

Microbial Ecology and Biogeography — OF THE — Southern Ocean

David Wilkins

Submitted in fulfillment of the requirements for the Degree of Doctor of Philosophy.

SCHOOL OF BIOTECHNOLOGY AND BIOMOLECULAR SCIENCES
UNIVERSITY OF NEW SOUTH WALES, SYDNEY

April 2013

"I hereby declare that this submission is my own work and to the best of my knowledge it contains no materials previously published or written by another person, or substantial proportions of material which have been accepted for the award of any other degree or diploma at UNSW or any other educational institution, except where due acknowledgement is made in the thesis. Any contribution made to the research by others, with whom I have worked at UNSW or elsewhere, is explicitly acknowledged in the thesis. I also declare that the intellectual content of this thesis is the product of my own work, except to the extent that assistance from others in the project's design and conception or in style, presentation and linguistic expression is acknowledged."

Parts of this thesis which have been previously published, or to which writing has been contributed by a person other than the author, are clearly marked with a statement in a sans-serif typeface preceding the relevant section. For example:

Sections of this chapter have been previously published in Wilkins D., Yau S., Williams T. J., Allen M. A., Brown M. V., DeMaere M. Z., Lauro F. M., and Cavicchioli R. (2012). Key microbial drivers in Antarctic aquatic environments. *FEMS Microbiology Reviews*.

Where experimental work has been performed by a person or people other than the author, this is indicated in a footnote.

Abstract

TODO write this

Contents

Abstract	iii
List of Figures	ix
List of Tables	xi
List of Acronyms	xv
Acknowledgements	xvii
1 Introduction	1
Physical oceanography of the Southern Ocean	1
Fronts and zones	1
Water masses and circulation	2
Effect of climate change	3
Microbial ecology of the Southern Ocean	3
Bacteria	4
Alphaproteobacteria	4
Roseobacter clade	4
SAR11	5
SAR116	6
Betaproteobacteria	6
Gammaproteobacteria	6
SAR86	6
OMG group	7
Ant4D3	7
GSO-EOSA-1	7
Deltaproteobacteria	8
CFB	8
Cyanobacteria	9
Verrucomicrobia	9
Other bacteria	9
Archaea	10
Viriplankton	11
Project aims	11
Aim 1	11
Aim 2	11
Aim 3	11
Aim 4	11
2 MINSPEC	13
Abstract	13
Introduction	13
Metagenomic analysis of microbial assemblages	13
The maximum parsimony approach	15

Methods	15
Implementation of MINSPEC	15
Validation of MINSPEC	16
Results	17
Discussion	17
Conclusions	17
3 The Polar Front	21
Abstract	21
Introduction	21
Methods	22
Sampling and metagenomic sequencing	22
Phylogenetic analysis of metagenomic data	25
BLAST comparison to RefSeq database	25
OTU abundances and variance between zones	25
Fragment recruitment to verify Operational Taxonomic Unit (OTU) identification	25
Additional samples to test “polynya hypothesis”	25
Functional analysis of metagenomic data	26
BLAST comparison to KEGG database	26
Analysis of functional potential	26
Taxonomic decomposition	26
Results	27
Metagenomic sequencing	27
Phylogenetic analysis of metagenomic data	27
Fragment recruitment to verify OTU identification	31
Additional samples to test alternative “polynya hypothesis”	31
Functional analysis of metagenomic data	31
Discussion	31
Taxonomic groups differentiating the zones	31
GSO-EOSA-1	31
Ammonia-oxidizing Crenarchaeota	36
Cyanobacteria	36
SAR11 and SAR116 clades	37
Bacteroidetes	37
Rhodobacterales	38
Alteromonadales	38
Verrucomicrobia	38
Functional capacities differentiating the zones	38
Conclusions: Biogeographic role of the Polar Front	41
4 Deep water formation	43
Abstract	43
Methods	43
Results and Discussion	45
5 The advection effect	47
Abstract	47
Introduction	47
Methods	48
Sampling	48
DNA extraction	49
Sequencing	50
Taxonomic assignment	50
Physicochemical and spatial distances	51
Generation of advection distance matrix	51
Ordination of distance matrices and comparison to water masses	52

Testing of advection effect	52
Differential influence of advection on different OTUs	52
Results	53
Sequencing and taxonomic assignment	53
Environment and distance effects	56
Testing the advection effect	58
Testing advection effect mechanisms	60
Discussion	61
Future work	62
References	63

List of Figures

1.1	Major fronts and water masses of the Southern Ocean	2
2.1	Results of MINSPEC validation	18
3.1	Map showing sites of seawater samples used in the Polar Front study	24
3.2	Rank-abundance curves for OTUs in each zone and size fraction	27
3.3	Contribution of OTUs to variance between the North and South zones	29
3.4	Tree of GSO-EOSA-1 related 16S rRNA genes	34
3.5	Read recruitment to reference genomes	35
3.6	Taxonomic decomposition of KEGG modules	39
4.1	Map showing sites of preliminary Antarctic Bottom Water (AABW) samples	44
4.2	Non-Metric Multidimensional Scaling (nMDS) of AABW, North Zone (NZ) and South Zone (SZ) samples	46
5.1	Map showing sites of samples used in the advection study	49
5.2	OTU assignments in the advection study.	56
5.3	nMDS of advective distances between samples.	57
5.4	nMDS of advective distances between samples.	57
5.5	dbRDA ordination of relationship between environment and community.	59
5.6	nMDS of advective distances between samples.	60
5.7	Advection effect at different taxonomic resolutions	61

List of Tables

2.1 Examples of spurious OTU identifications	14
3.1 Details of samples used in Polar Front study	23
3.2 Additional samples used to test polynya hypothesis	26
3.3 Twenty most abundant OTUs	28
3.4 Highest-contributing OTUs to the difference between the North and South zones	30
3.5 Contributions of KEGG modules to variance between the North and South zones	32
3.6 Contributions of KEGG ortholog groups to variance between the North and South zones	33
4.1 AABW samples used in the preliminary analysis	43
4.2 Twenty most abundant OTUs in preliminary AABW samples	45
5.1 Full sample data for advection study	54
5.1 (cont.) Full sample data for advection study.	55
5.2 Correlations between dbRDA axes and physicochemical variables	58

List of Acronyms

PASSAGE 2 Pattern Analysis, Spatial Statistics and Geographic Exegesis version 2.

GAAS Genome relative Abundance and Average Size.

MEGAN Metagenome Analyzer.

QIIME Quantitative Insights Into Microbial Ecology.

AABW Antarctic Bottom Water.

AAD Australian Antarctic Division.

AAIW Antarctic Intermediate Water.

AAP Aerobic Anoxygenic Phototrophic.

AC Antarctic Convergence.

ACC Antarctic Circumpolar Current.

anammox Anaerobic Ammonium Oxidation.

ANOSIM Analysis of Similarities.

AOA Ammonia-Oxidizing Archaea.

AOB Ammonia-Oxidizing Bacteria.

AP Antarctic Peninsula.

ASW Antarctic Surface Water.

AZ Antarctic Zone.

BW Bottom Water.

CASO Climate of Antarctica and the Southern Ocean.

CDW Circumpolar Deep Water.

CEAMARC Collaborative East Antarctic Marine Census.

CFB Cytophaga-Flavobacterium-Bacteroides.

CMS Connectivity Modeling System.

CTD Conductivity, Temperature and Depth.

dbRDA Distance-based Redundancy Analysis.

DCM Deep Chlorophyll Maximum.

DFAA Dissolved Free Amino Acids.

DGGE Denaturing Gradient Gel Electrophoresis.

distLM Distance-based Linear Models.

DMSP dimethylsulfoniopropionate.

DOC Dissolved Organic Carbon.

DOM Dissolved Organic Matter.

ECCO Estimating the Circulation and Climate of the Ocean.

FISH Fluorescence *In Situ* Hybridization.

GOS Global Ocean Sampling expedition.

GSO-EOSA-1 Gammaproteobacterial Sulfur Oxidizer-EOSA-1.

HMW High Molecular Weight.

HNLC High Nutrient, Low Chlorophyll.

IP Integer Programming.

IPCC Intergovernmental Panel on Climate Change.

ITS Internal Transcribed Spacer.

KEGG Kyoto Encyclopedia of Genes and Genomes.

KEOPS Kerguelen Ocean and Plateau Compared Study.

LCD Lower Circumpolar Deep.

LCDW Lower Circumpolar Deep Water.

LP Linear Programming.

LWM Low Molecular Weight.

MGI Marine Group I Crenarchaeota.

MGII Marine Group II Euryarchaeota.

MMPA methylmercaptopropionate.

NADW North Atlantic Deep Water.

nMDS Non-Metric Multidimensional Scaling.

NZ North Zone.

OMG Oligotrophic Marine Gammaproteobacteria.

OTU Operational Taxonomic Unit.

PF Polar Front.

PFZ Polar Frontal Zone.

POM Particulate Organic Matter.

RCA Roseobacter Clade Affiliated.

SACCF Southern Antarctic Circumpolar Current Front.

SAF Subantarctic Front.

SAM Southern Annular Mode.

SAMW Subantarctic Mode Water.

SAZ Subantarctic Zone.

SB Southern Boundary of the Antarctic Circumpolar Current.

SIMPER Similarity Percentages.

SO Southern Ocean.

SOSE Southern Ocean State Estimate.

SSU Small Subunit.

STF Subtropical Front.

SZ South Zone.

THC Thermohaline Circulation.

UCD Upper Circumpolar Deep.

UCDW Upper Circumpolar Deep Water.

Acknowledgements

Chapter 1

Introduction

Sections of this chapter have been previously published in Wilkins D., Yau S., Williams T. J., Allen M. A., Brown M. V., DeMaere M. Z., Lauro F. M., and Cavicchioli R. (2012). Key microbial drivers in Antarctic aquatic environments. *FEMS Microbiology Reviews*.

Physical oceanography of the Southern Ocean

The Southern Ocean (SO) is large ($\sim 36,000,000 \text{ km}^2$), oceanographically complex and an important part of the world's hydro- and biospheres. It drives global Thermohaline Circulation (THC): Antarctic Bottom Water (AABW) formed off the Antarctic Coast is the major source of the World Ocean's Bottom Water (BW) (Jacobs, 2004), the sinking of which is one of two major engines for the THC "global conveyor belt" (the other being BW formation in the North Atlantic). The SO also supports a large fraction of global marine primary production: the upwelling of Circumpolar Deep Water (CDW) south of the Polar Front (PF) returns nutrients transported to the deep ocean by sinking particulate matter (Rath *et al.*, 1998) to the surface, and SO phytoplankton may perform as much as 15% of global carbon fixation (Huntley *et al.*, 1991).

These important functions are closely linked to the SO's unique oceanography. Like the Arctic Ocean, the SO is circumpolar, entailing physical features such as low surface water temperatures, strong seasonal cycles in temperature and solar irradiation, the seasonal formation of sea ice and exposure to surface sheer forces from strong high-latitude winds. Unlike the Arctic Ocean, however, the SO has broad interfaces with the tropical oceans and circumpolar circulation uninterrupted by any major land mass, and in Antarctic coastal waters experiences powerful katabatic winds off the Antarctic ice cap. These properties shape the SO's unique physical oceanography.

Fronts and zones

Definitions of the SO's extent vary. Features commonly used to define its northern boundary include the 60th parallel south and the Antarctic Convergence (AC), while most Australian cartographic and governmental bodies consider the SO to begin at Australia's southern coastline, or approximately the 45th parallel south. As these distinctions have no biological relevance, for simplicity the Australian definition will be used in this thesis.

The surface of the SO is composed of several distinct zones, separated by circumpolar fronts (Fig. 1.1). Step transitions in the temperature and density of surface waters define the locations and extent of these fronts (Sokolov and Rintoul, 2002; Orsi *et al.*, 1995). The northernmost front is the Subtropical Front (STF), which lies at $\sim 40\text{--}45^\circ \text{ S}$, separating the Subantarctic Zone (SAZ) from the warmer and saltier tropical oceans to its north (Sokolov and Rintoul, 2002). Across the STF, potential temperature at 150 m depth decreases from > 12 to $< 10^\circ \text{ C}$.

Moving southwards, the southern extent of the SAZ is defined by the Subantarctic Front (SAF). The SAF is the northernmost and primary current core of the multiply-branched Antarctic Circumpolar Current (ACC) (Sokolov and Rintoul, 2009), and its position is thus defined by that of the ACC which varies considerably with longitude (Moore *et al.*, 1999). As with the STF, there is a drop in potential

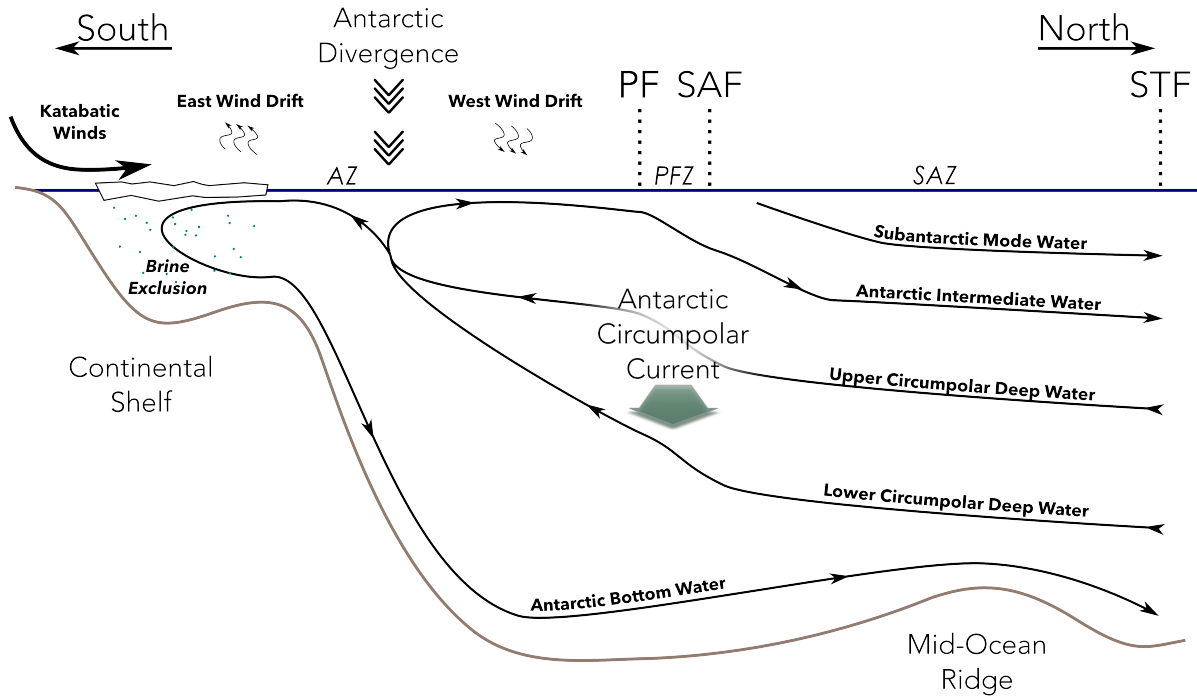


Figure 1.1: North–South cross-section of the Southern Ocean, showing major fronts and water masses. This map is schematic only and not to scale. Acronyms are as follows: Subtropical Front (STF); Subantarctic Zone (SAZ); Subantarctic Front (SAF); Polar Frontal Zone (PFZ); Polar Front (PF); Antarctic Zone (AZ).

temperature of 2–4 °C across the front (Sokolov and Rintoul, 2002). The SAF also marks the northern boundary of the Polar Frontal Zone (PFZ), where the SAZ and colder Antarctic Zone (AZ) waters meet and mix. Although both the SAF and PF represent large step changes in surface characteristics, the PFZ itself is relatively constant (Whitworth III and Nowlin Jr., 1987). This zone, and particularly its bounding fronts, are regions of high primary productivity (e.g. Laubscher *et al.*, 1993; Abell and Bowman, 2005b).

The southern boundary of the PFZ is the PF, also a current core of the ACC, and associated with a potential temperature drop of ~1–1.5 °C (Moore *et al.*, 1999). The waters south of the PF constitute the AZ, the southernmost and coldest (< 2 °C, Sokolov and Rintoul (2002)) major zone. The AZ can be further subdivided by several minor features, including the Southern Antarctic Circumpolar Current Front (SACCF) and Southern Boundary of the Antarctic Circumpolar Current (SB), both weaker southern branches of the ACC. However, these do not represent significant step transitions in physical properties.

Water masses and circulation

In addition to these surface features, the SO comprises several distinct water masses (Fig. 1.1), the circulation of which forms a major component of global THC. The most extensive of these is CDW, which consists of two layers. The Upper Circumpolar Deep Water (UCDW), characterised by a nutrient maximum and oxygen minimum, originates in the western Indian and south-eastern Pacific oceans (Orsi *et al.*, 1995). The Lower Circumpolar Deep Water (LCDW), characterised by a salinity maximum, originates as sinking North Atlantic Deep Water (NADW) (Whitworth III and Nowlin Jr., 1987). Both layers of CDW shoal southwards across the ACC.

South of the PF is the Antarctic Divergence, a region of transition between dominant easterly and westerly winds. As a consequence of Ekman (i.e. wind-forced) flow, surface currents are divergent, with those to the north driven further northwards by the westerlies (the West Wind Drift) while those to the south are forced southwards by the easterlies (the East Wind Drift) (Foldvik and Gammelsrød, 1988). This generates a region of upwelling, where the UCDW meet and interact with the upper ocean layers and atmosphere.

Between the divergence and the PF, the surface layer (~100–300 m depth) consists of Antarctic Surface Water (ASW), which is colder, less saline and better ventilated (i.e. more oxygenated) than the CDW. Driven by Ekman transport in the West Wind Drift, the ASW moves northwards towards the PF, with isopycnals (surfaces of constant potential density) sloping gently downwards towards the north. At the PF, the ASW sinks rapidly to form the Antarctic Intermediate Water (AAIW) (~500–1500 m depth), a layer of low-salinity water which underlies SAZ and, moving northwards, contributes to the intermediate water of the subtropical oceans (Foldvik and Gammelsrød, 1988). (Note that both the SAF and PF can be defined as the locations where the temperature minimum associated with AAIW rapidly decreases in depth (Whitworth III and Nowlin Jr., 1987).) Overlying the AAIW in the SAZ is the Subantarctic Mode Water (SAMW), which forms the surface layer north of the SAF (Speer *et al.*, 2000). Although the SAF is nominally the southern boundary of the SAMW, the surface discontinuity may sometimes occur several degrees to the south of the sub-surface front (e.g. Deacon, 1982; Orsi *et al.*, 1995).

Surface and CDW waters south of the Antarctic Divergence do not move northwards to form AAIW, but instead are driven southwards by the East Wind Drift. The region between the Antarctic Divergence and the coast is the site of dense, cold AABW formation. Katabatic winds from the Antarctic continent form polynyas and cool the surface waters, while brine exclusion during sea ice formation increases the waters' density. This newly formed cold and dense AABW sinks rapidly and flows down the continental shelf and margin to form an abyssal layer beneath the entire SO (Orsi *et al.*, 1999; Foldvik and Gammelsrød, 1988). AABW formation does not occur along the entire continental margin; rather, it is concentrated in the Weddell and Ross seas, and to a lesser extent the D'Urville sea off the Adélie Land coast. AABW is a major source of abyssal water to the World Ocean, and its formation drives global THC. Because AABW is ventilated in the SO before sinking rapidly, AABW is relatively enriched in oxygen compared to other deep layers of the World Ocean, which are oxygen-depleted due to the heterotrophic oxidation of sinking organic matter.

Effect of climate change

Anthropogenic climate change is having a significant effect on the ACC and the water masses it defines. Changes in the Southern Annular Mode (SAM), a regular pattern of Southern Hemisphere atmospheric circulation characteristics, are leading to an intensification of the westerly winds (Thompson and Solomon, 2002) which drive the ACC. As a consequence of this and other climate change-related effects, the mean annual path of the ACC and its associated fronts and isopycnals has moved ~50 km southwards since the 1950s (Gille, 2002). Waters on the poleward side of the ACC have become warmer and more saline, while those to the north cooler and fresher (Böning *et al.*, 2008). The ACC itself is warming and freshening (Böning *et al.*, 2008), from the surface to 900 m depth (Aoki *et al.*, 2003).

Fyfe and Saenko (2005), using a wind-driven model of the southward shift of the ACC, predicted that with conservative assumptions about future anthropogenic greenhouse gas emissions (Intergovernmental Panel on Climate Change (IPCC) A2 and B2 scenarios), the ACC can be expected to move ~1.4° southwards by the year 2100. They note that this is equivalent to reducing the volume of the SO south of the ACC by about $16 \times 10^6 \text{ km}^3$, or approximately the volume of the Arctic Ocean.

Aside from the oceanographic effects, these changes can be expected to effect the biology of the SO. In particular, even neglecting the changes in temperature and salinity of the water masses defined by the ACC, the southward migration of the ACC and concomitant change in the relative volumes (and surface areas) of the water masses it defines are a significant change in the size of the microbial habitats these masses represent. Predicting the effects this will have on SO ecosystems and ecosystem functions requires an understanding of the microbial ecology of the SO, and its biogeography relative to the ACC and its associate fronts and water masses. The following section gives an overview of the current state of knowledge.

Microbial ecology of the Southern Ocean

As in all the World Ocean, microorganisms perform key ecosystem functions in the SO, driving carbon, nitrogen, sulfur and other major cycles. There is evidence that the PF and other SO fronts are

biogeographic boundaries between distinct bacterioplankton communities (e.g. Selje *et al.*, 2004; Abell and Bowman, 2005b; Giebel *et al.*, 2009; Weber and Deutsch, 2010). This section reviews the current state of knowledge on the abundance, biogeography and ecosystem functions of microorganisms in the SO, with a focus on molecular studies.

Eukaryotic phytoplankton and protists are a major component of the SO microbial ecosystem. In particular, they perform a large proportion of primary production in coastal and continental shelf AZ waters (e.g. El-Sayed, 2005). Additionally, the production and deposition of biogenic silica by SO diatoms composes a large fraction of the global silica flux (Tréguer *et al.*, 1995). However, as the work described in this thesis focuses on bacteria and archaea, eukaryotic plankton will not be considered except where relevant to bacteria, archaea or viruses (e.g. grazing).

Bacteria

Alphaproteobacteria

Roseobacter clade The Roseobacter clade is an abundant and ecologically significant group of marine bacteria, found at high (> 15%) abundance in most marine surface environments (Buchan *et al.*, 2005, and references therein). Unlike some other major proteobacterial groups that are strongly associated with a particular ecological niche (e.g. the SAR11 clade), roseobacters have diverse metabolic abilities, with members capable of (for example) aerobic anoxygenic phototrophy (Biebl *et al.*, 2005; Béjà *et al.*, 2002), degradation of dimethylsulfoniopropionate (DMSP) by at least two pathways (Miller and Belas, 2004; Moran *et al.*, 2003), carbon monoxide oxidation (King, 2003) and heterotrophic utilisation of a broad range of substrates (reviewed in Brinkhoff *et al.*, 2008). Roseobacters are found in the planktonic fraction as well as in commensal association with phytoplankton and metazoans (reviewed in Buchan *et al.*, 2005).

Several 16S rDNA-based studies have identified the Roseobacter Clade Affiliated (RCA) subgroup as ubiquitous and abundant in SO surface waters and to a depth of at least 2200 m, composing ~10–30% of surface bacteria (and the majority of roseobacters) in the Subantarctic and Antarctic zones (Giebel *et al.*, 2009; Murray and Grzymski, 2007; Ghiglione and Murray, 2011) and a major fraction of the population in coastal waters (Murray and Grzymski, 2007; Koh *et al.*, 2011). Two major RCA phylotypes appear to be present in the SO and form the majority of the Roseobacter population. The phylotypes are strictly segregated by the PF, coexisting only within the PFZ (Selje *et al.*, 2004; Giebel *et al.*, 2009) where they may outnumber even the SAR11 clade. There is some evidence that the AZ RCA phylotype originates from the North Atlantic; Giebel *et al.* (2009) noted CDW at 2200 m in the South Zone (SZ) had an identical temperature-salinity signature to NADW. NADW is formed by the sinking of dense, saline waters from the surface north Atlantic, and is transported to the SO via global thermohaline circulation to become CDW (Callahan, 1972). Consistent with the upwelling of CDW in the AZ south of the PF, (Selje *et al.*, 2004) reported in a global study of RCA 16S rDNA gene fragments that the surface phylotype south of the PF was identical to one found in the Arctic Ocean, while differing by 3 bp from that north of the PF.

Little is known about the functional capabilities of RCA as only two isolated representatives have been described to date. (Giebel *et al.*, 2010) isolated “*Candidatus Planktomarina temperata*” from the North Sea, where it was the dominant phylotype. The authors’ identification of the pufM gene encoding a bacteriochlorophyll a subunit suggests at least this member of the RCA is capable of performing aerobic anoxygenic photosynthesis, a function of potentially large ecological significance. Mayali *et al.* (2008) isolated an apparently heterotrophic RCA member from subtropical waters, and found *in vitro* evidence that they colonised and increased mortality in blooming dinoflagellates, but did not investigate photosynthetic potential.

Roseobacters, and particularly the RCA, have been strongly associated with phytoplankton blooms in the SO. Two separate 16S rDNA-based studies of a naturally fertilised bloom in the Kerguelen islands region (West *et al.*, 2008; Obernosterer *et al.*, 2011) found that RCA and the Roseobacter NAC11-7 and NAC11-6 clusters were dominant bacterial Operational Taxonomic Units (OTUs) in the bloom patch, suggesting they play a role in heterotrophic degradation of bloom products. Unlike the other clusters, however, RCA representatives were also relatively abundant and metabolically active outside of the patch. Both Giebel *et al.* (2009) and Obernosterer *et al.* (2011) found that in SO vertical profiles RCA abundances often peaked at the Deep Chlorophyll Maximum (DCM), again suggesting an

association with phytoplankton.

RCA abundance may follow a seasonal cycle in the SO. Giebel *et al.* (2009) found that RCA phylotypes composed at most 8% of all bacterial 16S rDNA genes during winter but up to 36% in the coastal current and Weddell sea during autumn, while Ghiglione and Murray (2011) found the proportion to peak in January in coastal waters off the Antarctic Peninsula and in February off the Kerguelen islands.

A metagenomic study of SO waters off West Antarctica found that Roseobacter clade Small Sub-unit (SSU) rRNA sequences were much more abundant in summer than in winter, with *Sulfitobacter* sequences the most abundant within this clade (Grzymski *et al.*, 2012). This is consistent with the association of roseobacters with phytoplankton (Moran *et al.*, 2003). Nevertheless, Roseobacter clade representatives in these polar waters are metabolically active in both seasons, expressing high-affinity uptake systems (ABC, TRAP) for capturing labile nutrients such as sugars, polyamines, amino acids, and oligopeptides (Williams *et al.*, 2012a).

SAR11 The SAR11 clade of Alphaproteobacteria is probably the most abundant class of marine microorganisms worldwide (Morris *et al.*, 2002). “*Candidatus Pelagibacter ubique*” strain HTCC1062, the first and most intensively studied SAR11 isolate, has one of the smallest genomes and gene complements of any known free-living cell as well as a very small cell volume (Giovannoni *et al.*, 2005). The small volume, streamlined genome and high proportion of ABC nutrient-uptake transporter genes are all consistent with an oligotrophic lifestyle, scavenging a wide range of substrates using high-affinity, broad-specificity transporters (Giovannoni *et al.*, 2005; Lauro *et al.*, 2009; Sowell *et al.*, 2009). SAR11 cells probably preferentially consume low over high molecular weight Dissolved Organic Matter (DOM) (Malmstrom *et al.*, 2005) and their relative contribution to uptake of DOM may decrease as substrate concentration increases (Alonso and Pernthaler, 2006). A consequence of this oligotrophic strategy is that SAR11 members are probably unable to take advantage of sudden nutrient influxes, such as during phytoplankton blooms, to rapidly increase cell density (Tripp *et al.*, 2008).

SAR11 has been consistently detected at high abundances in molecular surveys of the SO, in all open ocean regions as well as at depth and in coastal waters, and is usually the dominant alphaproteobacterial, if not bacterial, group (Giebel *et al.*, 2009; Murray and Grzymski, 2007; López-García *et al.*, 2001; Straza *et al.*, 2010; Jamieson *et al.*, 2012; García-Martínez and Rodríguez-Valera, 2000; Ghiglione and Murray, 2011; Murray *et al.*, 2011; Piquet *et al.*, 2011). It is probably more abundant in the epipelagic than at depth (Giebel *et al.*, 2009).

SAR11 seems to exhibit biogeographic partitioning in the SO, and is probably represented by two major ecotypes with a temperature-driven boundary in the region of the PF (Brown *et al.*, 2012). It is probably more abundant in the SAZ and PFZ zones than in the AZ (Giebel *et al.*, 2009; Ghiglione and Murray, 2011). This may be related to a competitive advantage of the oligotrophic SAR11 in the High Nutrient, Low Chlorophyll (HNLC) SAZ relative to the AZ, where blooming phytoplankton lead to increased concentrations of High Molecular Weight (HMW) DOM and Particulate Organic Matter (POM). Straza *et al.* (2010) found SAR11 accounted for the largest fraction of leucine uptake among all bacterial groups in continental shelf waters off the West Antarctic Peninsula, but a comparatively small fraction of protein uptake, consistent with a role as a Low Molecular Weight (LWM) DOM specialist. West *et al.* (2008), examining 16S rDNA profiles in and out of a natural phytoplankton bloom on the Kerguelen Plateau (SAZ), found SAR11 to be a dominant group in HNLC waters outside the bloom patch but relatively less abundant in it. A separate study of the same bloom found SAR11 had a markedly smaller relative contribution to bulk leucine incorporation in the patch than out, suggesting it was not a major contributor to DOM degradation (Obernosterer *et al.*, 2011). Interestingly, SAR11 did dominate in abundance and leucine incorporation at an additional site where a recent and transient phytoplankton bloom had taken place, implying a time lag in the succession between the baseline HNLC and bloom populations. The authors additionally noted that SAR11 abundances at the bloom station began to climb towards non-bloom levels once the bloom had peaked and begun declining. An Antarctic Peninsula SAR11 metaproteome was dominated by ABC transport proteins for the capture and uptake of labile substrates, especially taurine, polyamines and amino acids, and also included DMSP demethylase (Williams *et al.*, 2012a). Finally, despite an apparently negative correlation between SAR11 and blooming phytoplankton, Ghiglione and Murray (2011) found only small seasonal changes in abundance during an annual cycle at the Antarctic Peninsula (AP) and Kerguelen Island. These studies are all consistent with the view of SAR11 as a typically non-opportunistic oligotroph specialising in LWM Dissolved Organic Carbon (DOC).

One of the most interesting physiological features of SAR11 representatives is their expression of the retinal-binding pigment proteorhodopsin, which has been shown to act as a proton pump when exposed to light (Beja *et al.*, 2000) and has therefore been implicated in photoheterotrophy. Surprisingly, given very low light levels in Antarctic waters during austral winter, SAR11 proteorhodopsin is present throughout the annual cycle (Williams *et al.*, 2012a). This may be consistent with the observation that many marine proteorhodopsins do not appear tuned to maximise energy conversion from available light, which has led Fuhrman *et al.* (2008) to propose at least some proteorhodopsins may perform non-energetic functions such as photoregulatory sensing. Alternatively, constitutive expression of proteorhodopsin for light harvesting in SAR11 may facilitate the ability to immediately respond to cellular energy deficits caused by carbon starvation (Steindler *et al.*, 2011).

SAR116 The SAR116 clade of Alphaproteobacteria has been detected throughout the world ocean, including in molecular studies of the SO (West *et al.*, 2008; Topping *et al.*, 2006). Topping *et al.* (2006) using Fluorescence *In Situ* Hybridization (FISH) estimated it composed $13.1\% \pm 8.6$ to $31.9\% \pm 13.7$ of bacterioplankton in the West and East regions of the Scotia Sea respectively.

The only isolated and fully sequenced SAR116 representative, “*Candidatus Puniceispirillum marinum*”, has been reported to have a versatile repertoire of genes for aerobic CO fixation, C1 metabolism and dimethylsulfoniopropionate degradation, suggesting it may occupy a “marine generalist” niche similar to that of SAR11 and some roseobacters (Oh *et al.*, 2010). Proteins for ABC and TRAP transport and C1 metabolism with high matches to SAR116 bacteria were detected in both the summer and winter metaproteomes of coastal waters of the Antarctic Peninsula, consistent with a preference for labile compounds and C1 substrates (Williams *et al.*, 2012a).

Betaproteobacteria

The Betaproteobacteria are a large and cosmopolitan class with a range of ecological roles in the World Ocean (reviewed in Kirchman, 2008). Hollibaugh *et al.* (2002) detected *Nitrosospira*-like 16S rRNA sequences in Ross Sea and Antarctic Peninsula surface waters, and noted that the ribotype appeared similar to one found in the Arctic. While not found at high abundance (Gentile *et al.*, 2006; Ghiglione and Murray, 2011; Jamieson *et al.*, 2012), there is evidence that Betaproteobacteria perform significant ecological functions. Most known Ammonia-Oxidizing Bacteria (AOB) belong to the Betaproteobacteria (Head *et al.*, 1993; Teske *et al.*, 1994). Metagenomic and metaproteomic analyses of surface coastal waters off the Antarctic Peninsula show evidence of Calvin cycle carbon fixation and ammonia oxidation in winter by Betaproteobacteria (Grzymski *et al.*, 2012; Williams *et al.*, 2012a).

The OM43 clade of Betaproteobacteria has been associated with coastal phytoplankton blooms (Morris *et al.*, 2006) and shown to be an obligate methylotroph capable of using methanol and formaldehyde as carbon and energy sources (Giovannoni *et al.*, 2008). As it has the smallest reported genome for a free-living cell, OM43 seems to be highly specialized for this unusual niche (the “genome streamlining” hypothesis, Mira *et al.* (2001)). OM43 has been detected in a 16S rDNA library in a naturally fertilised bloom in the SAZ (West *et al.*, 2008), where it was the only betaproteobacterial representative, and in a metaproteomic survey of coastal waters on the AP, where methanol dehydrogenase from OM43 was detected (Williams *et al.*, 2012a). Although the source of methanol in the marine environment is not yet clear, it may be a byproduct of phytoplankton growth (Heikes *et al.*, 2002), which would be consistent with OM43’s observed association with coastal blooms. This possibility suggests OM43, and perhaps other C1 specialists, play an underexplored role in the marine microbial loop. Alternative methanol sources are atmospheric deposition (Sinha *et al.*, 2007) or photochemical degradation of organic material (Dixon *et al.*, 2011). The latter is of particular interest in Antarctic waters, given the high levels of solar irradiation during the austral summer.

Gammaproteobacteria

SAR86 The gammaproteobacterial SAR86 clade is an abundant group in the surface ocean, being e.g. the most abundant genome of an uncultured organism in the Global Ocean Sampling expedition (GOS) dataset (Dupont *et al.*, 2011). While it has been detected in the Southern Ocean (Abell and Bowman, 2005b; Topping *et al.*, 2006; West *et al.*, 2008; Obernosterer *et al.*, 2011), little is known of its distribution or ecological role. (Topping *et al.*, 2006) estimated on the basis of FISH activity that

SAR86 cells composed $7.8\% \pm 8.2$ and $18.3\% \pm 17.0$ of total bacterioplankton in the western and eastern Scotia Sea respectively, suggesting that at least in the SAZ it is a major component of the surface community. Genomic analysis of partial SAR86 genomes assembled from metagenomes found the clade have streamlined genomes and are specialized for utilizing lipids and carbohydrates, suggesting minimal competition between SAR86 and SAR11 for DOC (Dupont *et al.*, 2011). This may be reflected by the simultaneous high abundance and activity of SAR11 and SAR86 in the HNLC waters of the SAZ (Obernosterer *et al.*, 2011)

OMG group The term Oligotrophic Marine Gammaproteobacteria (OMG) was named for a group of physiologically diverse heterotrophs that belong to previously detected environmental rRNA clades (OM60, BD1-7, KI89A, OM182, SAR92) (Cho and Giovannoni, 2004). Cultured OMG isolates have been shown to be obligately oligotrophic (Cho and Giovannoni, 2004). Nevertheless, SAR92 is associated with nutrient-rich waters with high phytoplankton abundances (Stingl *et al.*, 2007; Pinhassi *et al.*, 2004). Reports of SAR92 in the SO corroborate this ecology: both West *et al.* (2008) and Obernosterer *et al.* (2011) found SAR92-affiliated OTUs to be far more abundant inside the Kerguelen Ocean and Plateau Compared Study (KEOPS) phytoplankton bloom patch than in typically HNLC SAZ waters outside of it, with abundance declining as the bloom aged. This, combined with the observation that SAR92 growth is highly carbon-limited (Stingl *et al.*, 2007), suggests the clade plays an important role in degradation of organic carbon produced by phytoplankton blooms. It has also been detected in coastal AP and Kerguelen Islands waters (Ghiglione and Murray, 2011). Metaproteomic and metagenomic surveys of coastal waters at Palmer station found OMG to be more abundant in the summer than winter (Williams *et al.*, 2012a). TonB-dependent receptor systems from OMG were highly abundant in the metaproteome, indicating that this is the preferred uptake system of ambient substrates (Williams *et al.*, 2012a). Certain OMG strains encode proteorhodopsin (HTCC2207, Stingl *et al.* (2007); HTCC2143, Oh *et al.* (2010)), also indicated in the metaproteomic study in both seasons (Williams *et al.*, 2012a).

Ant4D3 In a study of six fosmids from nearshore waters at Palmer station, Grzymski *et al.* (2006) identified a uncultured gammaproteobacterium, Ant4D3. It has since been reported as one of the dominant proteobacterial groups in the SO. In waters off the western Antarctic Peninsula, Ant4D3 was reported to compose 10% of the total community and half the gammaproteobacterial community, and 68% of cells incorporating amino acids (Straza *et al.*, 2010). The authors also reported that the clade appears to have low diversity, based on detected rDNA sequences. Like SAR86, Ant4D3 cells were more active in HNLC than bloom conditions on the Kerguelen Plateau (West *et al.*, 2008). However, Ghiglione and Murray (2011) reported that 16.5% of tag-pyrosequenced 16S Denaturing Gradient Gel Electrophoresis (DGGE) bands from summer AP waters were affiliated to Ant4D3, dominating the Gammaproteobacteria and outnumbering winter and Kerguelen Island waters. Murray *et al.* (2011) similarly found Ant4D3 clones to be highly abundant in a 16S library from waters in the vicinity of Antarctic icebergs. Little is known about the group's function or ecological position, although it has been detected in Arctic waters where it appeared to occupy a DOM utilisation niche different from that of other major heterotrophs e.g. SAR11 (Nikrad *et al.*, 2012).

GSO-EOSA-1 The GSO-EOSA-1 cluster of sulfur-oxidizing Gammaproteobacteria, which includes the uncultivated ARCTIC96BD-19 and SUP05 lineages as well as cultivated chemoautotrophic clam symbionts, has been reported in global mesopelagic waters (Swan *et al.*, 2011) and oxygen minimum zones (Walsh *et al.*, 2009; Canfield *et al.*, 2010). Three studies have recently identified GSO-EOSA-1 representatives at high abundance in coastal and AZ waters. A metagenomic survey of coastal waters at Palmer station found GSO-EOSA-1 winter bacterioplankton were dominated by Gammaproteobacteria (19.7% of the winter library compared to 2.7% of the summer library) falling into five closely-related (0.03 distance) bins that were affiliated with the GSO-EOSA-1 complex. Grzymski *et al.* (2012), in a metaproteomic survey of coastal waters at Palmer station, found GSO-EOSA-1 proteins composed a large fraction of all gammaproteobacterial proteins detected and were significantly more abundant in winter than summer (20% vs 3%). In a companion metaproteomic analysis of the same sites, Williams *et al.* (2012a) confirmed this high abundance and seasonal pattern, although GSO-EOSA-1 appeared to be metabolically active at the surface in both summer and winter.

Genomic and metaproteomic analyses of GSO-EOSA-1 representatives, particularly SUP05, have revealed the potential for carbon fixation via the Calvin cycle and sulfur oxidation, even in well-oxygenated waters (Walsh *et al.*, 2009; Swan *et al.*, 2011; Grzymski *et al.*, 2012). Grzymski *et al.* (2012) estimated from rRNA abundances that 18–37% of the winter bacterioplankton community comprises OTUs with the potential for chemolithoautotrophy, including GSO-EOSA-1, suggesting winter chemolithoautotrophy may contribute significantly to SO carbon fixation.

Deltaproteobacteria

Deltaproteobacteria are rarely detected at abundance in global surface waters (see e.g. Venter *et al.*, 2004), and this pattern appears to hold in the Southern Ocean (Murray and Grzymski, 2007; West *et al.*, 2008; Ghiglione and Murray, 2011; Murray *et al.*, 2011; Ducklow *et al.*, 2011; Jamieson *et al.*, 2012). However, they may increase in abundance in mesopelagic waters (Wright *et al.*, 1997; Pham *et al.*, 2008; Zaballos *et al.*, 2006). At a 3000 m deep site at the PF in the Drake Passage, López-García *et al.* (2001) detected several deltaproteobacterial 16S rDNA sequences, all of which clustered with the marine deltaproteobacterial clade SAR324 previously identified in the mesopelagic Sargasso Sea (Wright *et al.*, 1997). Whole-genome analysis of SAR324 indicates an ecology that includes carbon fixation via the Calvin cycle and sulfur oxidation, as well as oxidation of methylated compounds (Swan *et al.*, 2011). SAR324 may therefore be significant contributors to chemoautotrophy in the dark ocean (Swan *et al.*, 2011).

CFB

Bacteria of the group Cytophaga-Flavobacterium-Bacteroides (CFB) are cosmopolitan and abundant in the world ocean (Glöckner *et al.*, 1999). While the CFB often form a major fraction of planktonic taxa (Fandino *et al.*, 2001), they are particularly prevalent in particle-attached communities (DeLong *et al.*, 1993) and are associated with blooming phytoplankton (Pinhassi *et al.*, 2004). Isolated CFB representatives have a well-described aptitude for the degradation of HMW DOM, particularly biopolymers which may be recalcitrant to utilisation by other bacterial heterotrophs (reviewed in Kirchman, 2002), suggesting they play an important role in remineralisation of primary production products. Of the CFB, the class Flavobacteria seem to be in the majority worldwide in both freshwater and marine environments (O'Sullivan *et al.*, 2004; Cottrell *et al.*, 2005) including the Southern Ocean (Abell and Bowman, 2005b).

CFB in the SO are strongly biogeographically partitioned. Abell and Bowman (2005b), using DGGE and 16S sequencing with Flavobacteria-specific primers, found significantly higher abundance and diversity of particle-attached Flavobacteria in the nutrient- and phytoplankton-rich waters south of the PF relative to the HNLC waters of the Subantarctic. This difference in abundance may be largely attributable to the low iron availability in the Subantarctic, which probably limits primary production (Boyd *et al.*, 2007). Both natural and artificial iron fertilization events in the Subantarctic have resulted in high abundances of bacterial heterotrophs (Christaki *et al.*, 2008; Oliver *et al.*, 2004); West *et al.* (2008) identified the CFB as a major component of the bacterial response to blooms induced by natural iron input on the Kerguelen plateau. The higher abundance of CFB in the AZ may also relate to their prevalence in sea ice (Brinkmeyer *et al.*, 2003; Brown and Bowman, 2001), from which they would be released into AZ waters during seasonal melting. Two groups, the uncultured agg58 cluster and the genus *Polaribacter*, appear to dominate CFB populations and activity in the SO (Murray and Grzymski, 2007; Abell and Bowman, 2005a,b; Obernosterer *et al.*, 2011; West *et al.*, 2008; Ghiglione and Murray, 2011; Ducklow *et al.*, 2011; Straza *et al.*, 2010).

There is some evidence that planktonic and particle-attached CFB, rather than being an integrated population with cells opportunistically shifting between phases, may comprise at least partially distinct groups of phylotypes. In a mesocosm experiment examining colonisation of diatom detritus in SO seawater, 16S DGGE and sequencing analysis showed a large proportion of flavobacterial phylotypes present in the planktonic phase failed to colonise detrital particles during the course of the experiment (Abell and Bowman, 2005a). The authors suggest these phylotypes may be slower-growing, perhaps comprising a secondary group of colonisers which only come to dominate when the more accessible detrital nutrients have been exhausted and the primary colonisers have secreted useful secondary metabolites. Alternatively, some flavobacterial groups may not use particle attachment as a primary

strategy.

Kirchman (2002) suggests 16S clone libraries may systematically underestimate the abundance of CFB in environmental samples, noting that in two studies where both FISH and 16S analysis were employed at the same site there were common discrepancies in CFB abundance estimates between the two methods (Cottrell and Kirchman, 2000; Eilers *et al.*, 2000). Additionally, both FISH and PCR based methods may underestimate CFB abundance relative to metagenomic surveys, due to probe specificity biased against Bacteroidetes 16S rDNA (Cottrell *et al.*, 2005; O'Sullivan *et al.*, 2004).

Polaribacter is a gas-vacuolated, proteorhodopsin-expressing flavobacterial genus prevalent in Arctic and Antarctic seawater. Its genome indicates a preference for polymers obtained from algal detritus rather than labile exudates (e.g. taurine, polyamines) (González *et al.*, 2008). An Antarctic Peninsula coastal metagenome found *Polaribacter*-related sequences to be dominant in summer, consistent with an association with phytoplankton blooms and/or input from melting sea-ice (Grzymski *et al.*, 2012). Flavobacterial proteins (including those with the best matches to *Polaribacter* spp.) were similarly much more abundant in the summer than winter metaproteome from the same sites, with components of TonB-dependent receptor systems predominating (Williams *et al.*, 2012a).

Cyanobacteria

Cyanobacteria, dominated by the genera *Prochlorococcus* and *Synechococcus*, are the most abundant photosynthetic organisms on Earth (Scanlan *et al.*, 2009, and references therein), but little molecular research has been performed on their role in SO ecosystems. This may be because it has been generally accepted that there are no cyanobacteria in AZ waters (Ghiglione and Murray, 2011; Zubkov *et al.*, 1998; Evans *et al.*, 2011), although recent and metaproteomic results (Williams *et al.*, 2012a) challenge this assumption. It is not infeasible that cyanobacteria survive at Antarctic temperatures, as (apparently psychrophilic or psychrotolerant) *Synechococcus* and *Prochlorococcus* strains have been identified in several marine-derived Antarctic lakes, including at sub-zero water temperatures (Bowman *et al.*, 2000; Powell *et al.*, 2005; Lauro *et al.*, 2011). Regardless, it is clear that cyanobacteria, if present in the AZ, are at very low abundance (Marchant *et al.*, 1987) and probably of little ecological significance. Cyanobacteria also appear to be at low abundance in the SAZ (Abell and Bowman, 2005b; Topping *et al.*, 2006).

Verrucomicrobia

Verrucomicrobia is a recently described phylum, members of which are ubiquitous in the marine environment, and which appears to be composed of several physiologically distinct lineages (Freitas *et al.*, 2012). A small number of Verrucomicrobia representatives have been detected in the SO (Murray *et al.*, 2011; West *et al.*, 2008; Gentile *et al.*, 2006; Murray and Grzymski, 2007), and Ghiglione and Murray (2011) reported a higher abundance of 16S rDNA clones affiliating with the Verrucomicrobia at a Kerguelen Island site relative to a site near Palmer Station on the Antarctic Peninsula. Little else is known regarding their abundance, diversity or ecological role in the SO.

Other bacteria

Other bacterial groups have been reported at low abundance in SO waters, including Actinobacteria (Bowman and McCuaig, 2003; Brinkmeyer *et al.*, 2003; Abell and Bowman, 2005b; Gentile *et al.*, 2006; Murray and Grzymski, 2007; Murray *et al.*, 2011; Ghiglione and Murray, 2011; Piquet *et al.*, 2011; Jamieson *et al.*, 2012), Epsilonproteobacteria (Gentile *et al.*, 2006; Murray and Grzymski, 2007), and Firmicutes (Murray and Grzymski, 2007; Lo Giudice *et al.*, 2011; Murray *et al.*, 2011). Little is known about their respective ecological roles, although Actinobacteria have been associated with marine aggregates (Grossart *et al.*, 2004); interestingly, their terrestrial counterparts have diverse HMW substrate degradation capabilities (reviewed in Kirchman, 2008). A strong negative correlation has been reported between actinobacterial abundance and latitude in a global survey of 16S rDNA clone libraries (Pommier *et al.*, 2007), with higher abundances in tropical and subtropical waters, as for Cyanobacteria.

Bacteria of the phylum Planctomycetes have been detected at low abundance in SO molecular surveys (Gentile *et al.*, 2006; López-García *et al.*, 2001; Jamieson *et al.*, 2012; Murray *et al.*, 2011; Abell and Bowman, 2005b). The Planctomycetes are emerging as organisms of interest in marine microbial

ecology, for example as performers of Anaerobic Ammonium Oxidation (anammox) (Strous *et al.*, 1999). They have been identified in a metaproteome from West Antarctic coastal waters (Williams *et al.*, 2012a), where they and members of the phylum Nitrospirae were implicated in nitrification using nitrite generated by Ammonia-Oxidizing Archaea (AOA) and AOB.

Archaea

DeLong *et al.* (1994) first reported the high abundance (up to 34%) of archaea in Antarctic coastal surface waters, a surprising discovery at a time when the Archaea were generally considered a rare group of strict extremophiles. The majority of rDNA clones they identified were affiliated with the Marine Group I Crenarchaeota (MGI), while the remainder represented the Marine Group II Euryarchaeota (MGII). Subsequent rRNA-based studies are likewise in agreement that MGI are the dominant group of archaea in surface waters of coastal Antarctica, followed by MGII (Gerlache Strait, Massana *et al.* (1998); near Anvers Island, Murray *et al.* (1998)). Further rRNA-based analysis showed the widespread distribution of Antarctic marine archaea (Murray *et al.*, 1999; Topping *et al.*, 2006; Jamieson *et al.*, 2012), and identified a significant MGI community in benthic sediments on the Antarctic coast (Bowman and McCuaig, 2003).

For MGI, ammonia-oxidizing chemolithoautotrophy is likely the dominant metabolic lifestyle (Ingalls *et al.*, 2006; Berg *et al.*, 2007), suggesting they play major roles in nitrification and carbon fixation in the SO. In a winter coastal Antarctic metaproteome, MGI proteins made up 30% of all identified proteins from bacteria or archaea; no MGI proteins were detected in the summer metaproteome (Williams *et al.*, 2012a). The winter metaproteome included MGI proteins from the 3-hydroxypropionate/4-hydroxybutyrate cycle, the pathway used by ammonia-oxidizing MGI for carbon fixation, and for ammonium transport and oxidation, supporting a nitrification role for Southern Ocean MGI (Williams *et al.*, 2012a). The complementary metagenomic analysis of Grzymski *et al.* (2012) proposed chemolithoautotrophy carried out by ammonia-oxidizing MGI and sulfur-oxidizing Gammaproteobacteria (see GSO-EOSA-1, above) to be the major drivers of winter carbon fixation in AZ waters. In summer autotrophic carbon assimilation is driven by algal-driven oxygenic photoautotrophy, consistent with high light availability and intensity, whereas in the polar winter “dark” chemoautotrophy by archaea and bacteria plays a major role in carbon fixation.

Murray *et al.* (1998) found that total archaeal rRNA levels decreased during summer, and noted a negative correlation between archaeal rRNA levels and chlorophyll *a* concentration. Massana *et al.* (1998) also observed a decline in archaeal rRNA levels during spring. Church *et al.* (2003) found a significantly higher (44% increase) abundance of MGI in surface waters in winter than summer. Ammonia-oxidizing MGI have been shown to be especially sensitive to photoinhibition (Merbt *et al.*, 2012), which might account for their decline during periods of extended illumination. It has also been speculated that the decline of archaea during spring/summer represents competition with non-archaeal microbes during phytoplankton blooms (Massana *et al.*, 1998), or that the majority of MGI were chemoautotrophic and therefore more competitive than heterotrophs during carbon-scarce winter conditions (Murray *et al.*, 1998). Genomic evidence suggests MGII are motile, proteorhodopsin-expressing photoheterotrophs that specialize in protein and lipid degradation (Iverson *et al.*, 2012). This is consistent with evidence that this group, in contrast to MGI, was more relatively abundant at the surface than at depth (Massana *et al.*, 1998). Murray *et al.* (1998) noted an increase in MGII in autumn in waters off Anvers Island; but otherwise the seasonal distribution of this group in Antarctic waters is not well understood.

The numerical dominance of MGI over other archaeal groups in surface and photic zone waters has also become well established (e.g. DeLong *et al.*, 1994; Massana *et al.*, 2000), although not in aphotic waters; López-García *et al.* (2001) detected only euryarchaeotal sequences in a sample from 3000 m depth at the PF in the Drake Passage, including marine groups II and III and a novel marine group IV. However, these studies also illustrated a potential hazard of probe-dependant methods, namely the high variability of abundance estimates depending on probe design. For example, (Simon *et al.*, 1999) did not detect any DAPI-positive archaeal cells in a summer transect between the polar front and ice edge using the archaea-specific probes ARCH334 and ARCH915, in contrast to the results of several other studies reviewed herein. López-García *et al.* (2001) detected only one archaeal phylotype (an euryarchaeon) in their initial clone library constructed with one archaeal primer pair. This prompted the authors to design an additional five primer pairs, resulting in both a higher number and greater

diversity of clones. Such results illustrate both the importance of primer selection and the value of whole genome shotgun (i.e. primer-independent) approaches to community analysis.

Virioplankton

The “viral shunt”, by which nutrients are released via lysis from marine microorganisms and returned to the dissolved and particulate pools, may mediate the flux of a quarter of all organic matter in the microbial loop (Wilhelm and Suttle, 1999) and the viral release of iron from bacterioplankton may be crucial for phytoplanktonic growth (Poorvin *et al.*, 2004). Viral production, and by inference the viral shunt, has been shown to be highly active in HNLC Subantarctic (Evans *et al.*, 2009), iron-fertilized Subantarctic (Weinbauer *et al.*, 2009) and coastal waters, where viral-mediated carbon flux may account for 50–100% of all heterotrophic production (Guixa-Boixereu *et al.*, 2002). Despite this crucial ecosystem role, molecular analysis of the diversity and function of SO virioplankton has been sparse. Two studies (Short and Suttle, 2002, 2005) used probes with specificity to algal virus and cyanophage marker genes respectively, and succeeded in detecting both in SO waters. Williams *et al.* (2012a) and Grzymski *et al.* (2012), in complementary metaproteomic and metagenomic studies of sites near Palmer station on the Antarctic Peninsula, also detected cyanophage (cyanobacterial virus) genes and proteins as well as a single major capsid protein from *Phaeocystis pouchetii* virus PpV01. While these studies are only preliminary, they suggest that the more abundant viruses are phytoplanktonic predators.

Project aims

Aim 1

The PF is a major current core of the ACC, and represents the surface transition between CDW which dominates the AZ and SAMW which dominates the SAF and northwards. Previous studies (e.g. Abell and Bowman, 2005b; Giebel *et al.*, 2009; Selje *et al.*, 2004) have suggested the PF is a biogeographic barrier for certain microbial taxa, but this has not yet been established on the community level, a necessary prerequisite for a comparative study of the two zones. This project aimed to determine whether the microbial communities to the north and south of the PF are significantly different.

Aim 2

In order to predict the effects of climate change-driven changes in the location and properties of the ACC on the SO’s microbial ecosystems, this project aimed to characterise the microbial communities to the north and south of the PF.

Aim 3

Picoplankton in the SO perform numerous important ecosystem functions, for example primary production and heterotrophic utilisation of recalcitrant organic compounds. This project aimed to characterise those ecosystem functions, and in particular the ways in which those functions differ north and south of the PF.

Aim 4

Findings flowing from the three previous questions will be useful in predicting the effects of climate change-driven change in the physical oceanography of the SO. However, an underlying assumption has been that the distribution and abundance of microorganisms is determined solely by the physical properties of an environment; in other words, that “*everything is everywhere, but, the environment selects*” (quotation from Baas Becking (1934); English translation from de Wit and Bouvier (2006)). Recently, evidence has accumulated that physical transport (advection) may play a role in shaping marine microbial biogeography, but this hypothesis has yet to be directly tested. This project aimed to do so.

Chapter 2

MINSPEC, a bioinformatic tool for metagenomics

Sections of this chapter have been previously published in Wilkins D., Lauro F. M., Williams T. J., De-Maere M. Z., Brown M. V., Hoffman J. M., Andrews-Pfannkoch C., McQuaid J. B., Riddle M. J., Rintoul S. R., and Cavicchioli R. (2012). Biogeographic partitioning of Southern Ocean microorganisms revealed by metagenomics. *Environmental Microbiology*.

Abstract

Incorrect assignment of taxonomic identity to sequencing reads is a source of error in microbial metagenomic studies. Microbial genomes naturally share large amounts of very similar or identical genomic sequence as a result of common ancestry, horizontal gene transfer or convergent evolution. Thus, when a read is similar to more than one Operational Taxonomic Unit (OTU) in a reference database of microbial genomes, nucleotide identity alone is insufficient to determine the correct taxonomic assignment. This chapter presents a simple algorithm and software tool, MINSPEC, which determines the smallest set of OTUs that explains a given set of matches between metagenomic reads and a reference database. By removing OTUs not in this “maximum parsimony” set, MINSPEC reduces spurious OTU assignments (false positives) and thus increases the accuracy of relative abundance estimates. MINSPEC has been validated against simulated metagenomic experiments.

Introduction

Metagenomic analysis of microbial assemblages

The identification of the species or Operational Taxonomic Units (OTUs) that compose a microbial community is a primary aim of metagenomics. Typically this is achieved using one of two methods.

The first method is the identification, using a search and alignment algorithm such as BLAST, of specific marker genes or other sequences which are diagnostic for a particular OTU. Common targets in microbial ecology are the 16S or other ribosomal subunit rDNA sequences, and the Internal Transcribed Spacer (ITS) regions between 16S–23S rDNA sequences (e.g. Brown *et al.*, 2012). This method provides several advantages. The selected regions are usually highly conserved, and through cultivation and full-genome sequencing have been reliably associated with a particular OTU, allowing very accurate identification and analysis of diversity down to the ecotype level (e.g. Brown *et al.*, 2012). If the copy number of the gene or region is well known, this method also allows for accurate estimations of cell abundance from metagenomes. However, a disadvantage of this method is that the large majority of metagenomic reads will not cover the region of interest, and will contribute nothing to the analysis. Low-abundance OTUs will therefore be missed, as the region of interest is unlikely to have been sequenced.

Table 2.1: Selected examples of OTUs identified in a marine metagenome using the naïve method. These OTUs were identified in a single sample from the SO (sample 346; see Chapter 3). The sample was compared to the RefSeq database of full genomes using TBLASTX with an E-value maximum of 1.0×10^{-3} , i.e. only high-quality hits were included. Relative abundances were calculated using GAAS (Angly *et al.*, 2009).

Species	Relative Abundance (%)	Notes
<i>Encephalomyocarditis virus</i>	1.98	Human pathogen.
<i>Marek's disease virus type 1</i>	1.49	Chicken pathogen.
<i>Marek's disease virus type 2</i>	0.85	Chicken pathogen.
<i>Francisella philomiragia</i>	0.041	Human and animal pathogen.
<i>Agrobacterium vitis</i>	0.040	Plant and opportunistic human pathogen.
<i>Brucella suis</i>	0.011	Human and swine pathogen (causes brucellosis).
<i>Enterobacter</i> sp. 638	0.0085	Animal commensal/pathogen.
<i>Bordetella parapertussis</i>	0.0075	Mammalian pathogen (causes mild form of whooping cough).
<i>Neisseria meningitidis</i>	0.0074	Human pathogen.
<i>Yersinia pestis</i>	0.0060	Human/animal pathogen (causes bubonic plague).

The second method is to compare assembled or unassembled metagenomic reads to a reference database, using an algorithm such as BLAST, then use probabilistic methods to assign identifications and abundances with varying degrees of confidence. Most commonly, the reads are compared to a database of full genomes (e.g. Lauro *et al.*, 2011; Qin *et al.*, 2010). This method makes more efficient use of metagenomic data compared to the first, as any read can potentially yield a BLAST match and thus contribute to the identification of an OTU. However, interpretation of the results, and particularly calculation of abundances, is more complex. For example, the software tool Genome relative Abundance and Average Size (GAAS) makes use of BLAST match quality, number of matches and estimated genome size to estimate the relative abundances of OTUs in a sample (Angly *et al.*, 2009).

Such relative abundance estimates are confounded by the presence of multiple OTUs which can generate high-quality BLAST matches (“hits”) to a given read. Multiple high-quality hits to a single read are the norm, rather than the exception, in metagenomic studies for several reasons. A microbial assemblage will often include a number of closely-related OTUs (e.g. congeners) which share large sections of highly similar or identical genomic sequence. If several such OTUs are present in the reference database, a metagenomic read from one will yield high-quality BLAST hits to them all. Further, even distantly related OTUs are likely to share large regions of identity, and the selection of hit quality thresholds to discriminate between them (for example, a minimum bit score or maximum expectation value) is effectively arbitrary. Thus, while metagenomic studies using whole-genome comparisons almost always use such thresholds as the sole discriminators between OTUs, this method (hereafter the “naïve” method, after Ye and Doak (2009)) will almost inevitably result in the identification of OTUs which are not present in the assemblage, skewing the relative abundance estimates of those which are truly present.

This problem is compounded by a systematic overrepresentation within full genome databases of taxa of particular interest to humans, such as human and agricultural pathogens. Environmental OTUs are comparatively underrepresented. For example, Table 2.1 gives examples of terrestrial plant and animal pathogens, *a priori* unlikely to be truly present, which were identified in an open ocean metagenome with the naïve method.

One commonly used software tool to address this problem, Metagenome Analyzer (MEGAN), aggregates reads with hits to many OTUs to the most recent common ancestor of those OTUs, represented by a higher taxonomic rank e.g. family (Huson *et al.*, 2007). This approach increases the fidelity of the results, but comes at the cost of reduced taxonomic resolution. Particularly in marine assemblages where even fine genomic differences can represent distinct ecological functions (e.g. Brown *et al.*, 2012), a tool which reduces spurious identifications without compromising taxonomic resolution would clearly be valuable.

The maximum parsimony approach

Ye and Doak (2009) identified an analogous problem in the annotation of biochemical pathways in genomes and metagenomes. They noted that a common method is to annotate a pathway as present if a single protein within that pathway attracts at least one high-quality BLAST hit. However, because many proteins are shared by multiple pathways, and databases of orthologous genes are often incomplete, this method has resulted in many clearly spurious annotations, such as an ascorbic acid synthesis pathway in the human genome (humans require dietary vitamin C) and a mitochondrial pathway in *Escherichia coli* (annotated in the Kyoto Encyclopedia of Genes and Genomes (KEGG) PATHWAY database).

The authors developed a software tool, MINPATH, to combat this problem and increase the accuracy and fidelity of pathway annotations. MINPATH computes the smallest possible set of pathways (“maximum parsimony”) sufficient to explain a set of annotated proteins. As a simple example, if a genome is annotated with all the proteins that belong to pathway A, and one of those proteins also happens to belong to pathway B — that is, it is shared by both pathways — the naïve approach would annotate both pathways as present. However, the most parsimonious explanation is that pathway A is present, and B is not.

MINPATH was implemented by framing the construction of a maximum parsimony pathway set as an Integer Programming (IP) problem. IP is a subset of algorithms for solving Linear Programming (LP) problems, which seek to maximise the value of a linear function (the objective function) within a set of constraints. In this case, the objective function was maximised by decreasing the number of annotated biochemical pathways, while the constraint was that every high-quality protein annotation had to be represented at least once in the annotated pathways. Validation and testing of MINPATH showed it was successful in eliminating spuriously annotated pathways while retaining those genuinely present.

It was noted that this as this problem is isomorphic with that of spurious annotations in microbial metagenomes, the “maximum parsimony” method would also be likely to work in the latter domain. The aim of the project described in this chapter was thus to develop and test a software tool, MINSPEC, which would find the most parsimonious set of OTUs necessary to explain a set of observed BLAST hits generated by a metagenome, using the approach of Ye and Doak (2009) as a model.

Methods

Implementation of MINSPEC

A computational method to minimise false OTU identifications and increase the accuracy of OTU abundance estimates (MINSPEC) was developed and implemented in PERL¹. Following the approach of Ye and Doak (2009) to the parsimonious reconstruction of biochemical pathways (MINPATH), MINSPEC computes the smallest set of OTUs sufficient to explain a set of observed high-quality hits against RefSeq (or any other sequence database). The minimal set computation was framed as a IP problem and solved with GLPSOL (The GNU Linear Programming/MIP solver) (Free Software Foundation, Boston).

The objective function for the IP problem was constructed as follows (adapted from Ye and Doak, 2009):

$$\min \sum_{j=1}^s A_j$$

where s is the number of OTUs in the assemblage, and $A_j = 1$ if OTU j is in the assemblage, 0 if not. In other words, the objective function is satisfied by minimising the number of OTUs in the assemblage. The constraint function was constructed as follows (adapted from Ye and Doak, 2009):

$$\sum_{j=1}^s M_{ij}A_j \geq 1 \quad \forall i \in [1, n]$$

¹MINSPEC and the associated metagenomic simulation and validation scripts are open source and available at <https://github.com/wilcox/minspec>.

where $M_{ij} = 1$ if read i has a mapping (i.e. a high-quality BLAST hit) to OTU j , 0 if not, and $[1, n]$ is the set of all reads. In other words, the constraint function fails if any read does not have at least one of its high-quality BLAST hits represented in the assemblage.

This approach eliminates many of the spurious OTU identifications which result from reads with strong identity to more than one OTU. The “minimal OTU set” is liable to exclude some low-abundance OTUs, but gives more faithful abundance estimates and eliminates many false positives.

It was noted that in some special cases, it may be desirable to include an OTU in the assemblage even if it is not part of the minimal set, if that OTU generated a very large number of BLAST hits. An example of such a situation might be if the sample was known with certainty to contain a two very closely related OTUs at roughly equal abundance. In such a case, it would be expected that almost all metagenomic reads generated by each of these OTUs would also attract BLAST hits to the other, and MINSPEC would thus probably eliminate whichever happened to generate slightly fewer hits. To allow for this, an option was added such that MINSPEC will not eliminate OTUs to which a specified threshold number of reads attract high-quality hits.

Validation of MINSPEC

To establish the usefulness of MINSPEC, a validation method was devised to experimentally determine its error rates and efficacy (i.e. number of spurious OTUs identified and removed).

A set of simulated microbial OTUs was generated. To simulate genomic sequence identity between OTUs, each simulated OTU went through up to fifty rounds in which another OTU was selected at random and marked as having sequence identity with the first. This process was terminated with a 10% probability at each round, simulating an exponential curve of interrelatedness between OTUs. A random subset of the simulated OTUs were then selected to form a simulated microbial assemblage. Because of the previously established simulated sequence identity between OTUs, some OTUs in the assemblage would be marked as having identity to other OTUs both within the assemblage and outside of it.

A simulated metagenomic sampling was then performed. In each round, an OTU was selected at random. To produce a natural rank-abundance curve of OTU abundance within the assemblage, the probability that the selected OTU yielded a read was

$$\frac{1}{\ln(x) + 1}$$

where x is the OTU’s rank. Simulated BLAST matches to the OTU were generated for the read. These matches would include accurate high-quality “genuine” hits to the OTU that produced the read, as well as to other randomly selected OTUs both within and out of the assemblage which had been previously marked as having sequence identity to the “genuine” OTU.

To fully explore the limits and reliability of MINSPEC, the simulated metagenomic experiment described above was performed with all possible permutations of the following parameters: number of simulated OTUs [100; 1,000; 10,000; 50,000; 100,000]; size of simulated assemblage [1; 10; 100; 300; 500; 1,000; 10,000]; number of simulated metagenomic reads [10; 100; 1,000; 10,000; 100,000; 200,000; 500,000]. Each permutation was repeated five times, except for those where the size of the assemblage would exceed the number of OTUs simulated.

The resulting simulated BLAST outputs were processed with MINSPEC, and the false positive (percentage of OTUs not in the assemblage which nevertheless survived MINSPEC filtering) and false negative (percentage of OTUs present in the assemblage which were not present after MINSPEC filtering) rates calculated. Because a high false negative rate can arise from undersampling, a problem in metagenomic studies both real and simulated, an additional “false negative (MINSPEC)” metric was calculated, which excluded OTUs which were present in the assemblage but through random chance did not generate any reads, the equivalent of “unsampled rare taxa”. This rate thus represented only false negatives attributable to MINSPEC itself. Finally, as a measure of MINSPEC’s usefulness, the proportion of “false OTUs” — OTUs that generated BLAST matches but were not part of the assemblage — successfully removed by MINSPEC was calculated.

Results

Repeated simulated metagenomic experiments with a wide range of permutations of parameters showed that MINSPEC was reliable and able to substantially reduce the rate of false positive OTU identifications, although its effectiveness varied with the parameters of the assemblage and metagenomic experiment (Fig. 2.1).

Discussion

The false negative rate, or percentage of OTUs in the simulated assemblage which were absent from the BLAST results following MINSPEC processing, was generally high, ranging from ~20% under ideal conditions (a low assemblage / all OTUs ratio, and 500,000-read metagenomic sample) to ~90% in the worst case (a high assemblage / all OTUs ratio and a small metagenomic sample) (Fig. 2.1a). The assemblage / all OTUs ratio (hereafter referred to as “assemblage ratio”) indicates the proportion of simulated OTUs (“all OTUs”) that were chosen to form the simulated assemblage. A higher ratio means that any OTU is more likely on average to be part of the assemblage, and thus that any individual failure to detect a OTU is an error. This problem is mitigated with increasing the number of reads, as this makes it less likely that a given OTU would go unsampled. The extreme false negative rates, in some cases 100%, represent extreme simulated scenarios (e.g. an assemblage of 1 OTU drawn from a pool of 100,000), and thus do not reflect real metagenomic studies.

Because the majority of false negatives are attributable to undersampling and failure of OTUs to generate BLAST hits — properties the simulated metagenomic experiments share with real ones — a second metric, the false negative (MINSPEC) rate, was calculated (Fig. 2.1b). This is the proportion of OTUs in the assemblage that generated BLAST hits, but were incorrectly removed by MINSPEC. This rate thus represents error attributable only to MINSPEC. The false negative (MINSPEC) rate was generally low, ranging from ~0–1% for low assemblage ratios, to ~15–20% under high ratios. Surprisingly, increasing the number of reads only slightly decreased the rate, at both low and high assemblage ratios. This suggests MINSPEC is more affected by the degree of similarities between OTUs than by undersampling.

The false positive rate, or percentage of OTUs not in the assemblage which nevertheless generated high-quality BLAST matches that were not identified and removed by MINSPEC, was generally ~0–5% except for extremely small read sets and low assemblage ratios, where it reached as high as 60% (Fig. 2.1c). These results reinforce the value of larger read sets, and show that once a modest metagenome size is reached (~100,000 reads) very few false positives can be expected.

The proportion of false OTUs removed was calculated to measure MINSPEC’s efficacy in identifying and eliminating OTU which are not part of the sampled assemblage yet generate high-quality BLAST matches. This rate varied from 0–1 depending on the parameters of the assemblage (??). For simulations with a low assemblage ratio, the proportion was generally high (> 0.6), although there were simulated experiments with a low ratio where the proportion was low or zero. However, in all simulations with an assemblage ratio of 1, the proportion was 0, and the regression indicated a generally inverse relationship between the ratio and the proportion of false OTUs removed. This is likely because in assemblages with a higher assemblage ratio, there are fewer false OTUs to remove; in assemblages with a ratio of 1, there are none. The high proportion of false OTUs correctly identified in simulations with a low assemblage ratio is thus a good indication that MINSPEC is effective at identifying and removing false OTUs, especially as this proportion far exceeds the false positive and false negative (MINSPEC) rates for comparable experiments. As expected, increasing the number of reads improved MINSPEC’s accuracy.

Conclusions

Overall, the simulated experiments validated both the accuracy and usefulness of MINSPEC as a tool for reducing error in metagenomic studies. It is worth noting that the assemblage ratio is not an inherent property of an assemblage, although it is limited by the assemblage’s OTU richness. Rather,

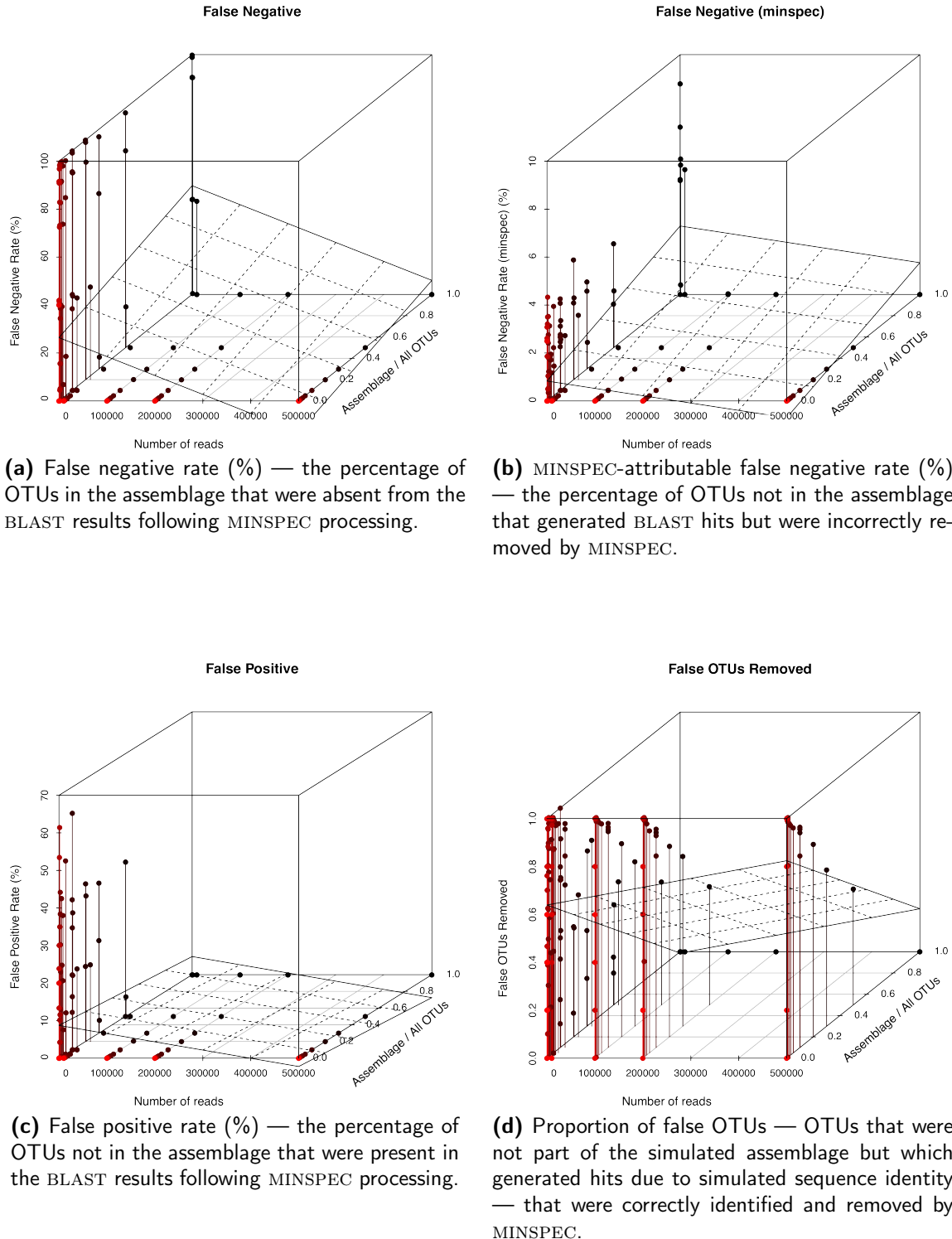


Figure 2.1: Results of repeated trials of MINSPEC on simulated metagenomic studies with multiple permutations of parameters (number of reads, number of simulated OTUs, size of simulated assemblage). The number of simulated OTUs and size of simulated assemblage are represented as a ratio on the z-axis ("assemblage / all OTUs"). Each permutation was repeated five times. A plane representing a linear regression has been overlaid on each plot to indicate the trend. Points have been tinted to aid the perception of depth; colour is not otherwise meaningful.

it can be decreased, and thus the accuracy of the metagenomic experiment improved, by performing BLAST searches against larger databases with finer taxonomic resolution. These results thus reinforce the value of both large read sets and comprehensive reference databases in obtaining high-quality metagenomic results.

At the time of writing, MINSPEC has been used in two published projects: Wilkins *et al.* (2012a) and Williams *et al.* (2012b).

Chapter 3

The Polar Front as a major biogeographic boundary in the Southern Ocean

Sections of this chapter have been previously published in Wilkins D., Lauro F. M., Williams T. J., De-Maere M. Z., Brown M. V., Hoffman J. M., Andrews-Pfannkoch C., McQuaid J. B., Riddle M. J., Rintoul S. R., and Cavicchioli R. (2012). Biogeographic partitioning of Southern Ocean microorganisms revealed by metagenomics. *Environmental Microbiology*.

Abstract

The Polar Front (PF) is a major oceanographic feature of the Southern Ocean (SO), dividing surface water masses with distinct physicochemical characteristics. To confirm and characterise the PF's role as a biogeographic barrier in the SO, sixteen metagenomic samples were collected on a latitudinal transect from waters near Hobart, Australia (44° S) to near the Mertz Glacier, Antarctica (67° S). The samples were shotgun sequenced, and the community composition and functional potential of the captured microorganisms were analysed. The SAR11 and SAR116 clades and the cyanobacterial genera *Prochlorococcus* and *Synechococcus* were strongly overrepresented north of the PF. Conversely, the Gammaproteobacterial Sulfur Oxidizer-EOSA-1 (GSO-EOSA-1) complex, the phyla Bacteroidetes and Verrucomicrobia and order Rhodobacterales were overrepresented in waters south of the PF. Functions enriched south of the PF included a range of transporters, sulphur reduction and histidine degradation to glutamate, while branched-chain amino acid transport, nucleic acid biosynthesis and methionine salvage were overrepresented north of the PF. The taxonomic and functional characteristics suggested a shift of primary production from cyanobacteria in the north to eukaryotic phytoplankton in the south, and reflected the different trophic states of the two regions. Overall, this study supported the PF as a defining biogeographic feature of the SO.

Introduction

The Southern Ocean (SO) consists of zones separated by circumpolar fronts, the locations of which vary with time and longitude (Whitworth, 1980; Orsi *et al.*, 1995; Sokolov and Rintoul, 2002). From north to south, the major fronts are the Subtropical Front (STF), the Subantarctic Front (SAF) and the Polar Front (PF) (Fig. 1.1). The SAF and PF are associated with the Antarctic Circumpolar Current (ACC), the world's largest ocean current and a defining oceanographic feature of the SO. Anthropogenic climate change may be driving the warming and freshening of the ACC (Böning *et al.*, 2008). It may also be shifting the ACC and associated fronts poleward; the mean path of the current has moved \sim 50 km south since the 1950s (Gille, 2002). If this migration continues, by 2100 it will have displaced a volume of water south of the ACC approximately equivalent to the Arctic Ocean (Fyfe and Saenko, 2005).

Climate change may also be affecting the zones separated by these fronts. The major zones of the SO are the Subantarctic Zone (SAZ), between the STF and SAF; the Polar Frontal Zone (PFZ), between the SAF and the PF; and the Antarctic Zone (AZ), between the PF and the Antarctic continent (Fig. 1.1). These zones have different physicochemical properties, such as density, salinity, temperature and nutrient concentrations (Sokolov and Rintoul, 2002), and the fronts represent stepwise transitions in these properties (Whitworth III and Nowlin Jr., 1987). However, as a consequence of climate change, waters on the poleward side of the ACC have become warmer and more saline, while those to the north cooler and fresher (Böning *et al.*, 2008).

The PF has been suggested to be a major biogeographic boundary in the distribution and abundance of both zooplankton (Chiba *et al.*, 2001; Hunt *et al.*, 2001; Esper and Zonneveld, 2002; Ward *et al.*, 2003) and bacterioplankton (Selje *et al.*, 2004; Abell and Bowman, 2005b; Giebel *et al.*, 2009; Weber and Deutsch, 2010). The effects of climate change on the physical oceanography of the SO may therefore have global ecological significance, particularly as the SO is a major site for sequestration of anthropogenic CO₂ (Sabine *et al.*, 2004; Mikaloff Fletcher *et al.*, 2006) through both physicochemical processes and the microbe-driven “biological pump” of CO₂ fixation (Thomalla *et al.*, 2011), potentially forming a feedback loop (Cox *et al.*, 2000). However, the microbial assemblages that inhabit the SO are generally poorly understood, and their diversity and functional capacity poorly characterised (reviewed in Murray and Grzymski, 2007). A community-level understanding is needed to predict the effects of a shifting ACC on the distribution, abundance and ecosystem functions of microorganisms.

Large scale metagenome surveys have not previously been performed in the SO. Compared to traditional environmental microbiological methods such as culture-based or DGGE surveys, metagenomic studies are able to offer both deeper (capture of sequence from rare taxa) and broader (larger sample sizes with greater statistical significance) data on the taxonomic makeup and functional capacities of marine microbial communities (e.g. Rusch *et al.*, 2007; Angly *et al.*, 2006; Dinsdale *et al.*, 2008). Metagenome sampling is also better suited to large-scale biogeographic studies, as it allows large numbers of samples to be taken across broad spatial and temporal scales with uniform sampling, storage and processing, compared to e.g. culture-based methods where technical replicability is more difficult.

This project is part of a metagenomic survey of the SO begun in the austral summer of 2006, based on the sampling design of the Global Ocean Sampling expedition (GOS) (Rusch *et al.*, 2007). The GOS sampling strategy involves size fractionation of plankton assemblages by passing seawater through a 20 µm prefilter then capturing planktonic biomass on sequential 3.0 µm, 0.8 µm and 0.1 µm filter membranes. As well as allowing deeper sequencing of metagenomes and thus better representation of low-abundance taxa (Rusch *et al.*, 2007), this approach allows comparison to other samples collected using the GOS methods (e.g. Brown *et al.*, 2012). This study will thus focus on the 0.1–20 µm fraction of the sampled microbial assemblages.

Methods

Sampling and metagenomic sequencing

Sampling¹ was conducted on board the RSV *Aurora Australis* during Australian Antarctic Division (AAD) cruise V3 Collaborative East Antarctic Marine Census (CEAMARC) / Climate of Antarctica and the Southern Ocean (CASO) from 13 December 2007–25 January 2008. This cruise occupied the SR3 latitudinal transect from Hobart, Australia (44° S) to the Mertz Glacier, Antarctica (67° S) within a longitudinal range of 140–150° E. Sixteen samples were obtained along almost the entire latitudinal range (Fig. 3.1).

A range of physicochemical data were recorded by integrated instruments on the RSV *Aurora Australis* including location, water column depth, water temperature, salinity, fluorescence and meteorological conditions (Table 3.1). These data were used to locate the PFZ based on a surface temperature gradient of ~1.35 °C across a distance of 45–65 km, placing the PF at approximately 59.70° S, consistent with previous descriptions (Moore *et al.*, 1999; Sokolov and Rintoul, 2002). Samples were accordingly grouped into “North” and “South” zones (Table 3.1). The North Zone (NZ) represents waters from the Subtropical, Subantarctic and PFZ regions, while the South Zone (SZ) represents the AZ.

¹Sampling was performed by Jeffrey M. Hoffman and Jeffrey B. McQuaid.

Table 3.1: Sampling time, location and physicochemical properties of samples used in this study. All data were retrieved from underway instruments aboard the RSV *Aurora Australis*.

Sample	Zone	Date	Latitude	Longitude	Water Column Depth (m)	Sample Depth (m)	Temperature (°C)	Salinity (PSU)	Fluorescence (µgL⁻¹)	Volume filtered (L)
346	North	20/12/2007	-59.31	142.59	4294	2	2.9	33.75	0.3	500
347	South	23/12/2007	-66.02	142.74	450	2	0.6	34.20	4.0	250
349	South	27/12/2007	-66.57	142.32	370	1.5	-1.3	34.40	2.3	250
351	South	28/12/2007	-66.56	143.43	823	1.5	-0.6	34.30	1.3	500
352	South	29/12/2007	-66.77	143.32	164	2.5	-0.8	34.30	3.1	500
353	South	30/12/2007	-67.05	144.68	180	2	-1.8	34.40	0.3	500
357	South	05/01/2008	-66.17	143.02	580	2	-0.4	34.15	2.5	500
358	South	09/01/2008	-64.30	150.03	3550	2	0	33.55	0.5	500
359	South	12/01/2008	-66.19	143.53	540	2	-0.2	34.21	2.5	500
360	South	13/01/2008	-66.58	141.02	316	2	-0.7	34.04	6.2	500
362	South	19/01/2008	-65.54	140.83	1064	2	0.7	32.20	0.5	500
363	North	22/01/2008	-60.00	141.31	4473	2	3.3	33.77	0.1	500
364	North	23/01/2008	-56.70	141.88	3693	2	4	33.70	0.5	500
366	North	24/01/2008	-52.02	144.14	3180	2	7.6	33.84	0.3	500
367	North	25/01/2008	-48.25	145.90	3490	2	11	34.43	0.2	500
368	North	26/01/2008	-44.72	145.78	3201	2	14.8	34.96	1.3	560

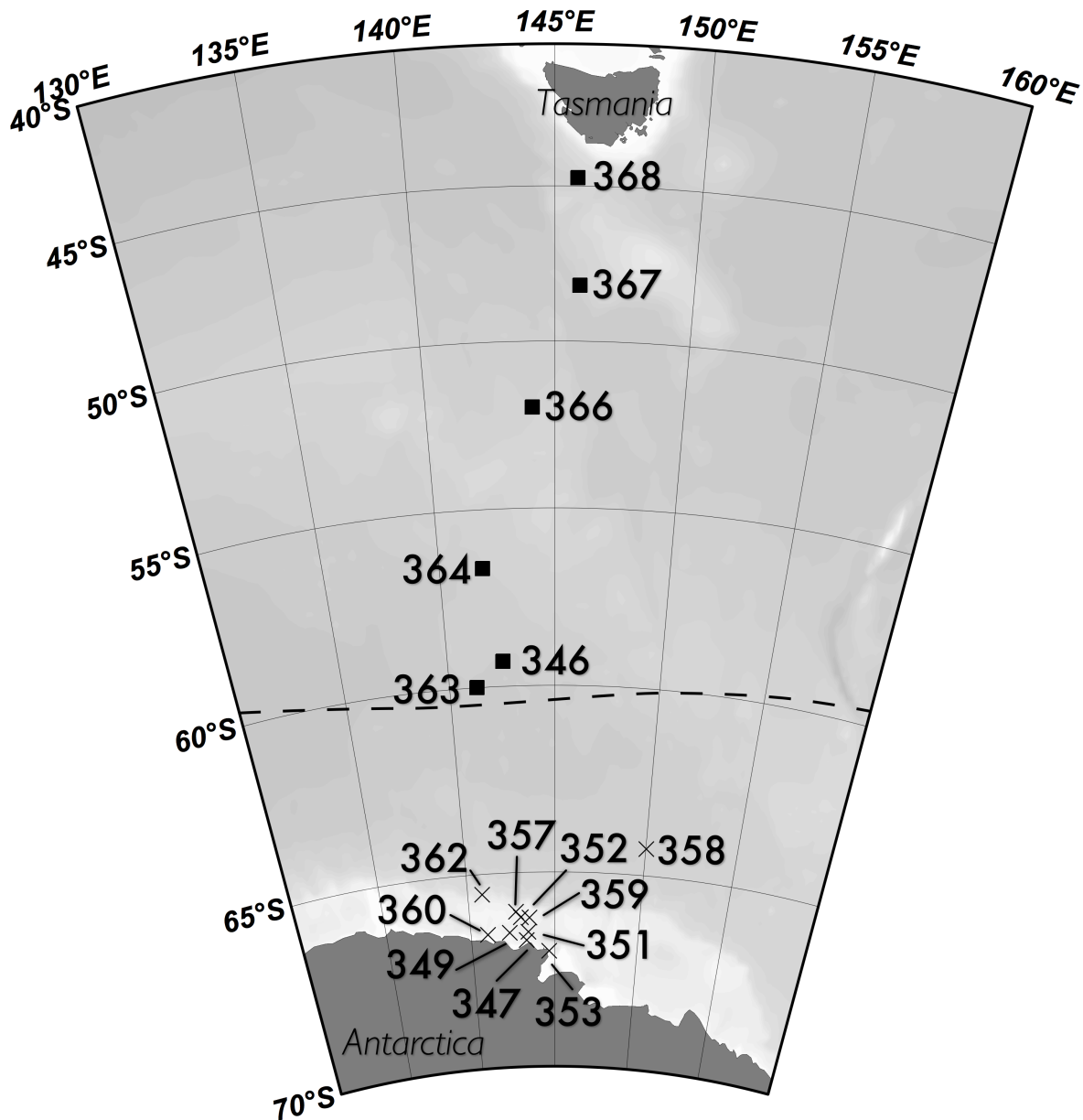


Figure 3.1: Sites of seawater samples used in this study. Squares indicate surface samples from the North Zone; crosses samples from the South Zone. The dashed line represents the Polar Front.

At each station, ~250–560 L of seawater was pumped from ~1.5–2.5 m below the sea surface into drums stored at ambient temperature on deck. Seawater samples were prefiltered through a 20 µm plankton net, then filtrate was captured on sequential 3.0 µm, 0.8 µm and 0.1 µm 293 mm polyethersulfone membrane filters (Pall, Port Washington, USA), and immediately stored at –20 °C (Rusch *et al.*, 2007; Ng *et al.*, 2010).

DNA extraction² was performed at the J. Craig Venter Institute (Rockville, USA) as described in Rusch *et al.* (2007). Pyrosequencing was performed on a GS20 FLX Titanium instrument (Roche, Branford, USA) also at the J. Craig Venter Institute as described in Lauro *et al.* (2011). Duplicate reads and reads with many pyrosequencing errors were removed as described in Lauro *et al.* (2011).

²DNA extraction was performed by Cynthia Andrews-Pfannkoch and others at the J. Craig Venter Institute.

Phylogenetic analysis of metagenomic data

BLAST comparison to RefSeq database

A subset of the RefSeq microbial (bacterial and archaeal) genome database (release 41, retrieved 31 May 2010 from <ftp://ftp.ncbi.nih.gov/refseq/release/>) was prepared by excluding sequences with the words “shotgun”, “contig”, “partial”, “end” or “part” in their headers (following Angly *et al.*, 2009). Because this database was not expected to contain representative genomes for every species present, Operational Taxonomic Units (OTUs) in this study are defined by the best species match to this database, and may for example represent congeners.

The metagenomic reads from each sample were compared against this database using TBLASTX, with default parameters except for: E-value threshold 1.0×10^{-3} , cost to open gap 11, cost to extend gap 1, masking of query sequence by SEG masking with lookup table only. The outputs of all TBLASTX searches against RefSeq were processed by MINSPEC, and hits not belonging to the minimal OTU sets were removed.

OTU abundances and variance between zones

The relative OTU abundances for each sample were determined using the PERL script Genome relative Abundance and Average Size (GAAS) (Angly *et al.*, 2009). Briefly, GAAS estimates the relative abundance of OTUs from the number and quality of BLAST matches (“hits”) to each OTU, taking into account differences in genome size. GAAS was run with the default settings. To normalise for reads which did not yield acceptable hits, the relative abundances for each sample were scaled by that sample’s effective BLAST hit rate. An OTU profile was generated for each sample by encoding the scaled relative abundance of each OTU from each size fraction as a separate variable.

To test the hypothesis that the oceanic zones harbour significantly different communities, Analysis of Similarities (ANOSIM) with 999 permutations was performed on a standardised, log-transformed Bray-Curtis resemblance matrix of OTU profiles. Similarity Percentages (SIMPER) analysis was performed to identify the contribution of individual OTUs to differences between the zones. All statistical procedures were performed in PRIMER 6 as described by Clarke and Warwick (2001).

Fragment recruitment to verify OTU identification

To confirm that identified OTUs were truly present, and not resulting from hits to small regions of genomic identity, plots of read recruitment and coverage to reference genomes were generated using R and PERL. Six samples, three from the SZ and three from the NZ, were randomly selected and their 0.1 μm fractions used as sources of recruited reads. As shotgun sequencing of a metagenome should be essentially random, it was predicted that these plots would show fairly even coverage of the reference genomes. Genomes where all recruited reads were concentrated in a few small regions would be likely candidates for OTUs which were not present, but shared a small genomic region with an OTU which was present.

Additional samples to test “polynya hypothesis”

Because many samples from the SZ were taken in the region of the Mertz Glacier polynya, an alternative hypothesis for any difference observed between the SZ and NZ would be that the difference represented the effect of the polynya, rather than the PF. A set of samples collected³ from waters south of the PF on different voyages and in a different longitudinal range were used to test this hypothesis. Sampling, DNA extraction and sequencing were performed as described above, although only the 0.1–0.8 μm size fraction was processed. The resulting metagenomic reads were compared to RefSeq and weighted relative abundances calculated with GAAS as described above.

Two ANOSIM tests were performed on the standardised and log-transformed Bray-Curtis resemblance matrices of the samples’ OTU abundance profiles and similarly prepared matrices representing only the 0.1 μm fractions of the SZ and NZ samples. In the first ANOSIM test (“polynya hypothesis”), all samples from the Mertz Glacier polynya region (i.e. all SZ samples apart from 358) were grouped

³Collection was performed by Ricardo Cavicchioli, Federico M. Lauro and Mark V. Brown. TODO who else was on these voyages?

Table 3.2: Dates and locations of additional samples used to falsify the hypothesis that the Mertz Glacier polynya was responsible for the observed biogeographic partitioning.

Sample	Date	AAD Voyage Number	Latitude	Longitude
388	20/10/2008	V1 2008–09	−63.8090	115.1613
398	22/10/2008	V1 2008–09	−64.8018	112.3730
390	30/10/2008	V1 2008–09	−64.8152	80.7204
392	13/12/2008	V2 2008–09	−64.1826	76.4537
393	15/12/2008	V2 2008–09	−55.2573	74.2531

together, while the samples from the open ocean were placed in a separate group. In the second test (“PF hypothesis”), the additional samples were grouped with all the SZ samples.

Functional analysis of metagenomic data

BLAST comparison to KEGG database

In order to identify functional differences between the zones, the set of metagenomic reads from each sample was compared against the Kyoto Encyclopedia of Genes and Genomes (KEGG) GENES database (retrieved 2 July 2010 from <ftp://ftp.genome.jp/pub/kegg/genes/fasta/genes.pep>) with BLASTX, with default parameters except for: maximum number of database sequence alignments 10; E-value threshold 1.0×10^{-3} ; gap opening penalty 11; gap extension penalty 1; masking of query sequence by SEG masking for lookup table only.

Analysis of functional potential

Genes identified by BLASTX were aggregated to KEGG ortholog groups according to the KEGG Orthology schema (<ftp://ftp.genome.jp/pub/kegg/genes/ko>, retrieved Mar 29 2011), and ortholog group abundances calculated for each sample. Following Coleman and Chisholm (2010), a read was considered a hit to a given ortholog group if the top three hits for that read (or all hits if fewer than three total hits) were to genes from the same ortholog group, and had bit scores > 40 . If the bit score difference between any two top hits was greater than 30, only the hits above this difference were considered.

Ortholog group counts were then used to calculate the abundance of KEGG modules. Because many ortholog groups are members of more than one module, the abundance a_m of each module m was calculated as

$$a_m = \sum_{K=1}^n \frac{C_K}{M_K}$$

where n is the number of ortholog groups K belonging to module m , C_K is the number of hits to ortholog group K , and M_K is the total number of modules to which K belongs. To account for differences in sequencing depth between samples, module abundances were scaled to 500,000 reads per sample. To test the hypothesis that the NZ and SZ harbour significantly different functional potential, one-way ANOSIM with 999 permutations was performed as above on a standardised, log-transformed Bray-Curtis distance resemblance matrix of the module and ortholog group profiles. A functional profile was generated for each sample by summing the scaled abundances of each module from all size fractions, and SIMPER performed as above to identify modules which contributed highly to the variation in functional potential between the two zones.

Taxonomic decomposition

To link modules with a high contribution to variance or otherwise of interest to specific OTUs (“taxonomic decomposition”), a script was written which decomposed each module to its constituent ortholog groups, then each ortholog group to each representative gene sequence in the KEGG database. Because each KEGG sequence is associated with a particular organism, this allowed the abundance

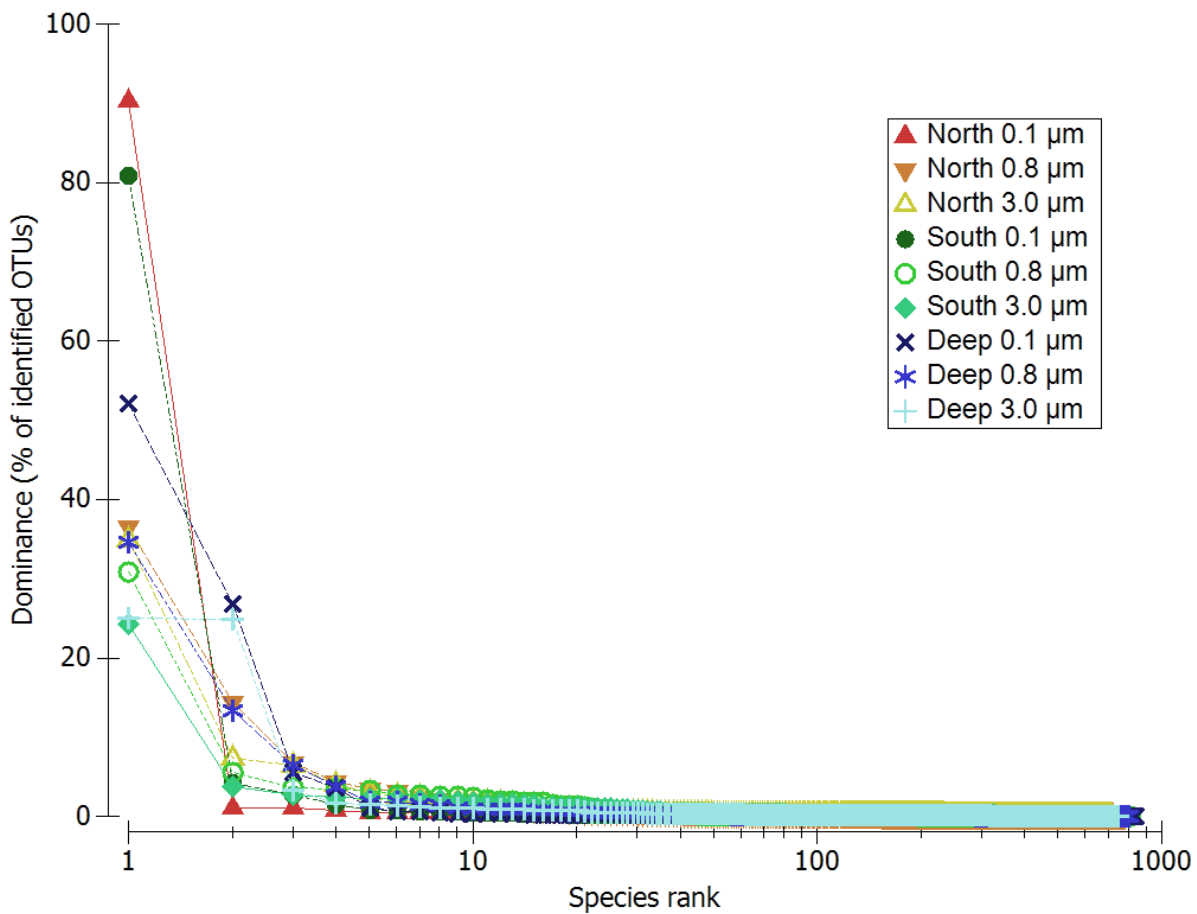


Figure 3.2: Rank-abundance curves for OTUs identified in each zone and size fraction. The dominance of a given OTU is its relative abundance as a percentage of all identified OTUs. The x-axis is scaled logarithmically. Generated using PRIMER 6.

of each module to be decomposed into the relative contribution from each of these organisms. This allowed functional contributions to be putatively assigned to genera which were not identified in our taxonomic analysis, as the database included gene sequences for organisms for which a full genome was not available. To aid interpretation of these results, the taxonomic decompositions for some modules were aggregated to higher taxonomic ranks, such as class or family.

Results

Metagenomic sequencing

6.6 Gbp of 454 sequence data representing microorganisms in the size range 0.1–3.0 μm was obtained from 16 samples. After removal of low-quality reads, 454 sequencing yielded 157,507–597,689 reads per sample (mean 354,399) of lengths ranging from 100 to 606 bp (mean 378).

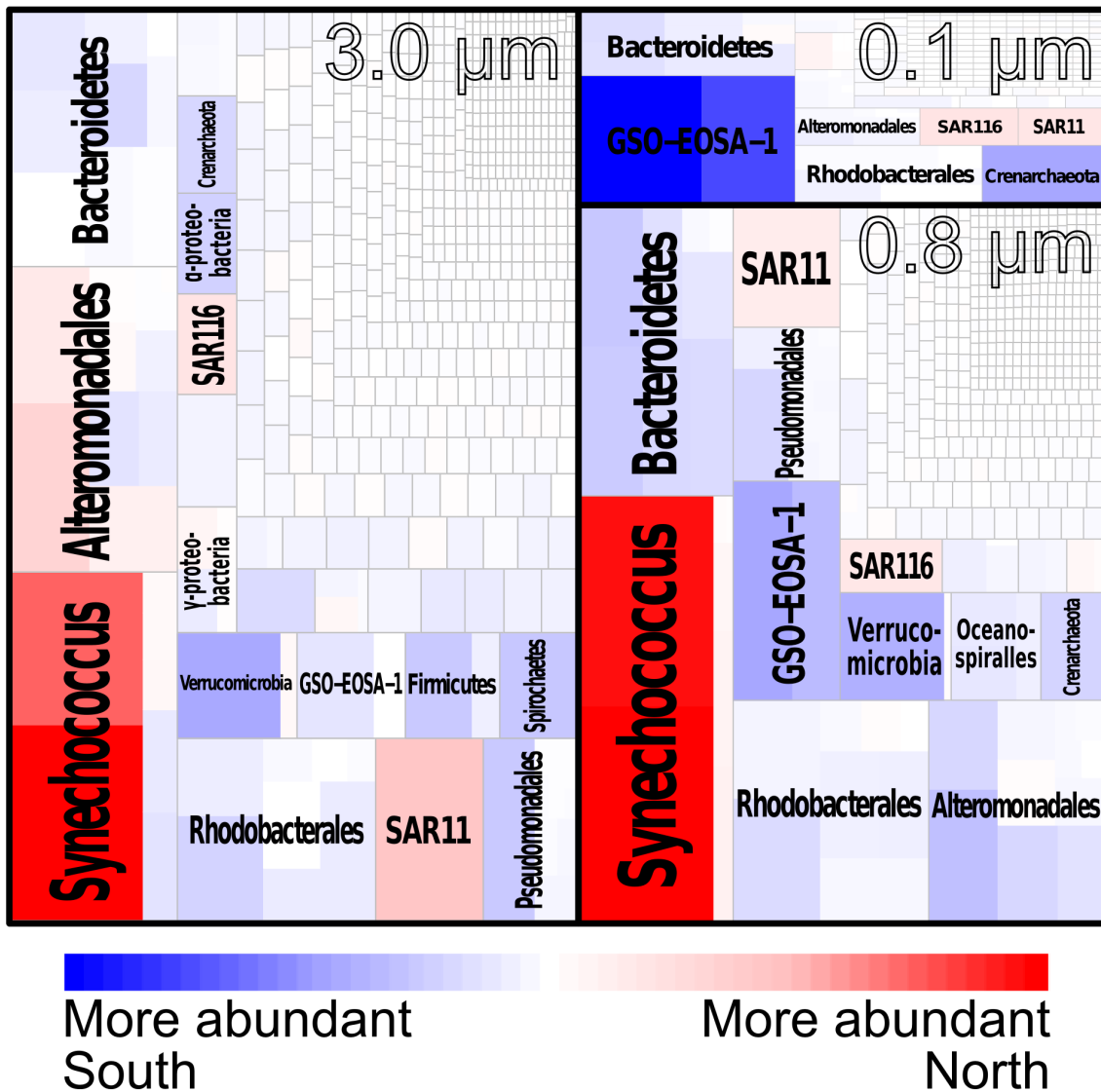
Phylogenetic analysis of metagenomic data

The proportion of reads in each sample which yielded hits to RefSeq ranged from 25–85% (mean 62%). The most abundant OTUs in each sample are given in Table 3.3 and a full list of OTU abundances in the supplementary material (PF-all-OTUs.csv). All samples and size fractions exhibited very low OTU evenness (Fig. 3.2).

Table 3.3: Relative abundances (as percentages) of the twenty most abundant OTUs identified in this study, in each zone and size fraction.

OTU	North			South		
	0.1 µm	0.8 µm	3.0 µm	0.1 µm	0.8 µm	3.0 µm
"Candidatus Pelagibacter ubique" HTCC1062	61.76	25.00	23.87	58.85	22.40	17.61
<i>Nitrosopumilus maritimus</i> SCM1	0.01996	0.01438	0.009508	1.076	1.309	1.210
"Candidatus Ruthia magnifica" str. Cm (<i>Calyptogena magnifica</i>)	0.6699	0.6458	0.5484	2.987	2.616	1.025
<i>Roseobacter</i> sp. OCh 114	0.3125	2.932	1.588	0.4477	3.994	2.657
<i>Synechococcus</i> sp. CC9902	0.1081	9.837	4.973	0.007484	0.004156	0.09733
<i>Silicibacter pomeroyi</i> DSS-3	0.2578	2.286	1.154	0.3070	2.505	1.576
<i>Gramella forsetii</i> strain KT0803	0.2412	1.210	1.755	0.4993	2.347	1.890
"Candidatus Vesicomysoscius okutanii" strain HA	0.4634	0.4642	0.2078	1.970	1.807	0.2174
<i>Robiginitalea biformalis</i> strain HTCC2501	0.2751	1.099	1.297	0.4722	1.878	1.405
<i>Flavobacterium psychrophilum</i> strain JIP02/86	0.1718	0.8409	1.224	0.4316	1.960	1.598
<i>Synechococcus</i> sp. CC9311	0.03014	4.624	4.409	0.007221	0.002778	0.02764
"Candidatus Puniceispirillum marinum" IMCC1322	0.6444	2.077	1.267	0.3586	1.377	0.7109
<i>Silicibacter</i> sp. TM1040	0.2274	1.652	0.8738	0.2709	1.803	1.233
<i>Jannaschia</i> sp. DFL-12	0.1776	1.378	0.7350	0.2443	1.692	0.8009
<i>Zunongwangia profunda</i> strain SM-A87	0.1522	0.7487	1.059	0.2968	1.410	1.204
<i>Colwellia</i> sp. 34H	0.02345	0.3636	2.736	0.05207	0.5140	1.041
<i>Coraliomargarita akajimensis</i> strain DSM 45221	0.03698	0.07573	0.1197	0.1154	1.543	1.680
<i>Jannaschia</i> sp. CCS1	0.1173	0.9344	0.4784	0.1711	1.230	0.8239
<i>Pseudoalteromonas atlantica</i> strain T6c	0.01251	0.4772	1.993	0.02270	0.4089	1.132
<i>Saccharophagus degradans</i> strain 2-40	0.06532	0.4325	0.5429	0.1289	1.072	0.8663
<i>Flavobacterium johnsoniae</i> strain UW101	0.08822	0.4220	0.6141	0.2034	0.9389	0.8578
<i>Capnocytophaga ochracea</i> strain DSM 7271	0.1143	0.4830	0.5399	0.2314	0.8815	0.6814
<i>Marinomonas</i> sp. MWYL1	0.03777	0.2529	0.3026	0.1514	1.30	0.7006
<i>Cellvibrio japonicus</i> strain Ueda107	0.05884	0.3080	0.3231	0.1155	0.9917	0.4713
<i>Marinobacter hydrocarbonoclasticus</i> VT8	0.04093	0.2889	0.3883	0.08418	0.7195	0.3848
<i>Pseudoalteromonas haloplanktis</i> strain TAC125	0.01389	0.2505	0.8896	0.03427	0.3561	0.6530
<i>Terediniibacter turnerae</i> strain T7901	0.05665	0.3051	0.3081	0.1138	0.9174	0.5127
<i>Acinetobacter baumannii</i> strain SDF	0.004886	0.007187	0.4073	0.006260	0.04218	1.459

ANOSIM analysis showed that the zones harbor significantly different microbial communities ($R = 0.451$, $p = 0.004$). SIMPER was performed in order to identify the contribution of individual OTUs to the difference between the NZ and SZ. The results for the highest contributors are provided in Table 3.4, and are graphically summarised for all OTUs in Fig. 3.3.



The SIMPER analysis found that no single OTU contributed more than 2.9% of variance and 74% of variance was contributed by OTUs with a contribution less than 1%. There was also a large difference in the contribution to variance of the three size fractions, with approximately 52% of all variance

Table 3.4: The thirty OTUs with the highest contributions to the difference between the NZ and SZ. Abundances are zonal averages and have been standardised and log-transformed. As each OTU on each size fraction was encoded as a separate variable in the SIMPER analysis, the size fraction is given after each OTU name.

OTU	Abundance South	Abundance North	Contribution to variance (%)
Synechococcus sp. CC9311 0.8 µm	0.00	1.08	2.88
Synechococcus sp. CC9902 0.8 µm	0.00	1.04	2.81
Synechococcus sp. CC9311 3.0 µm	0.01	0.98	2.59
Synechococcus sp. CC9902 3.0 µm	0.04	0.76	2.03
"Candidatus Pelagibacter ubique" HTCC1062 3.0 µm	1.97	2.40	1.97
"Candidatus Ruthia magnifica" str. Cm (<i>Calyptogena magnifica</i>) 0.1 µm	0.82	0.25	1.57
"Candidatus Ruthia magnifica" str. Cm (<i>Calyptogena magnifica</i>) 0.8 µm	0.34	0.66	1.32
"Candidatus Pelagibacter ubique" HTCC1062 0.8 µm	0.74	0.25	1.32
"Candidatus Vesicomyosocius okutanii" strain HA 0.1 µm	2.32	2.48	1.32
Coraliomargarita akajimensis strain DSM 45221 0.8 µm	0.62	0.18	1.20
Coraliomargarita akajimensis strain DSM 45221 3.0 µm	0.48	0.04	1.13
Roseobacter sp. OCh 114 0.8 µm	0.49	0.06	1.10
Pseudoalteromonas atlantica strain T6c 3.0 µm	1.01	0.81	1.08
"Candidatus Vesicomyosocius okutanii" strain HA 0.8 µm	0.38	0.54	1.08
Acinetobacter baumannii strain SDF 3.0 µm	0.57	0.19	1.04
Acinetobacter baumannii strain SDF 3.0 µm	0.45	0.18	0.95
Gramella forsetii strain KT0803 0.8 µm	0.72	0.43	0.94
Marinomonas sp. MWYL1 0.8 µm	0.46	0.11	0.92
Roseobacter sp. OCh 114 3.0 µm	0.76	0.54	0.91
Flavobacterium psychrophilum strain JIP02/86 0.8 µm	0.63	0.32	0.89
Silicibacter pomeroyi DSS-3 0.8 µm	0.75	0.69	0.86
Brachyspira hyodysenteriae strain WA1 3.0 µm	0.47	0.19	0.84
"Candidatus Ruthia magnifica" str. Cm (<i>Calyptogena magnifica</i>) 3.0 µm	0.34	0.21	0.82
Pseudoalteromonas haloplanktis strain TACI25 3.0 µm	0.22	0.33	0.77
Robiginitalea biformata strain HTCC2501 0.8 µm	0.61	0.40	0.74
Nitrosopumilus maritimus SCM1 0.1 µm	0.27	0.01	0.72
Gramella forsetii strain KT0803 3.0 µm	0.59	0.59	0.71
Lysinibacillus sphaericus strain C3-41 3.0 µm	0.29	0.02	0.71
Nitrosopumilus maritimus SCM1 0.8 µm	0.25	0.01	0.70
Silicibacter sp. TM1040 0.8 µm	0.59	0.55	0.69

contributed by OTUs from the 3.0 μm fraction, 37% by the 0.8 μm fraction, and 9% by the 0.1 μm fraction. Notably, OTUs within several taxonomic groups that had high contribution to variance covaried in their relative representation in the NZ and SZ. For example, Bacteroidetes and GSO-EOSA-1 representatives were on average more abundant in the SZ; while *Prochlorococcus* and *Synechococcus* species, SAR11 and SAR116 were on average more abundant in the NZ (Fig. 3.3). Some groups, such as the Alteromonadales, had variable relative representation depending on size fraction.

Fragment recruitment to verify OTU identification

As predicted, read recruitment to reference genomes produced fairly even coverage, especially in the high-abundance OTUs. This indicates that OTU identification was accurate and unlikely to be confounded by small regions of genomic identity. Fig. 3.5 gives examples of read recruitment plots to three high-abundance and three low-abundance OTUs.

Additional samples to test alternative “polynya hypothesis”

The ANOSIM analysis strongly supported the “PF hypothesis” ($R = 0.435$, $p = 0.002$), i.e. that the PF was primarily responsible for the difference observed between the NZ and SZ, over the “polynya hypothesis” ($R = 0.29$, $p = 0.005$) that the influence of the Mertz Glacier polynya was responsible. This also provides evidence that the PF effect is robust over a longitudinal range and over time.

Functional analysis of metagenomic data

ANOSIM analysis of the samples’ KEGG ortholog group and module profiles revealed that the zones had significantly different functional potential (ortholog group: $R = 0.642$, $p = 0.001$; module: $R = 0.871$, $p = 0.001$). SIMPER was performed on the profiles in order to identify the specific functional differences between the zones. The highest-contributing modules are given in Table 3.5, and a complete list in the supplementary material (PF-modules-SIMPER.csv). The highest-contributing ortholog groups are given in Table 3.6, and a complete list in the supplementary material (PF-ortholog-groups-SIMPER.csv). No single ortholog group or module contributed more than 2.2% of the variance, indicating a complex and diverse pattern of functional differences. There was a strong trend for ortholog groups and modules with higher contributions to variance to be overrepresented in the NZ in the 3.0 μm fraction but the SZ in the smaller fractions, indicating that the functional diversity of each zone was strongly segregated by size fraction.

Discussion

Taxonomic groups differentiating the zones

GSO-EOSA-1

The Gammaproteobacterial Sulfur Oxidizer-EOSA-1 (GSO-EOSA-1) cluster, represented in RefSeq by the OTUs “*Candidatus Vesicomyosocius okutanii*” strain HA and “*Candidatus Ruthia magnifica*” strain Cm. (*Calyptogena magnifica*) (Walsh *et al.*, 2009), made a large contribution to variance between the NZ and SZ, with higher abundance in the SZ: relative abundances of GSO-EOSA-1 in the SZ were 5.2%, 3.4% and 0.25% in the 0.1, 0.8 and 3.0 μm size fractions respectively, compared to 1.1%, 0.84% and 0.30% in the NZ (Table 3.3). The contribution to variance of this group was highest in the 0.1 μm size fraction, followed by 0.8 μm and 3.0 μm (Table 3.4). This pattern most likely represents a small cell size and lack of association with particulate matter.

“*Ca. R. magnifica*” and “*Ca. V. okutanii*” are chemoautotrophic endosymbionts of deep-sea bivalves (Kuwahara *et al.*, 2007; Newton *et al.*, 2007) and are thus unlikely to be present in open ocean surface waters. However, GSO-EOSA-1 representative ARCTIC96BD-19 has recently been reported at high abundance in Antarctic coastal waters (Ghilione and Murray, 2011; Grzymski *et al.*, 2012). The majority of 16S rRNA genes from this metagenome with best BLASTN hits to “*Ca. R. magnifica*” and “*Ca. V. okutanii*” clustered with ARTIC96BD-19 in a neighbour-joining phylogenetic tree (Fig. 3.4), indicating this is the dominant GSO-EOSA-1 representative.

Table 3.5: The thirty KEGG modules with the highest contributions to the difference between the NZ and SZ. Abundances are zonal averages and have been standardised and log-transformed.

KEGG module	Abundance South	Abundance North	Contribution to variance (%)
Photosystem II	0.42	0.57	2.21
Complex I (NADH dehydrogenase), NADH dehydrogenase I/diaphorase subunit of the bidirectional hydrogenase	0.01	0.24	1.80
Photosystem I	0.43	0.34	1.70
Pyrimidine deoxyribonucleotide biosynthesis, CDP/CTP → dCDP/dCTP,dTDP/dTTP	0.51	0.66	1.16
Histidine degradation, histidine → N-formiminoglutamate → glutamate	0.42	0.31	1.14
Methionine salvage pathway	0.29	0.43	1.14
sn-Glycerol 3-phosphate transport system	0.29	0.16	1.11
Complex I (NADH dehydrogenase), NADH dehydrogenase I	1.08	1.05	1.06
Branched-chain amino acid transport system	0.79	0.83	0.96
Dipeptide transport system	0.14	0.02	0.95
Adenine nucleotide biosynthesis, IMP → ADP/dADP,ATP/dATP	0.62	0.74	0.95
Glycine betaine/proline transport system	0.66	0.56	0.94
Sulfur reduction, sulfate → H ₂ S	0.54	0.44	0.91
Simple sugar transport system	0.46	0.39	0.90
Peptides/nickel transport system	0.99	0.98	0.89
Ribosome, eukaryotes	0.26	0.27	0.89
Multiple sugar transport system	0.55	0.55	0.86
Type II general secretion system	0.21	0.21	0.82
Sulfonate/nitrate/taurine transport system	0.45	0.37	0.82
Guanine nucleotide biosynthesis, IMP → GDP/dGDP,GTP/dGTP	0.72	0.82	0.81
RNA polymerase II, eukaryotes	0.11	0.20	0.76
Histidine biosynthesis, PRPP → histidine	0.94	0.86	0.76
Putrescine transport system	0.18	0.09	0.72
Leucine biosynthesis, pyruvate → 2-oxoisovalerate → leucine	1.29	1.37	0.71
C5 isoprenoid biosynthesis, non-mevalonate pathway	0.70	0.77	0.71
Leucine degradation, leucine → acetoacetate + acetyl-CoA	0.64	0.59	0.71
Thiamine transport system	0.13	0.05	0.69
Spliceosome, 35S U5-snRNP	0.18	0.20	0.68
Cytochrome b6f complex	0.14	0.12	0.67
Menaquinone biosynthesis, chorismate → menaquinone	0.25	0.27	0.66

Table 3.6: The thirty KEGG ortholog groups with the highest contribution to the difference between the NZ and SZ. Abundances are zonal averages and have been standardised and log-transformed. As each ortholog group on each size fraction was encoded as a separate variable in the SIMPER analysis, the size fraction is given after each ortholog group name.

KEGG ortholog group	Abundance South	Abundance North	Contribution to variance (%)
Hypothetical protein 3.0 μm	0.11	0.24	0.26
Hypothetical protein 0.8 μm	0.68	0.57	0.24
Ribonucleoside-diphosphate reductase alpha chain [EC:1.17.4.1] 0.8 μm	0.17	0.24	0.15
DNA polymerase III subunit alpha [EC:2.7.7.7] 0.8 μm	0.25	0.19	0.14
Hypothetical protein 0.1 μm	0.26	0.24	0.12
Proline dehydrogenase / delta 1-pyrroline-5-carboxylate 0.8 μm	0.10	0.04	0.12
Aminomethyltransferase [EC:2.1.2.10] 0.8 μm	0.25	0.19	0.12
Ribonucleoside-diphosphate reductase alpha chain [EC:1.17.4.1] 3.0 μm	0.02	0.08	0.12
Sarcosine oxidase, subunit alpha [EC:1.5.3.1] 0.8 μm	0.22	0.17	0.12
Integrator complex subunit 6 3.0 μm	0.07	0.05	0.11
Multicomponent $\text{Na}^+:\text{H}^+$ antiporter subunit D 0.8 μm	0.11	0.05	0.11
Glutamine synthetase [EC:6.3.1.2] 0.8 μm	0.24	0.19	0.11
Pyruvate dehydrogenase E1 component [EC:1.2.4.1] 0.8 μm	0.15	0.10	0.11
Cobaltochelatase CobN [EC:6.6.1.2] 0.8 μm	0.11	0.06	0.11
Formate dehydrogenase, alpha subunit [EC:1.2.1.2] 0.8 μm	0.15	0.10	0.11
DNA-directed RNA polymerase subunit beta [EC:2.7.7.6] 3.0 μm	0.03	0.08	0.11
Glutamate synthase (NADPH/NADH) large chain [EC:1.4.1.13 1.4.1.14] 0.8 μm	0.25	0.22	0.11
Dimethylglycine dehydrogenase [EC:1.5.99.2] 0.8 μm	0.17	0.14	0.11
Flagellin 0.8 μm	0.06	0.10	0.10
DNA-directed RNA polymerase subunit beta [EC:2.7.7.6] 3.0 μm^a	0.03	0.08	0.10
Photosystem II PsbA protein 0.8 μm	0.01	0.06	0.09
Aldehyde dehydrogenase (NAD+) [EC:1.2.1.3] 0.8 μm	0.17	0.13	0.09
Glutamate synthase (NADPH/NADH) large chain [EC:1.4.1.13 1.4.1.14] 3.0 μm	0.02	0.07	0.09
Thymidylate synthase (FAD) [EC:2.1.1.148] 0.8 μm	0.02	0.06	0.09
Topoisomerase IV subunit A [EC:5.99.1.-] 0.8 μm	0.11	0.07	0.09
DNA mismatch repair protein MutS 0.8 μm	0.13	0.08	0.09
Glutamate dehydrogenase [EC:1.4.1.2] 0.8 μm	0.07	0.03	0.09
DNA polymerase I [EC:2.7.7.7] 0.1 μm	0.12	0.11	0.09
GTP-binding protein 0.8 μm	0.26	0.21	0.09
GTP-binding protein 3.0 μm	0.03	0.07	0.09



Figure 3.4: Neighbour-joining tree of GSO-EOSA-1-like 16S rRNA gene sequences from the metagenomes in this study. Sequences labeled in black text are reads from the metagenomes. Red labels are 16S rRNA gene sequences from Gammaproteobacterial Sulfur Oxidizers (GSO) and other Gammaproteobacteria. The tree was constructed using ARB (Ludwig et al., 2004).

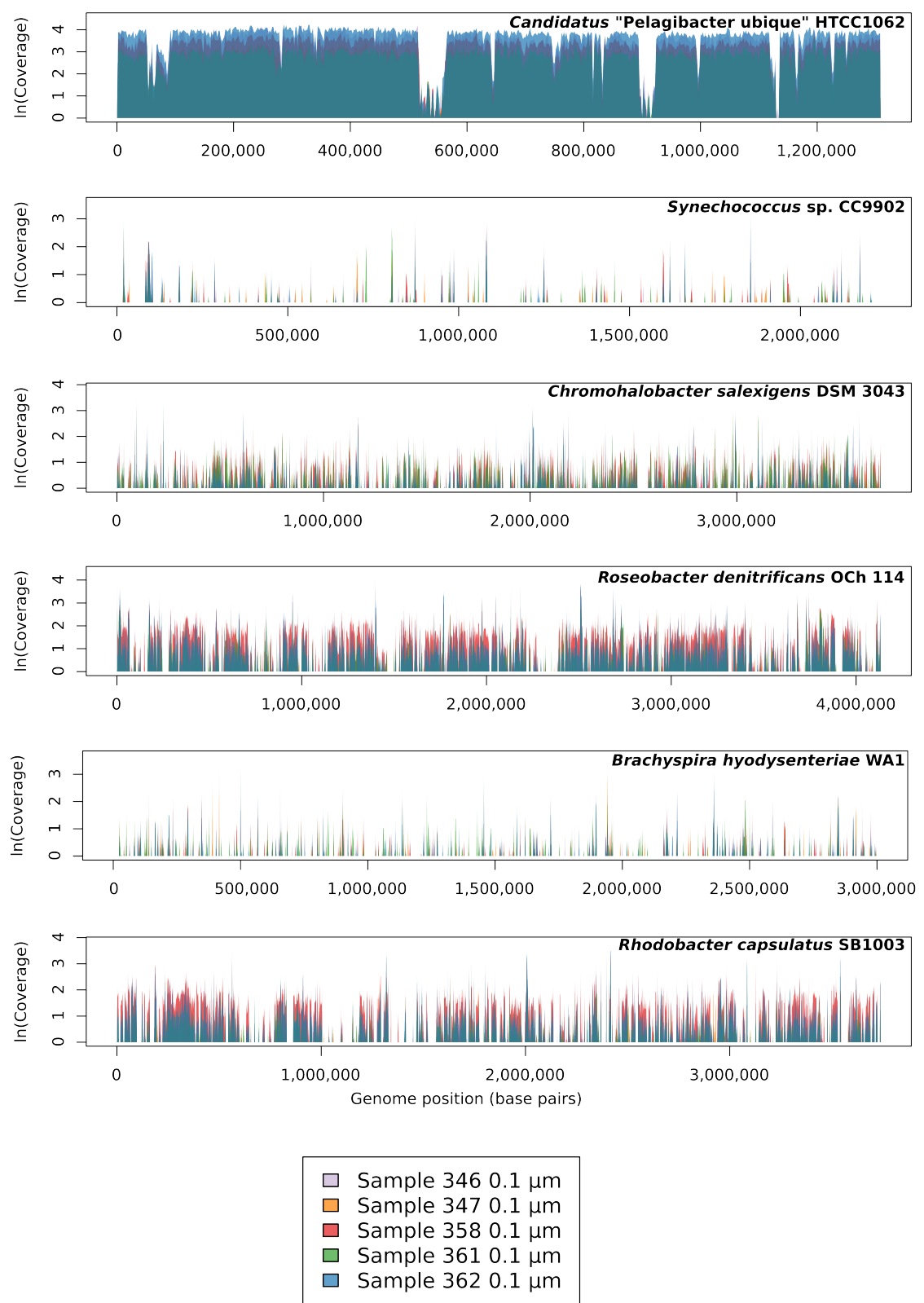


Figure 3.5: Examples of read recruitment (fragment recruitment) plots of metagenomic reads to reference genomes. The even distribution of recruitment sites across the genome suggests that OTUs identifications are relatively accurate; an OTU identification resulting from a small region of genomic identity would generate a plot with read recruitment concentrated in small islands.

Single-cell genomic analysis of ARCTIC96BD-19 from global mesopelagic waters indicates the lineage is probably mixotrophic, able to couple carbon fixation to oxidation of reduced sulphur compounds as well as assimilate organic carbon (Swan *et al.*, 2011). GSO-EOSA-1 cytochrome C oxidase (CoxII) has been identified in a winter metaproteome of Antarctic Peninsula coastal waters, suggesting the capacity for aerobic respiration (Williams *et al.*, 2012a). Taken together, this evidence suggests the GSO-EOSA-1 representative in Antarctic coastal waters is a versatile chemolithoautotroph capable of aerobic respiration.

It has been proposed that during the winter months, chemolithoautotrophy is dominant over photoautotrophy as the major carbon fixation process in AZ waters due to the lack of available light, both from seasonal darkness and ice shading (Grzymski *et al.*, 2012). The high relative abundance of GSO-EOSA-1 in SZ compared to NZ waters may therefore represent the remnants of an annual winter increase in population in the marginal ice zone which does not occur in the open ocean.

Ammonia-oxidizing Crenarchaeota

Nitrosopumilus maritimus SCM1 and *Cenarchaeum symbiosum* are chemolithoautotrophic, nitrifying members of the Marine Group I Crenarchaeota (MGI) (Preston *et al.*, 1996; Walker *et al.*, 2010) and are the only representatives in the reference database of the Ammonia-Oxidizing Archaea (AOA). The contribution of OTUs of *C. symbiosum* to the AOA signature was low. As *C. symbiosum* is a sponge symbiont (Preston *et al.*, 1996) and given the poor representation of AOA in RefSeq, it is likely this OTU has attracted sequences originating from planktonic AOA and *C. symbiosum* itself is not present. AOA were moderate contributors to variance between the NZ and SZ, and were overrepresented in the SZ in all size fractions (Fig. 3.3). As with the GSO-EOSA-1 cluster, MGI have been proposed to be abundant chemolithoautotrophs and therefore major drivers of winter carbon fixation in Antarctic coastal waters (Grzymski *et al.*, 2012; Williams *et al.*, 2012a).

Sample 353 had a particularly high relative abundance of *N. maritimus* OTUs (7.5% of the 0.1 µm fraction; 0.8 µm: 11%; 3.0 µm: 12%). This sample was taken closer to the Antarctic continent (3.7 km) than any other, in relatively shallow (180 m) waters 17.6 km from the Mertz Glacier. The high abundance of ammonia oxidizers may reflect an input of ammonia from terrestrial sources (e.g. penguin guano), or resuspension of benthic sediments in which MGI are abundant (Bowman and McCuaig, 2003) by near-shore turbulence and iceberg scouring. Breakdown of water column stratification has been previously suggested as a cause of increased AOA abundance in Antarctic coastal surface waters (Kalanetra *et al.*, 2009).

Cyanobacteria

OTUs of the cyanobacterial genera *Prochlorococcus* and *Synechococcus* were overrepresented in the NZ in all size fractions (Fig. 3.3). The mean relative abundance of cyanobacteria in samples 367 and 368, the two northernmost samples, was strikingly higher than the mean abundance across all other samples in the NZ. *Synechococcus* sp. CC9902 alone composed greater than 22% of the 0.8 µm fraction in these samples, consistent with *Synechococcus* species' average cell diameter of approximately 0.9 µm. The high abundance of both cyanobacterial genera on the 3.0 µm fraction has previously been reported (Lauro *et al.*, 2011) and may be attributable to aggregation (Lomas and Moran, 2011).

Samples 367 and 368 were separated from the other samples north of the PF by the STF. While the STF was not a significant boundary on the assemblage level, it may mark a significant biogeographic boundary for these cyanobacteria. *Synechococcus* and *Prochlorococcus* together represent a large proportion of both phytoplankton abundance and carbon fixation in temperate and tropical waters, in many regions contributing more than half of total primary production (Liu *et al.*, 1997, 1998; André *et al.*, 1999). The role of the STF in determining the latitudinal range of *Synechococcus* and *Prochlorococcus* is therefore important, as it will affect models of ocean productivity under changing climactic conditions, and warrants further investigation. Despite the high abundance of cyanobacteria north of the

STF, they were also a significant feature of the SAZ; for example, *Synechococcus* sp. CC9902 composed 3–5% of the 0.8 µm fraction in SAZ samples.

These results extend the latitudinal distribution of both *Prochlorococcus* and *Synechococcus* to include presence at very low abundance as far south as the Antarctic coast. *Prochlorococcus* have been reported to be restricted to tropical and subtropical waters within 40° of latitude (Partensky *et al.*, 1999), and to be a negligible (Ghiglione and Murray, 2011) or undetectable (Grzynski *et al.*, 2012) component of marine microorganisms in Antarctic waters. However, these findings are consistent with findings of a logarithmic relationship of cyanobacterial numbers with temperature, where cyanobacteria were found at concentrations of 10³–10⁴ cells per litre even in the coldest waters, approximately four orders of magnitude less than in waters around Tasmania (Marchant *et al.*, 1987). Cyanophage proteins have also been detected in a metaproteomic analysis of Antarctic Peninsula coastal surface waters (Williams *et al.*, 2012a).

SAR11 and SAR116 clades

“*Ca. P. ubique*” HTCC1062 is a good representative of total SAR11 abundance in this study, as it is a member of the SAR11 phylotype which is most abundant in SO waters (Brown *et al.*, 2012). “*Ca. P. ubique*” HTCC1062 was the most abundant OTU across all samples and fractions (NZ average: 62%, 25% and 24% of the 0.1 µm, 0.8 µm and 3.0 µm fractions respectively; SZ: 59%, 22% and 18%) and one of the most significant contributors to variance between the NZ and SZ. The high abundance of SAR11 in the 0.1 µm fraction is consistent with the small size of SAR11 cells (Rappé *et al.*, 2002). The higher representation in the NZ may reflect the competitiveness of SAR11 members in regions with low Dissolved Organic Carbon (DOC) concentrations due to low primary productivity (Giovannoni *et al.*, 2005; Alonso and Pernthaler, 2006), such as the High Nutrient, Low Chlorophyll (HNLC) SAZ. Overall, these findings are consistent with reports that SAR11 is ubiquitous in the world’s oceans (Mary *et al.*, 2006; Carlson *et al.*, 2009) and more abundant north of the ACC (Giebel *et al.*, 2009).

OTUs of “*Ca. P. marinum*” from the SAR116 clade were a moderate contributor to variance between the NZ and SZ with higher abundance in the NZ (Fig. 3.3). A genomic analysis reported “*Ca. P. marinum*” IMCC1322 to be a metabolic generalist with genes for aerobic CO fixation, C1 metabolism and a “*Ca. P. ubique*”-like dimethylsulfoniopropionate (DMSP) demethylase, suggesting SAR116 and SAR11 occupy similar ecological niches (Oh *et al.*, 2010). In the Scotia Sea, SAR116 abundance (determined using Fluorescence *In Situ* Hybridization (FISH)) was reported to be higher in more productive waters where SAR11 numbers were lower (Topping *et al.*, 2006). However, this analysis across an extended latitudinal transect indicates that overall SAR11 and SAR116 have similar biogeographic distributions.

Bacteroidetes

OTUs of the phylum Bacteroidetes, in particular members of the class Flavobacteria, were found to be abundant (NZ average: 1.2%, 5.0% and 6.9% of the 0.1 µm, 0.8 µm and 3.0 µm fractions respectively; SZ: 2.3%, 9.8% and 9.1%) and significant contributors to variance between the NZ and SZ (Fig. 3.3). Flavobacteria have been previously reported to compose the majority of both Bacteroidetes (Murray and Grzynski, 2007) and total planktonic biomass (Abell and Bowman, 2005b) in the SO, as well as being abundant in sea ice (Brown and Bowman, 2001). As heterotrophic degraders of High Molecular Weight (HMW) compounds in the form of both Dissolved Organic Matter (DOM) and Particulate Organic Matter (POM) (Kirchman, 2002), marine Flavobacteria are major components of marine aggregates (Rath *et al.*, 1998; Crump *et al.*, 1999; Zhang *et al.*, 2007). The higher abundance of Flavobacteria OTUs on the 0.8 µm and 3.0 µm fractions indicates their association with particulate matter. Similar size partitioning of SO Flavobacteria has previously been reported (Abell and Bowman, 2005b).

The higher abundance of OTUs of Flavobacteria in the SZ may reflect an input of cells from melting sea ice (Brown and Bowman, 2001), the higher rates of primary productivity in the south, and the role of the Flavobacteria as degraders of HMW DOM. Because deposition of marine snow is a major route for sequestration of fixed carbon in the ocean (e.g. Hessen *et al.*, 2004), the Flavobacteria that associate with this particulate matter represent a remineralising shunt, which would decrease carbon sequestration by this route.

Rhodobacterales

Members of the order Rhodobacterales were abundant (NZ average: 1.2%, 10% and 5.5% of the 0.1 µm, 0.8 µm and 3.0 µm fractions respectively; SZ: 1.6%, 13% and 7.9%) and high contributors to variance, overrepresented in the SZ on all size fractions. As several members of the Roseobacter clade have been shown to have symbiotic relationships with marine eukaryotic algae (Buchan *et al.*, 2005; Wagner-Döbler and Biebl, 2006), and their abundance in the SO has previously been linked to phytoplankton blooms (West *et al.*, 2008; Obernosterer *et al.*, 2011), it is likely that their overrepresentation in the SZ is related to the higher density of phytoplankton in the AZ.

OTUs of *Roseobacter denitrificans* Och114 and *Silicibacter pomeroyi* DSS-3 were consistently the most abundant Roseobacter clade representatives. *R. denitrificans* and *S. pomeroyi* fall within a subclade of Aerobic Anoxygenic Phototrophic (AAP) members of the Roseobacter clade (Swingley *et al.*, 2007). These species have diverse mixotrophic metabolisms, with genomic and experimental evidence of photoheterotrophic respiration of organic carbon, fixation of CO₂, oxidation of CO, oxidation of reduced sulfur compounds, and utilization of the abundant marine osmolyte DMSP (King, 2003; Moran *et al.*, 2004; Wagner-Döbler and Biebl, 2006; Swingley *et al.*, 2007; Brinkhoff *et al.*, 2008; Howard *et al.*, 2008). This metabolic diversity suggests a complex ecological role, particularly with respect to the capture and release of climatically active gases (CO₂, CO, dimethylsulfide) involved in carbon and sulfur cycling.

Alteromonadales

Members of the gammaproteobacterial order Alteromonadales were large contributors to variance. Most OTUs were overrepresented in the SZ but some were overrepresented in the NZ on the 3.0 µm fraction (Fig. 3.3). *Colwellia psychrerythraea* 34H was one of the most abundant OTUs in the Alteromonadales that exhibited this distribution (NZ average: 0.14%, 2.2% and 16% of the 0.1 µm, 0.8 µm and 3.0 µm fractions respectively; SZ: 0.52%, 5.1% and 10%). *C. psychrerythraea* 34H was isolated from Arctic sediment, grows well at low temperatures and secretes extracellular polysaccharides (Huston *et al.*, 2000; Junge *et al.*, 2003; Methé *et al.*, 2005). Similar to other *Colwellia* species grown under laboratory conditions, cells have widths of 0.4–0.8 µm and lengths of 1.5–4.5 µm (Jung *et al.*, 2006). Growth temperature can have a major impact on cell morphology, enzyme secretion and global gene expression in psychrophiles (e.g. Feller and Gerday, 2003; Junge *et al.*, 2003; Williams *et al.*, 2011; Cavicchioli, 2006; Campanaro *et al.*, 2011). Moreover, marine bacteria can alter their cell dimensions in response to nutrient flux (e.g. Kjelleberg *et al.*, 1987). It is therefore possible that the populations of Alteromonadales captured on the 3.0 µm filters (overrepresented in the NZ) had different physiological properties to those on the 0.1 and 0.8 µm filters (overrepresented in the SZ).

Verrucomicrobia

Two representatives of the phylum Verrucomicrobia, *Coraliomargarita akajimensis* and *Akkermansia* sp. Muc-30, were moderate contributors to variance and overrepresented in the SZ (Fig. 3.3). Surprisingly given the small cell size of *C. akajimensis* (Yoon *et al.*, 2007), its contribution to variance increased with size fraction. A global survey reported a similar fractionation pattern, and suggested marine Verrucomicrobia may be predominantly particle attached (Freitas *et al.*, 2012). However, little else is known about the distribution and ecological roles of marine Verrucomicrobia (Freitas *et al.*, 2012).

Functional capacities differentiating the zones

A number of modules with transport functions (sn-glycerol 3-phosphate transport system, dipeptide transport system, peptides/nickel transport system, simple sugar transport system, sulfonate/nitrate/taurine transport system) were overrepresented in the SZ (Table 3.5). As the genomes of copiotrophic bacteria have evolved to have a higher number of narrow-specificity transporters relative to oligotrophic genomes (Lauro *et al.*, 2009), these differences may reflect the higher nutrient availability and thus a dominance of copiotrophs in the SZ. The taxonomic contributors to these modules were varied, although members of the Rhodobacterales were prominent (Fig. 3.6).

The glycine betaine/proline transport module was also overrepresented in the SZ, though this probably reflects glycine betaine's role as an osmo- and cryoprotectant in the colder SZ waters. This



Figure 3.6: Decomposition of KEGG modules of interest to contributing classes, orders or genera. The left side of each stack (S) indicates the proportion of the module abundance contributed by each class, order or genus in the South Zone, while the right side (N) represents the North Zone. As the contributions are relative and represent unitless module abundances, no axis is given and proportions are not comparable between modules. Contributing classes, orders or genera are arranged in descending order of the difference in the relative contributions between the zones. Only the eight highest contributors for each module are shown, with the remainder collapsed into the “Other” group. The taxonomic ranks to which each module was decomposed are as follows: sn-glycerol 3-phosphate transport, peptide-nickel transport, simple sugar transport and sulfonate/nitrate/taurine transport were decomposed to order; glycine betaine/proline transport and branched-chain amino acid transport to genus; pyrimidine deoxyribonucleotide biosynthesis, adenine nucleotide biosynthesis and guanine nucleotide biosynthesis to order; methionine salvage to genus; sulphur reduction to class; photosystem I and photosystem II to genus; histidine degradation to glutamate and histidine biosynthesis to class.

is supported by the major taxonomic contributor to this module, genus *Psychromonas*, which includes several psychrophilic species.

One exception to this pattern was the branched-chain amino acid transport system module, overrepresented in the NZ. The genera *Pelagibacter* and *Puniceispirillum* were major contributors to this module’s overabundance in the NZ (Fig. 3.6). As both SAR11 (Giovannoni *et al.*, 2005) and SAR116 (Grote *et al.*, 2011) representatives encode branched-chain amino acid transporters, the abundance of this module is likely to represent taxonomic differences between the zones.

Biosynthesis pathways for all major nucleic acids (pyrimidine deoxyribonucleotide biosynthesis, adenine nucleotide biosynthesis, guanine nucleotide biosynthesis) were consistently high contributors to variance and overabundant in the NZ. This pattern seems inconsistent with the more oligotrophic nature of the NZ, as oligotrophic cells generally have smaller genomes (Lauro *et al.*, 2009) and slower growth rates than copiotrophs, and would therefore be expected to require a lower rate of de novo nucleotide biosynthesis. A possible explanation for this is that SZ cells have higher availability of extracellular DNA as a byproduct of decaying phytoplankton (Lomas and Moran, 2011), which can be imported and salvaged for nucleic acids (Paul *et al.*, 1988) thus reducing the requirement for de novo synthesis. No single taxonomic group contributed a large fraction of the difference in this module (Fig. 3.6), suggesting this is a widespread adaptation.

The methionine salvage pathway module had a large contribution to variance between the zones and was overrepresented north of the PF. This may reflect the higher availability of DMSP in the SZ as a byproduct of blooming eukaryotic algae. DMSP is a major carbon and sulfur source for marine microorganisms, and is commonly assimilated by bacteria through demethylation to methylmercaptopyruvate (MMPA), followed by further catabolism to the climatically important compounds dimethylsulfide or methanethiol (review in Curson *et al.*, 2011). However, when DMSP is scarce, MMPA may be derived from methionine through the alternative methionine salvage pathway (Reisch *et al.*, 2011). The genus *Synechococcus*, a noted contributor to marine DMSP uptake and assimilation (Vila-Costa *et al.*, 2006), was a very high contributor to the abundance of this module in the NZ (Fig. 3.6), suggesting *Synechococcus* species may use this route when DMSP is unavailable.

The sulfur reduction module was overrepresented in the SZ, and it is likely that this result is strongly driven by taxonomic differences. While the taxonomic breakdown indicated a large number of genera contributed to the difference, the Gammaproteobacteria were the highest-contributing class (Fig. 3.6). This module also includes the assimilatory sulfate reduction pathway, which is widespread in marine bacteria, but is absent from SAR11, with known representatives reported to lack genes for assimilatory sulfate reduction (cysDNCHI) (Tripp *et al.*, 2008). The higher relative abundance of SAR11 in the NZ may therefore contribute to the lower abundance of genes for assimilatory sulfate reduction in that zone.

The sulfur reduction module also included adenylylsulfate reductase (APS reductase, encoded by aprAB), an enzyme implicated in sulfite detoxification during heterotrophic growth on organosulfonates (Meyer and Kuever, 2007) (N.B. in recent KEGG releases, aprA is no longer included in this module). As the GSO-EOSA-1 representative SUP05 has been found to encode APS reductase, the overabundance of this module may reflect sulfur oxidation through the reverse dissimilatory sulfate reduction pathway (Walsh *et al.*, 2009). Also, Roseobacter clade bacteria are involved in the decomposition of abundant organic sulfur compounds (e.g. DMSP, organosulfonates), and hence have been

accorded an important role in marine sulfur cycling (Moran *et al.*, 2007).

The photosystem II module was overrepresented in the NZ. Given the underrepresentation of cyanobacterial OTUs in the SZ, this may reflect a dominance of primary production by eukaryotic algae south of the PF and cyanobacteria to the north. Decomposition of the taxonomic affiliations of ortholog groups contributing to this module found OTUs of *Synechococcus* and *Prochlorococcus* to be major contributors to the difference (Fig. 3.6). Variation in the photosystem I module, which was marginally overrepresented in the SZ, could largely be attributed to diatoms and other eukaryotic phytoplankton (Fig. 3.6), again supporting a dominance of eukaryotic phytoplankton in SZ primary production. Diatoms have previously been reported at higher abundance south of the PF, and their distribution is likely to be linked to the higher concentration of dissolved silica in that region (Trull *et al.*, 2001). As both eukaryotic phytoplankton and cyanobacteria would be expected to encode both complete photosystems, the differences in module abundance probably reflect the degree of similarity between the photosystem I and II genes in the KEGG database and those found in the sampled environments.

The histidine degradation to glutamate module, which comprises four ortholog groups mediating the degradation of histidine to glutamate via N-formiminoglutamate, was overrepresented in the SZ. The histidine biosynthesis module was also overrepresented in the SZ. While the concentration of dissolved histidine in the SO is generally low (Kawahata and Ishizuka, 2000), blooming eukaryotic phytoplankton (which are more prevalent in the SZ) may deplete nitrate while releasing Dissolved Free Amino Acids (DFAA). As DFAA become available, they are used by bacteria to sense the decaying bloom. Histidine may therefore act as a proxy for DFAA to regulate the expression of bacterial aminopeptidases, which are involved in lysing diatoms (Bidle and Azam, 2001). The class Bacteroidetes, while a small contributor to the histidine biosynthesis module in the SZ, was a large contributor to histidine degradation (Fig. 3.6), supporting an association between Bacteroidetes and phytoplanktonic bloom products. It is also possible that uptake and degradation of histidine to glutamate (which generates ammonia as a by-product) may function as a limited nitrogen source.

Conclusions: Biogeographic role of the Polar Front

These results show that there are major taxonomic and functional differences across the PF. The differences in functional potential between the NZ and SZ reflect both their taxonomic profiles and fundamental trophic and ecological differences. In particular, they provide genomic support that the NZ is more oligotrophic than the SZ (Pollard *et al.*, 2002; Giovannoni *et al.*, 2005; Alonso and Pernthaler, 2006; Lauro *et al.*, 2009), and are consistent with the observation that primary production is higher south of the PF (Strutton *et al.*, 2000; Williams *et al.*, 2010). Our findings extend previous work in defining the PF as a strong biogeographic boundary which shapes not only the composition, but also the functional capacity of microbial communities in the SO.

These results do not exclude the possibility that other major SO fronts, particularly the STF and SAF, are also significant biogeographic boundaries, as has been reported in some previous reports for specific taxonomic groups (e.g. Abell and Bowman, 2005b). While the sampling resolution in this study was not sufficient to resolve the effects of other fronts, there are some indications in the data of further structure within the zones. The two samples north of the STF had significantly larger cyanobacterial populations than the remaining NZ samples (see discussion of *Prochlorococcus* and *Synechococcus*, above). Future sampling across these fronts at higher resolution will provide the data necessary to investigate finer biogeographic patterns.

The nature and function of microbial communities in the SO are of global significance. Knowledge of these communities and their biogeographic drivers has relevance for understanding and predicting the long-term effects of climate change. These findings provide a basis for predicting how climate change-driven shifts in the SO may affect microbial communities; in particular, the effects of changes in the nature and location of the ACC on the ecosystem functions of SO microorganisms.

Chapter 4

Preliminary analysis of Antarctic Bottom Water (AABW) samples suggests advective transport of microbial cells

Abstract

During sampling for the study presented in Chapter 3, additional samples were collected of AABW on the Antarctic continental shelf and from the sea floor in the vicinity of the mid-ocean ridge. Metagenomic analysis found that the community composition of the continental shelf samples was surprisingly similar to that of surface samples in the same area, despite the significant differences in environmental factors such as pressure and light availability. This may have resulted from the rapid advection of cells in the sinking of surface waters to form AABW (deep water formation; see Chapter 1). These results led to the study described in Chapter 5.

Methods

Three samples of AABW were opportunistically obtained and analysed during the project described in Chapter 3 (Fig. 4.1). Two of these samples (356 and 361) were of newly formed AABW waters on the Antarctic continental shelf, while one (365) was of abyssal AABW from the South Australian basin (Table 4.1). DNA extraction, sequencing and construction of a taxonomic profile by BLAST comparison to the RefSeq database and processing with Genome relative Abundance and Average Size (GAAS) were performed using the methods described in Chapter 3. A standardised and log-transformed Bray-Curtis resemblance matrix was constructed including the taxonomic profiles of the AABW samples as well as the North Zone (NZ) and South Zone (SZ) samples described in Chapter 3.

Table 4.1: Sampling time, location and physicochemical properties of AABW samples used in this preliminary study. All data were retrieved from the CTD (SeaBird, Bellevue, USA) instrument used to collect the samples.

Sample	Date	Latitude	Longitude	Sample Depth (m)	Temperature (°C)	Salinity (PSU)	Volume filtered (L)
356	03/01/2008	-66.7617	144.4138	920	-1.9	34.69	230
361	14/01/2008	-66.4727	140.5572	1170	-1.8	34.56	225
365	23/01/2008	-56.6967	141.9125	3693	0.5	34.69	230

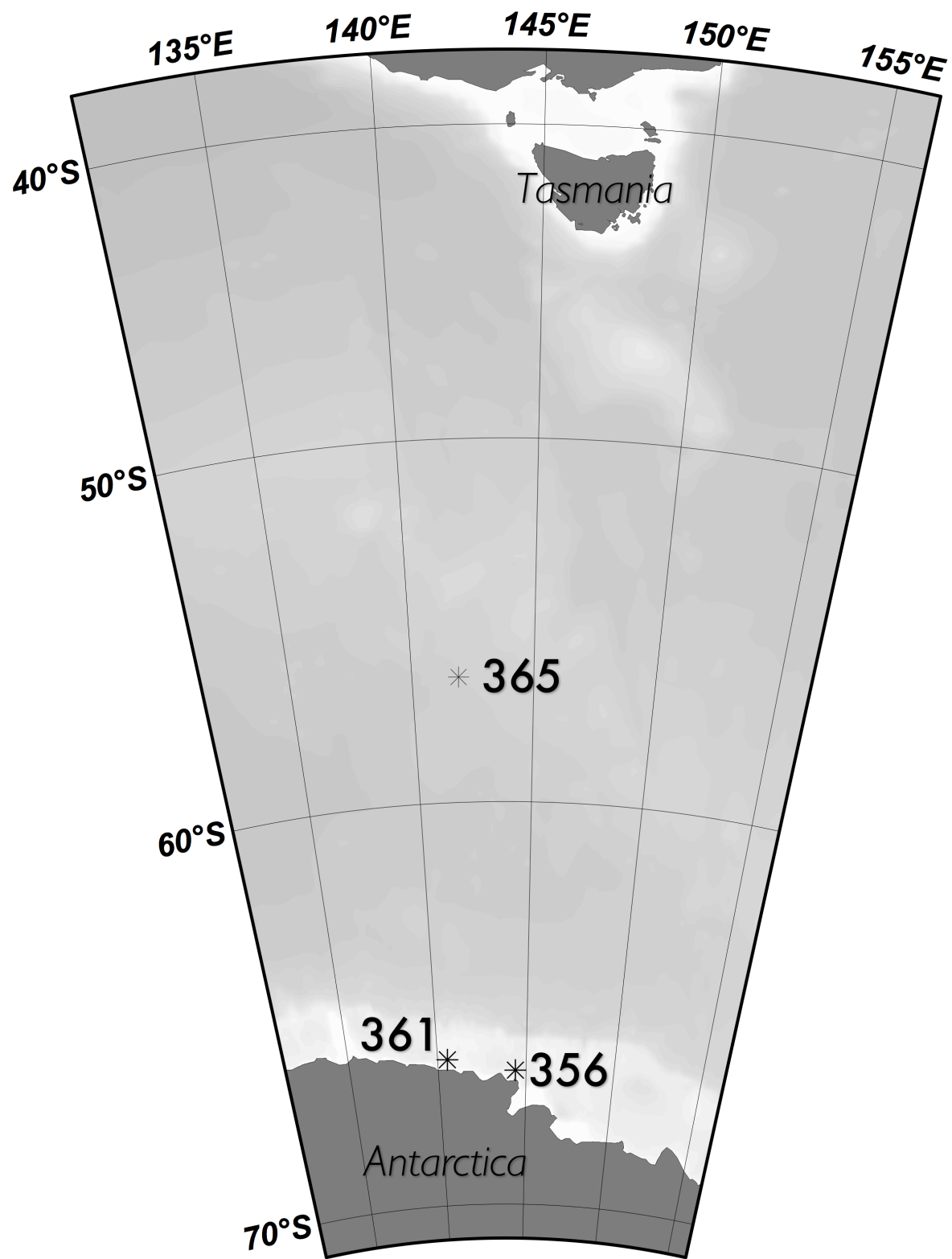


Figure 4.1: Sites of preliminary AABW samples.

Table 4.2: Relative abundances (as percentages) of the twenty most abundant OTUs identified in the preliminary study of AABW samples.

OTU	Sample 356			Sample 365		
	0.1 µm	0.8 µm	3.0 µm	0.1 µm	0.8 µm	3.0 µm
"Candidatus Pelagibacter ubique" HTCC1062	48.40	32.32	32.85	19.02	22.31	3.880
<i>Nitrosopumilus maritimus</i> SCM1	11.92	9.289	13.99	30.17	7.790	22.74
"Candidatus Ruthia magnifica" str. Cm (<i>C. magnifica</i>)	3.780	4.563	2.356	2.844	1.504	0.2599
"Candidatus Vesicomyosocius okutanii" strain HA	2.349	2.757	1.396	1.859	0.8025	0.08227
<i>Roseobacter</i> sp. OCh 114	0.1412	1.166	0.6845	0.08564	0.6662	0.4851
"Candidatus Puniceispirillum marinum" IMCC1322	0.3180	1.103	0.6403	0.4218	0.8223	0.4202
<i>M. hydrocarbonoclasticus</i> VT8	0.06999	0.4091	0.3976	0.2476	1.050	2.338
<i>S. pomeroyi</i> DSS-3	0.1081	0.8406	0.4996	0.1290	0.4630	0.3621
<i>R. biformata</i> strain HTCC2501	0.2813	0.6433	0.7417	0.1769	0.2739	0.4978
<i>P. haloplanktis</i> strain TAC125	0.02530	0.4540	0.1958	0.2836	2.817	0
<i>A. borkumensis</i> strain SK2	0.09262	0.3163	0.4281	0.1049	0.5674	1.985
<i>G. forsetii</i> strain KT0803	0.3096	0.6465	0.7405	0.1254	0.2670	0
<i>Colwellia</i> sp. 34H	0.04289	0.4512	1.020	0.07200	0.4532	0.7727
<i>F. psychrophilum</i> strain JIP02/86	0.2417	0.4722	0.6353	0.07943	0.1645	0.5072
<i>P. staleyi</i> strain DSM 6068	0.003149	0.2477	0.3093	0.08767	1.401	0.7732
<i>Jannaschia</i> sp. DFL-12	0.07995	0.6770	0.3841	0.03865	0.2030	0.1025
<i>P. atlantica</i> strain T6c	0.02312	0.1653	0.1941	0.03856	0.3235	1.728
<i>Z. profunda</i> strain SM-A87	0.1830	0.3499	0.4826	0.1036	0.1362	0.3825
<i>Silicibacter</i> sp. TM1040	0.09568	0.5448	0.3455	0.03477	0.2014	0.1740
<i>C. ochracea</i> strain DSM 7271	0.1251	0.2916	0.4491	0.03893	0.1542	0.5332

A Non-Metric Multidimensional Scaling (nMDS) plot was then constructed from this matrix. All statistical procedures were performed in PRIMER 6 as described by Clarke and Warwick (2001).

Results and Discussion

Although the three AABW samples were taken in deep, cold and aphotic waters (Table 4.1) compared to the surface Antarctic Zone (AZ) and SZ samples, the nMDS plot suggested that the two continental shelf AABW samples (356 and 361) were surprisingly similar to those of the AZ, particularly sample 353 (Fig. 4.2). Further, the indicated the presence of several Operational Taxonomic Units (OTUs) which would not be expected to be present at significant abundance in deep, aphotic waters (Table 4.2). For example, *R. denitrificans* OCh 114, a model organism for aerobic anoxygenic photosynthesis, was the fifth most abundant OTU of the continental shelf samples. Numerous Cytophaga-Flavobacterium-Bacteroides (CFB) representatives, typically associated with Particulate Organic Matter (POM) and the utilisation of High Molecular Weight (HMW) phytoplankton products (e.g. Williams *et al.*, 2012b), were also unexpectedly high.

A possible explanation for these observations is that the continental shelf samples represent AABW recently formed in the D'Urville sea, and the observed assemblage therefore represents advection rather than selection by environmental factors. The project described in Chapter 5 was designed to test and explore this hypothesis.

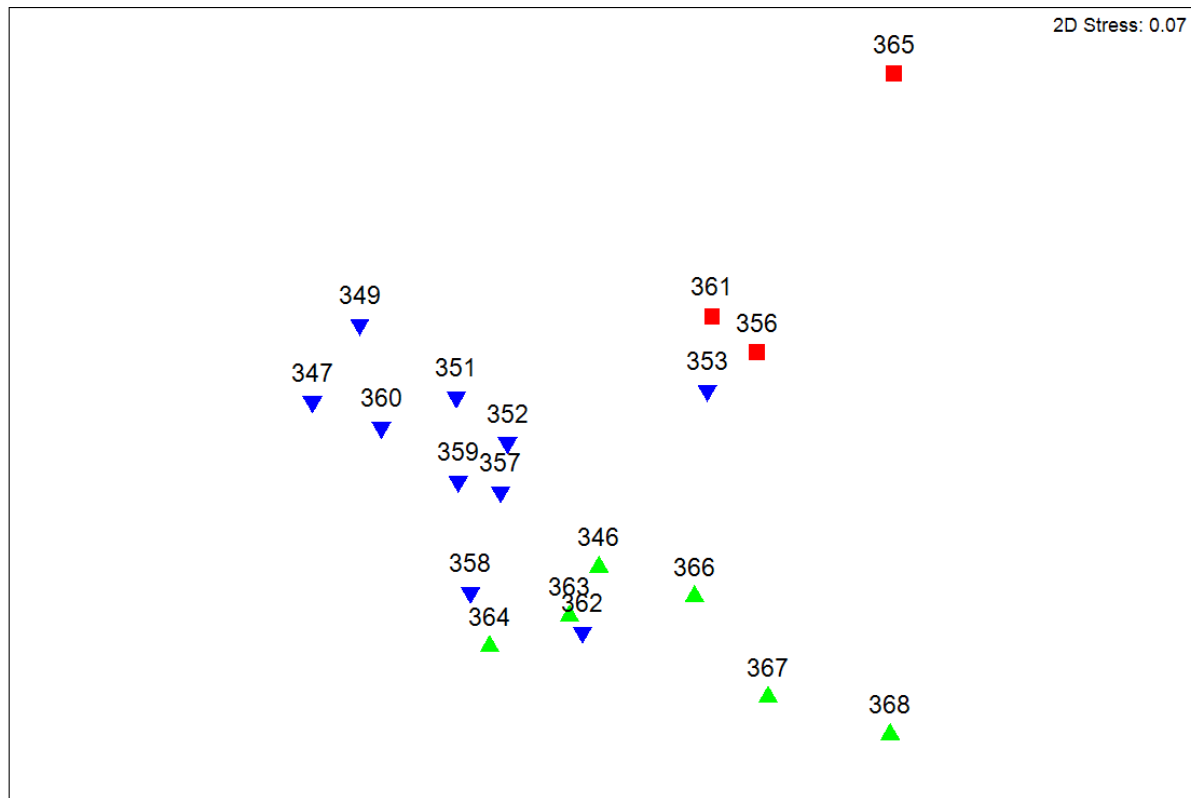


Figure 4.2: nMDS plot showing distance between AABW, NZ and SZ samples. Green triangles represent samples from the NZ; blue inverted triangles from the SZ; and red squares from AABW.

Chapter 5

The advection effect as a driver of microbial biogeography

Sections of this chapter have been previously published in

Abstract

The distribution and abundance of marine microbes are shaped by environmental factors and spatial separation. The physical transport of cells by ocean currents (advection) is also frequently invoked when describing marine microbial biogeography, but the role of advection has never been directly confirmed or measured. In this study, the microbial communities at 25 sites in the Southern Ocean were sampled and compared to a model of particle advection between the sites. Even when environmental factors and spatial separation were controlled for, the “advection effect” explained 7% of variation in community composition. Further investigation confirmed that this effect was directional, and likely represented an increase in the colonisation of distant sites by small numbers of cells. This study provides further evidence that microbial dispersal potential is far from total, and supports the role of ocean currents in shaping marine microbial ecosystems.

Introduction

The central goal of microbial biogeography is to understand how the distribution and abundance of microorganisms are shaped by their physical context. The Baas Becking hypothesis — that “*everything is everywhere, but, the environment selects*” (Baas Becking, 1934; de Wit and Bouvier, 2006) — posits that the rapid dispersal of microorganisms means microbial community structure is determined entirely by environmental selection. This stands in contrast to macroorganism biogeography, which has long been recognised as being under the control of historical (in addition to contemporary environmental) factors, particularly spatial influences such as barriers to dispersal. Microbial biogeography studies have begun to show that historical factors may also shape the distribution of microorganisms (Martiny *et al.*, 2006), e.g. a correlation between spatial and genetic distance (a “distance effect”) in fluorescent *Pseudomonas* strains in soils (Cho and Tiedje, 2000). This study, among others (Ramette and Tiedje, 2007; Storch and Sizling), also demonstrated the importance of taxonomic resolution in describing such biogeographic patterns. Other studies have found that dispersal potential varies between microbial species, leading to different or absent distance effects (Bissett *et al.*, 2010). When combined with contemporary environmental selection (“environment effect”), distance effects explain some but not all variation between microbial communities, and the mechanism(s) by which a distance effect arises are not always clear (Hanson *et al.*, 2012).

In the ocean, several recent studies have found that microbial communities can be endemic to hydrographically distinct water masses. Surveys in the Arctic (Galand *et al.*, 2009) and North Atlantic (Agogué *et al.*, 2011) oceans have found that bacterial assemblages within the same water mass can be similar across a range of thousands of kilometres, but assemblages can differ between water masses

across a range of hundreds of meters. Water masses are defined by their distinct physicochemical properties, so such patterns do not directly imply the existence of factors beyond environmental selection. However, in some cases a water mass-community relationship has been shown to persist even when environment effects are statistically controlled for (Hamilton *et al.*, 2008; Hamdan *et al.*, 2013).

During the study on the biogeographic effect of the Polar Front (PF) described earlier in this volume, it was found that microbial communities in surface waters of the Mertz Glacier region, a site of deep water formation, were very similar to those at the bottom of the water column, despite the very different environmental conditions (see Chapter 4). One hypothesis explaining both this observation and water mass endemicity is that microbial assemblages are influenced by the advection (physical transport) of cells by ocean currents. Higher dispersal rates cause the microbial community composition at a given site to increasingly resemble the dispersed colonisers, and less reflect local environmental selection and stochastic effects such as genetic drift (Hanson *et al.*, 2012). Hence, it would be expected that locations that are closely connected by advection (e.g. those within the same water mass, or different levels of the water column at a site of deep water formation) would have more similar compositions than those that are not, even when the environment effect is accounted for. Indeed, advection is often invoked to explain observations of microbial diversity or abundance which do not seem attributable to environmental selection (e.g. Sul *et al.*, 2013; Ghiglione *et al.*, 2012; Giebel *et al.*, 2009; Lauro *et al.*, 2007). The exchange of very small volumes of water between marine microbial mesocosms has been found to greatly reduce their β -diversity even under consistent environmental conditions (Declerck *et al.*, 2013). This suggests that advection of even small numbers of cells could have a large homogenizing effect independent of environmental selection. However, the existence of a relationship between advection and community composition that is independent of environment and distance effects has not been directly tested.

The Southern Ocean (SO) is composed of several water masses, which are physicochemically distinct but linked by circulation (see Chapter 1 for a full description; see also Fig. 5.1). This study aimed to determine whether advection shapes the community structure of bacteria and archaea, independent of environment and distance effects. By sampling each of the SO water masses (depths from surface to \sim 6 km), dissimilarity between microbial communities over a large spatial distance (\sim 3000 km) and range of environments could be determined, in order to test whether advection played a role in shaping their composition.

Methods

Sampling

Sampling¹ was conducted on board the RSV *Aurora Australis* during cruise V3 from 20 January–7 February 2012. This cruise occupied a latitudinal transect from waters north of Cape Poinsett, Antarctica (65° S) to south of Cape Leeuwin, Australia (37° S) within a longitudinal range of 113–115° E.

Sampling was performed as described in Chapter 3, with sites and depths selected to provide coverage of all major SO water masses. At each surface station, \sim 250–560 L of seawater was pumped from \sim 1.5–2.5 m depth. At some surface stations, an additional sample was taken from the Deep Chlorophyll Maximum (DCM), as determined by chlorophyll fluorescence measurements taken from a Conductivity, Temperature and Depth (CTD) cast at each station. Samples of mesopelagic and deeper waters (\sim 120–240 L) were also collected at some stations using Niskin bottles attached to the CTD. Sampling depths were selected based on temperature, salinity and dissolved oxygen profiles to capture water from the targeted water masses. Profiles were generated on the CTD descent, and samples collected on the ascent at the selected depths. Deep water masses were identified by the following criteria: Circumpolar Deep Water (CDW) = oxygen minimum (Upper Circumpolar Deep (UCD)) or salinity maximum (Lower Circumpolar Deep (LCD)); Antarctic Bottom Water (AABW) = deep potential temperature minimum; Antarctic Intermediate Water (AAIW) = salinity minimum (Foldvik and Gammelsrød, 1988). Surface zones were identified relative to the major fronts of the SO, which are marked by strong latitudinal gradients in temperature and salinity (Sokolov and Rintoul, 2002; Orsi *et al.*, 1995). The Antarctic Zone (AZ) lies south of the PF (\sim 51° S at the time of sampling), while the Polar Frontal Zone (PFZ) lies between the PF and the Subantarctic Front (SAF). Subantarctic

¹Sampling was performed by David Wilkins, Timothy J. Williams and Sheree Yau.

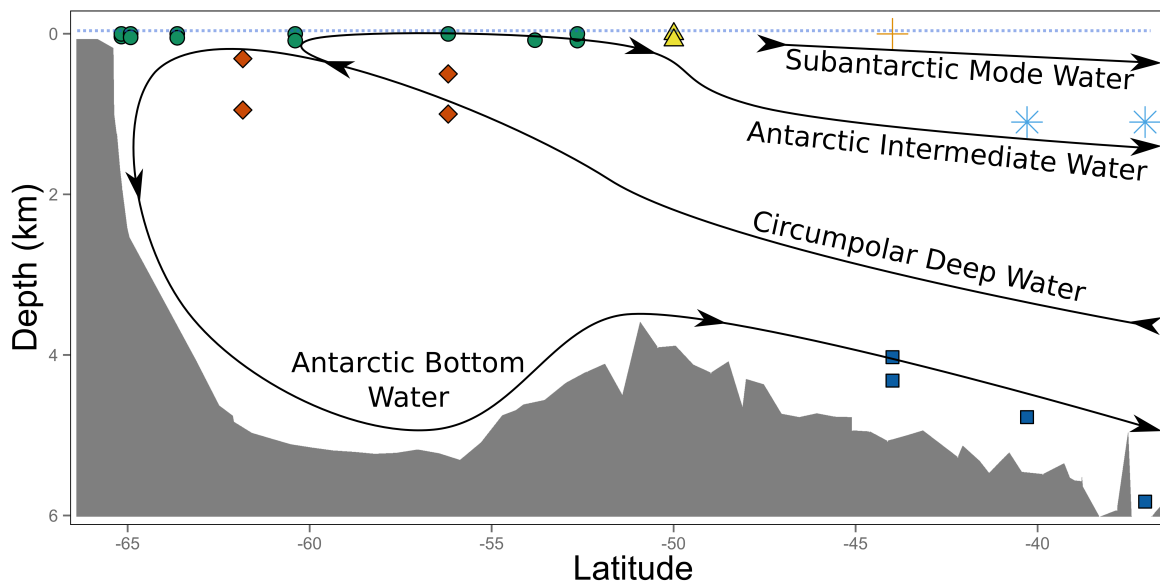


Figure 5.1: Antarctic Intermediate Waters (AAIW), light blue stars; Subantarctic Mode Water (SAMW), orange crosses; Antarctic Bottom Water (AABW), dark blue squares; Antarctic Zone (AZ), green circles; Polar Frontal Zone (PFZ), yellow triangles; Circumpolar Deep Water (CDW), red diamonds; sea surface, blue dashed horizontal line. Bathymetry is an approximate representation for 115° E, and is indicative only.

Mode Water (SAMW) overlays AAIW north of the SAF. In total, 25 samples from the AZ, PFZ, SAMW, AAIW, CDW and AABW were collected for this study (Fig. 5.1).

Seawater samples were prefiltered through a 20 µm plankton net, then filtrate was captured on sequential 3.0 µm 0.8 µm and 0.1 µm 293 mm polyethersulfone membrane filters (Pall, Port Washington, USA), and immediately stored at –20 °C (Rusch *et al.*, 2007; Ng *et al.*, 2010).

DNA extraction

DNA extraction was performed using a modified version of the phenol-chloroform method described in Rusch *et al.* (2007). Samples were thawed in a 37 °C water bath. Half of the storage buffer (~10 mL) was decanted into a clean 50 mL centrifuge tube. If the volume decanted was less than 10 mL, the difference was made with sterile water (Sigma-Aldrich, St. Louis, USA). An equal volume of 50% sucrose lysis buffer (50 mM TRIS-HCl, 40 mM EDTA, 0.75 M Sucrose, pH 8) was added such that the final concentration was 25% sucrose lysis buffer. A small pinch of lysozyme (Sigma-Aldrich, St. Louis, USA) (final concentration ~2.5 mg/mL) and 1 mL TRIS-EDTA (10 mM TRIS, 1 mM EDTA, pH 8) was added.

The filter membrane was removed from the storage tube and cut in half aseptically. One half was returned to the storage tube, which was refrozen at –80 °C. The remaining half was cut in half again, and one quarter-filter placed atop the other such that the biomass (filtrand) on each piece was facing outwards. Keeping the filters together, they were cut into very fine (~3 mm by 10 mm) strips, which were placed in the 50 mL centrifuge tube containing the buffer and lysozyme mixture. This tube was mixed by gentle inversion, then tapped such that all filter strips collected at the bottom of the tube and were covered by lysis buffer. The tube was then incubated in a 37 °C shaking water bath at 275 RPM for 30–60 min.

200 µL of 20 mg/mL Proteinase K (Sigma-Aldrich, St. Louis, USA) was added to the tube, which was mixed by gentle inversion. The tube was gently tapped such that all filter strips collected at the bottom covered by lysis buffer. The tube was then subjected to three freeze-thaw cycles, each cycle consisting of 20–30 min in a –80 °C freezer followed by 20–30 min in a 55 °C water bath. After the final complete thaw, 200 µL of 20 mg/mL Proteinase K and 2 mL of 10% SDS (Sigma-Aldrich, St. Louis, USA) were added to the tube. The tube was mixed by gentle inversion then gently tapped such that

all filter strips collected at the bottom covered by lysis buffer. It was then incubated in a 55 °C shaking water bath at 175 RPM for two hours.

The supernatant was pipetted from the tube using a genomic tip and split evenly into two new 50 mL centrifuge tubes. An equal volume of buffer-saturated (10 mM TRIS HCl, 1 mM EDTA, pH 8) phenol (Sigma-Aldrich, St. Louis, USA) was added to each of the tubes, which were mixed by gentle inversion. The mixtures were then fractionated in a fixed-angle rotor centrifuge for 15 min at 3700 RPM at room temperature. The bottom layer of each tube was removed by pipette into a new 50 mL centrifuge tube. Each of these two tubes was then made to 50 mL with sterile water (Sigma-Aldrich, St. Louis, USA). After mixing by gentle inversion, each 50 mL mixture was then split evenly into two new 50 mL centrifuge tubes, resulting in four tubes each containing 25 mL of mixture. These tubes were then made to 50 mL with 1-propanol (Sigma-Aldrich, St. Louis, USA). The mixtures were homogenised by gentle inversion and incubated at 4 °C overnight.

Following incubation, the tubes were centrifuged using a fixed-angle rotor for 30 min at 7500 RPM and room temperature. The majority of the supernatant was removed by decanting, and the tubes left to sit until the remaining supernatant (~1 mL) collected at the bottom over the precipitated pellet. The pellet was then resuspended by gentle pipetting with a genomic tip, and the suspension placed in a new 1.5 mL microcentrifuge tube (four tubes total). These tubes were then centrifuged in a microcentrifuge for 10 minutes at 13,000 RPM and room temperature. The supernatant was removed by pipette and the tubes placed in a 37 °C heat block with the lids opened and covered by a sterile KimWipe (Kimberly-Clark, Irving, USA) for 10 min, or longer if the supernatant did not evaporate completely in that time. 93.75 µL of TRIS-EDTA was added to each tube, and the tubes were incubated at 4 °C for one hour to allow the DNA pellet to redissolve.

After this incubation, the pellets were gently pipetted with a genomic tip to ensure complete resuspension. The suspensions from all four tubes were combined, and an additional 750 µL of TRIS-EDTA added. This was then split evenly into two new 1.5 mL microcentrifuge tubes (~562.5 µL per tube).

750 µL of buffer-saturated phenol was added to each tube, and the tubes mixed gently by inversion until a visible emulsion formed. Phase separation was performed by centrifugation for 5 min at 13,000 RPM and room temperature. The upper (aqueous) phase was removed to a new 1.5 mL microcentrifuge tube using a genomic tip.

750 µL of phenol-chloroform-isoamyl alcohol (25:24:1) mixture (Sigma-Aldrich, St. Louis, USA) was added to each tube, and the tubes mixed by gentle inversion until a visible emulsion formed. Phase separation was performed by centrifugation for 5 min at 13,000 RPM and room temperature. The upper (aqueous) phase was removed to a new 1.5 mL microcentrifuge tube using a genomic tip.

75 µL of 3 M sodium acetate (pH 8) and 750 µL of 1-propanol was added to each tube. The tubes were centrifuged at 13,000 RPM and room temperature for 30 min to precipitate the DNA. The supernatant was removed by pipetting, and 100 µL of 70% ethanol added. The tubes were centrifuged again at 13,000 RPM and room temperature for 5 min. The supernatant was removed by pipetting and the DNA pellet dried in a 37 °C heat block. The DNA was dissolved overnight in 40–200 µL of TRIS-EDTA, depending on the expected yield.

Sequencing

Tag pyrosequencing was performed by Research and Testing Laboratory (Lubbock, USA) on a GS FLX+ platform (Roche, Branford, USA), using a modification of the standard 926F/1392R primers targeting the V6–V8 hypervariable regions of bacterial and archaeal 16S rRNA genes (926wF: AAA-CTY-AAA-KGA-ATT-GRC-GG, 1392R: ACG-GGC-GGT-GTG-TRC). The additional wobble bases have been found to amplify a greater range of environmental bacteria and archaea, particularly Euryarchaeota, than the standard primers (Federico M. Lauro, personal communication). Denoising, chimera removal and trimming of poor quality read ends were performed by the sequencing facility.

Taxonomic assignment

Using Quantitative Insights Into Microbial Ecology (QIIME) 1.6.0 (Caporaso *et al.*, 2010), tag pyrosequencing reads were clustered at the 97% sequence similarity level against the SILVA database of rRNA sequences (release 108, eukaryote and chloroplast sequences removed) (Quast *et al.*, 2013), with

non-clustering reads discarded. QIIME was used to assign to each Operational Taxonomic Unit (OTU) cluster a description representing the most detailed lineage common to at least 90% of the clustered reads, with ranks labelled “uncultured” or “other” ignored. To generate a taxonomic profile for each sample, the relative abundances of reads assigned to each OTU in each size fraction were encoded as variables. To account for the reads discarded during clustering, abundances in each size fraction were standardised by the proportion of reads retained from that fraction. The abundances were square root transformed and Bray-Curtis dissimilarity indices between samples calculated in PRIMER 6 (PRIMER-E, Lutton, UK).

Physicochemical and spatial distances

Environmental data were collected from CTD casts at each sample site. Pressure, dissolved oxygen concentration and water temperature measurements were collected with CTD instruments. Salinity and concentrations of dissolved phosphate, nitrate and silicate were obtained from hydrochemical analysis of seawater samples collected in Niskin bottles during CTD casts (Rosenberg and Rintoul, 2012). These samples were collected at discrete depths, and the hydrochemical sample closest to the depth of the relevant biological sample was selected. The exceptions were samples 32 and 33 (49.5° S, 115° E), for which nitrate concentrations were not available, and sample 29 (53.2° S, 115° E) for which phosphate concentration was not available. In these cases, a reading from the appropriate depth was substituted from the nearest available cast (50.0° S, 115° E for samples 32 and 33; 53.8° S, 115° E for sample 29). Pressure values were $\log(x + 1)$ transformed to reduce right-skew (Clarke and Gorley, 2006) and the combined instrument and hydrochemical data were used to create environmental profiles for each sample. The variables were normalised and a Euclidean distance matrix generated in PRIMER 6.

Distance-based Linear Models (distLM) multivariate analysis (Legendre and Anderson, 1999) was performed to confirm the selection of physicochemical variables and explore their relationship with taxonomic composition. In PRIMER 6, all possible combinations of variables (“BEST selection”) were explored by distLM, and the models (sets of variables) that best fit the taxonomic dissimilarity matrix (adjusted R^2 as the fitness measure) were selected. The relationship between the resulting model and the taxonomic dissimilarity between samples was visualised by Distance-based Redundancy Analysis (dbRDA) ordination.

To generate a spatial distance matrix, pairwise ellipsoidal distances between samples (including difference in depth) were calculated using INVERS3D (National Oceanic and Atmospheric Administration, Silver Springs, USA).

Generation of advection distance matrix

Erik van Sebille contributed to writing the following paragraph.

Advection distances between the sites were computed using three-dimensional velocity data from a hydrodynamic numerical ocean model in combination with a Lagrangian trajectory toolset². The ocean model used was the Southern Ocean State Estimate (SOSE) (Mazloff *et al.*, 2010), a numerical model of the SO based on the Estimating the Circulation and Climate of the Ocean (ECCO) machinery (Wunsch and Heimbach, 2007) and constrained by a large set of in situ and remote-sensed observations. SOSE has been validated in the SO (Cerovečki *et al.*, 2011; Firing *et al.*, 2011). Here, the five-day averaged three-dimensional velocity fields for the period January 2005–December 2007 were used, on a $1/6^{\circ}$ horizontal resolution and with 42 vertical levels. The Connectivity Modeling System (CMS) (Paris *et al.*, 2013) 1.1 was used to integrate virtual Lagrangian particles within the SOSE velocity fields. For each site, 100 particles were released every 5 days (total of 2.2×10^4 per site). The particles were released at the latitude and depth of the site, evenly spaced in a 1° longitudinal line centred at the site longitudes. The particles were then advected for 100 years, looping through the 3 years of available velocity fields as described in van Sebille *et al.* (2012). Three-dimensional locations of the particles were saved every 5 days.

The trajectory of each particle was analysed to detect encounters between particles and sample sites. An encounter was defined as the vector between any two consecutive 5 day particle locations

²Modelling was performed by Erik van Sebille.

intersecting a box bounded by $\pm 0.2^\circ$ of latitude, $\pm 0.5^\circ$ of longitude and ± 50 m of depth from a sample site. Only the first encounter between any particle and sample was counted. Four pairs of samples (10/11; 12/13; 16/17; 21/22), where a DCM sample was taken directly below a surface sample within the mixed layer, were too close to act as separate particle release sites. For these samples, simulated particle releases were performed for only one of the pair, and the generated encounters were attributed to both. For all samples, the mean time in seconds between a particle being released from one sample and encountering another was calculated. Pairwise advective distance between samples was defined as the mean of the two directional mean times between each sample in the pair. This metric was selected to ensure advective flows which may be of high biological relevance, such as a small number of particles quickly transported between sites, were appropriately weighted when paired with flows of lower biological relevance, such as a large number of particles transported between sites over decades. To ensure the results were robust to the choice of metric, subsequent statistical tests were repeated with pairwise advective distance redefined as the mean time for all pairwise encounters. The pairwise distance between the surface/DCM samples discussed above was set to zero. For pairs of samples that did not yield mutual encounters (47 pairs, all including at least one AABW sample; see Results), this was set to the maximum run time of the simulation (100 years). Subsequent statistical tests were rerun with the DCM and AABW samples excluded to ensure these constraints were not unduly influencing the results (see “Testing of advection effect”, below).

Ordination of distance matrices and comparison to water masses

Ordinations of the taxonomic, environmental and advection distance matrices were produced by Non-Metric Multidimensional Scaling (nMDS) in PRIMER 6. Analysis of Similarities (ANOSIM) was also performed in PRIMER 6 to test for statistically significant differences between water masses in each of these three factors. Right-tailed p-values for each test were computed using 999 random label permutations of one of the test matrices.

Testing of advection effect

Mantel tests were performed using Pattern Analysis, Spatial Statistics and Geographic Exegesis version 2 (PASSAGE 2) (Rosenberg and Anderson, 2011). To test for and quantify distance and environment effects, partial Mantel tests were performed comparing the taxonomic matrix to the spatial then environmental matrices, with the remaining matrix held constant. To test the hypothesis that advection shapes SO microbial assemblages independent of distance and environment effects, a partial Mantel test was performed comparing the taxonomic and advection matrices, with both the spatial and environmental matrices held constant. Right-tailed p-values for all tests were calculated using 999 random label permutations of one the test matrices.

To ensure that the result was not unduly influenced by the samples to which the 100 year ceiling was applied (all AABW, see Results) and those for which particle releases were not simulated (samples 11, 13, 17 and 22), the test was repeated with these samples removed.

To confirm that the advection effect was directional, i.e. that “upstream” sites were acting as sources of diversity to “downstream” sites, SOURCETRACKER (Knights *et al.*, 2011) was used to identify sources of OTUs in each sample. Each sample was sequentially designated a sink, with the remaining samples as potential sources, and the most probable proportion of OTUs originating from each potential source determined over 100 randomised trials per sample. Spearman’s rank correlation was then calculated between the SOURCETRACKER predicted source proportions and particle encounter source proportions for each sample pairwise, with right-tailed p-value determined by permutation.

Differential influence of advection on different OTUs

It was hypothesised that some OTUs may be more amenable than others to advective dispersal: for example, cells able to form dormant states (Bissett *et al.*, 2010). A modified form of the BVSTEP algorithm (Clarke and Warwick, 1998) was developed to investigate this.

BVSTEP seeks to find a subset of a community of OTUs, the inter-sample resemblance pattern of which best matches that of the entire community. The quality of the match is defined as the rank correlation (typically Spearman’s ρ) between the Bray-Curtis similarity matrix for the OTU subset and

that of the full set. As the number of potential subsets grows exponentially with the number of OTUs ($2^s - 1$ subsets for s OTUs (Clarke and Warwick, 1998)), it is computationally impractical to test each individually. Hence, BVSTEP uses a stepwise approach to efficiently explore the space of possible subsets.

The algorithm proceeds through successive rounds of forward and backward selection, beginning with a randomly selected subset of (typically six) OTUs. In the forward selection round, each OTU not currently in the subset is tested as a potential addition to the subset. The OTU that by its addition maximally increases the correlation of the subset to the full set is added to the subset, and forward selection is repeated. If no OTU can improve the current subset, forward selection is terminated and backward selection begins.

In the backward selection round, each OTU currently in the subset is tested as a candidate for removal. As with forward selection, the OTU that by its removal maximally increases the correlation of the subset to the full set is removed, and backward selection is repeated. If no such OTU exists, backward selection is terminated and a new round of forward selection begins. Successive rounds of forward and backward selection proceed until either the correlation exceeds 0.95, or no further increase in the correlation can be achieved by either forward or backward selection.

Typically, the algorithm will be run with multiple restarts, each with a randomly selected starting subset, and the resulting subsets compared. This allows an estimation of the “structural redundancy” of the community: the number of unique, high-correlation subsets of OTUs which can be extracted from the total set without replacement.

The BVSTEP implementation used in this study differs from the canonical version (Clarke and Warwick, 1998) in two main ways. Most significantly, each potential OTU subset is not compared to the full set of OTUs by Spearman’s rank correlation. Instead, the Bray-Curtis resemblance matrix between samples is generated for each tested subset, and compared to the advection distance matrix using a partial Mantel test holding the spatial and environmental distances constant. This modified form of the algorithm thus addressed the question of whether some subset of OTUs were as (or more) affected by advection as the entire set. Unlike the standard algorithm, where the best possible “subset” is simply the full set of samples ($\rho = 1$), with this modified algorithm it is possible for a subset to yield a better correlation than the full set.

Additionally, after the random selection of six OTUs to form the starting subset, only the single OTU with the highest correlation is retained. This was because it was observed that the starting subset of OTUs were very rarely retained through the entire selection process, presumably because the total number of OTUs was high and the random selection of representative OTUs thus unlikely. Removing five of the starting OTUs immediately thus eliminates many unnecessary rounds of selection.

Results

Sequencing and taxonomic assignment

After trimming, denoising and chimera removal, the 25 samples (each with three separately sequenced size fractions) yielded 1,008,963 pyrosequencing reads of length 251–561 bp (mean 426 bp). Individual fractions yielded 3,687–52,192 reads (mean 13,453). After clustering against the SILVA database, 2,295–30,760 (mean 9,618) reads per fraction were retained for taxonomic assignment.

1417 unique OTUs were identified across all fractions of all samples. The Chao 1 statistic was calculated, and estimated OTU were under-sequenced by 0–50% across all samples (mean 26%) (Table 5.1). In all water masses, decreasing numbers of reads yielded OTU assignments as size fraction increased (Fig. 5.2). This probably reflects an increasing number of eukaryotic cells (which were excluded from OTU assignment) on the higher fractions.

Table 5.1: Full location, summary of taxonomic assignments and full physicochemical data for each of the 25 samples in this study. Units are given in column headers. Water mass abbreviations are Antarctic Intermediate Waters (AAIW); Subantarctic Mode Water (SAMW); Antarctic Bottom Water (AABW); Antarctic Zone (AZ); Polar Frontal Zone (PFZ); Circumpolar Deep Water (CDW).

Sample	Fraction (μm)	Date	Latitude ($^{\circ}$)	Longitude ($^{\circ}$)	Depth (m)	Water mass	OTU count	Chao 1	Pressure (dbar)	Dissolved O ₂ ($\mu\text{mol/L}$)	Temperature ($^{\circ}\text{C}$)	Phosphate ($\mu\text{mol/L}$)	Nitrate ($\mu\text{mol/L}$)	Silicate ($\mu\text{mol/L}$)	Salinity (PSU)
10	0.1	20/01/2012	-65.17	113.1	35	AZ	431	570	36	348.1	-1.125	1.82	26.73	60.6	33.6
10	0.8	20/01/2012	-65.17	113.1	35	AZ	444	593	36	348.1	-1.125	1.82	26.73	60.6	33.6
10	3.0	20/01/2012	-65.17	113.1	35	AZ	148	293	36	348.1	-1.125	1.82	26.73	60.6	33.6
11	0.1	20/01/2012	-65.17	113.1	2	AZ	433	655	2	365.7	-0.798	1.66	25.13	57.8	33.4
11	0.8	20/01/2012	-65.17	113.1	2	AZ	241	422	2	365.7	-0.798	1.66	25.13	57.8	33.4
11	3.0	20/01/2012	-65.17	113.1	2	AZ	145	202	2	365.7	-0.798	1.66	25.13	57.8	33.4
12	0.1	21/01/2012	-64.92	113.3	2	AZ	294	387	2	356.4	-0.358	1.70	25.87	55.0	33.7
12	0.8	21/01/2012	-64.92	113.3	2	AZ	68	79	2	356.4	-0.358	1.70	25.87	55.0	33.7
12	3.0	21/01/2012	-64.92	113.3	2	AZ	158	232	2	356.4	-0.358	1.70	25.87	55.0	33.7
13	0.1	21/01/2012	-64.92	113.3	45	AZ	259	363	46	314.9	-1.604	2.05	30.17	65.8	34.2
13	0.8	21/01/2012	-64.92	113.3	45	AZ	299	418	46	314.9	-1.604	2.05	30.17	65.8	34.2
13	3.0	21/01/2012	-64.92	113.3	45	AZ	115	160	46	314.9	-1.604	2.05	30.17	65.8	34.2
16	0.1	22/01/2012	-63.64	113.3	2	AZ	245	338	2	355.9	0.500	1.62	24.60	47.1	33.8
16	0.8	22/01/2012	-63.64	113.3	2	AZ	210	307	2	355.9	0.500	1.62	24.60	47.1	33.8
16	3.0	22/01/2012	-63.64	113.3	2	AZ	135	222	2	355.9	0.500	1.62	24.60	47.1	33.8
17	0.1	22/01/2012	-63.64	113.3	50	AZ	169	219	50	319.1	-1.352	2.06	29.69	63.3	34.2
17	0.8	22/01/2012	-63.64	113.3	50	AZ	227	315	50	319.1	-1.352	2.06	29.69	63.3	34.2
17	3.0	22/01/2012	-63.64	113.3	50	AZ	199	290	50	319.1	-1.352	2.06	29.69	63.3	34.2
18	0.1	24/01/2012	-61.84	113.5	310	CDW	474	666	314	186.8	1.909	2.35	34.09	83.2	34.6
18	0.8	24/01/2012	-61.84	113.5	310	CDW	466	676	314	186.8	1.909	2.35	34.09	83.2	34.6
18	3.0	24/01/2012	-61.84	113.5	310	CDW	136	172	314	186.8	1.909	2.35	34.09	83.2	34.6
19	0.1	24/01/2012	-61.84	113.5	950	CDW	138	205	962	202.4	1.624	2.18	31.59	95.1	34.7
19	0.8	24/01/2012	-61.84	113.5	950	CDW	124	153	962	202.4	1.624	2.18	31.59	95.1	34.7
19	3.0	24/01/2012	-61.84	113.5	950	CDW	214	315	962	202.4	1.624	2.18	31.59	95.1	34.7
21	0.1	25/01/2012	-60.40	115.0	2	AZ	287	385	2	335.8	2.462	1.75	26.62	16.2	33.9
21	0.8	25/01/2012	-60.40	115.0	2	AZ	217	296	2	335.8	2.462	1.75	26.62	16.2	33.9
21	3.0	25/01/2012	-60.40	115.0	2	AZ	153	240	2	335.8	2.462	1.75	26.62	16.2	33.9
22	0.1	25/01/2012	-60.40	115.0	85	AZ	318	458	86	336.4	1.724	1.96	28.52	24.7	33.9
22	0.8	25/01/2012	-60.40	115.0	85	AZ	298	418	86	336.4	1.724	1.96	28.52	24.7	33.9
22	3.0	25/01/2012	-60.40	115.0	85	AZ	323	420	86	336.4	1.724	1.96	28.52	24.7	33.9
25	0.1	27/01/2012	-56.19	115.0	500	CDW	297	423	506	187.7	2.296	2.39	35.09	72.9	34.5
25	0.8	27/01/2012	-56.19	115.0	500	CDW	595	736	506	187.7	2.296	2.39	35.09	72.9	34.5
25	3.0	27/01/2012	-56.19	115.0	500	CDW	307	396	506	187.7	2.296	2.39	35.09	72.9	34.5
26	0.1	27/01/2012	-56.19	115.0	1000	CDW	257	316	1012	190.1	2.107	2.23	32.90	80.7	34.7
26	0.8	27/01/2012	-56.19	115.0	1000	CDW	438	510	1012	190.1	2.107	2.23	32.90	80.7	34.7
26	3.0	27/01/2012	-56.19	115.0	1000	CDW	380	584	1012	190.1	2.107	2.23	32.90	80.7	34.7
27	0.1	27/01/2012	-56.19	115.0	2	AZ	368	491	2	324.8	4.159	1.64	25.32	9.60	33.8
27	0.8	27/01/2012	-56.19	115.0	2	AZ	318	454	2	324.8	4.159	1.64	25.32	9.60	33.8
27	3.0	27/01/2012	-56.19	115.0	2	AZ	288	394	2	324.8	4.159	1.64	25.32	9.60	33.8

Continued on following page.

Table 5.1: (cont.) Full sample data for advection study.

Sample	Fraction (μm)	Date	Latitude ($^{\circ}$)	Longitude ($^{\circ}$)	Depth (m)	Water mass	OTU count	Chao 1	Pressure (dbar)	Dissolved O ₂ ($\mu\text{mol/L}$)	Temperature ($^{\circ}\text{C}$)	Phosphate ($\mu\text{mol/L}$)	Nitrate ($\mu\text{mol/L}$)	Silicate ($\mu\text{mol/L}$)	Salinity (PSU)
29	0.1	28/01/2012	-53.81	115.0	80	AZ	281	394	80	324.4	4.399	1.66	24.78	7.80	33.8
29	0.8	28/01/2012	-53.81	115.0	80	AZ	261	377	80	324.4	4.399	1.66	24.78	7.80	33.8
29	3.0	28/01/2012	-53.81	115.0	80	AZ	271	403	80	324.4	4.399	1.66	24.78	7.80	33.8
30	0.1	29/01/2012	-52.65	115.0	85	AZ	217	341	86	330.8	3.517	1.73	26.27	15.7	33.8
30	0.8	29/01/2012	-52.65	115.0	85	AZ	244	358	86	330.8	3.517	1.73	26.27	15.7	33.8
30	3.0	29/01/2012	-52.65	115.0	85	AZ	269	393	86	330.8	3.517	1.73	26.27	15.7	33.8
31	0.1	29/01/2012	-52.65	115.0	2	AZ	392	486	2	332.2	3.941	1.70	26.15	15.4	33.8
31	0.8	29/01/2012	-52.65	115.0	2	AZ	317	470	2	332.2	3.941	1.70	26.15	15.4	33.8
31	3.0	29/01/2012	-52.65	115.0	2	AZ	332	425	2	332.2	3.941	1.70	26.15	15.4	33.8
32	0.1	30/01/2012	-49.99	115.0	2	PFZ	297	407	2	306.9	7.412	1.40	22.74	4.00	33.9
32	0.8	30/01/2012	-49.99	115.0	2	PFZ	269	337	2	306.9	7.412	1.40	22.74	4.00	33.9
32	3.0	30/01/2012	-49.99	115.0	2	PFZ	225	304	2	306.9	7.412	1.40	22.74	4.00	33.9
33	0.1	30/01/2012	-49.99	115.0	80	PFZ	325	422	80	300.3	7.061	1.39	23.02	4.20	34.0
33	0.8	30/01/2012	-49.99	115.0	80	PFZ	352	547	80	300.3	7.061	1.39	23.02	4.20	34.0
33	3.0	30/01/2012	-49.99	115.0	80	PFZ	326	473	80	300.3	7.061	1.39	23.02	4.20	34.0
38	0.1	03/02/2012	-43.99	115.0	2	SAMW	383	494	2	279.1	13.02	0.59	4.540	1.40	34.7
38	0.8	03/02/2012	-43.99	115.0	2	SAMW	215	220	2	279.1	13.02	0.59	4.540	1.40	34.7
38	3.0	03/02/2012	-43.99	115.0	2	SAMW	177	181	2	279.1	13.02	0.59	4.540	1.40	34.7
39	0.1	03/02/2012	-43.99	115.0	4320	AABW	520	682	4400	217.5	0.8497	2.30	32.92	127	34.7
39	0.8	03/02/2012	-43.99	115.0	4320	AABW	158	215	4400	217.5	0.8497	2.30	32.92	127	34.7
39	3.0	03/02/2012	-43.99	115.0	4320	AABW	129	152	4400	217.5	0.8497	2.30	32.92	127	34.7
40	0.1	03/02/2012	-43.99	115.0	4028	AABW	77	102	4100	216.9	0.8503	2.29	32.94	126	34.7
40	0.8	03/02/2012	-43.99	115.0	4028	AABW	156	203	4100	216.9	0.8503	2.29	32.94	126	34.7
40	3.0	03/02/2012	-43.99	115.0	4028	AABW	42	48	4100	216.9	0.8503	2.29	32.94	126	34.7
44	0.1	05/02/2012	-40.29	115.0	4775	AABW	248	303	4866	217.9	0.8716	2.28	33.15	130	34.7
44	0.8	05/02/2012	-40.29	115.0	4775	AABW	405	497	4866	217.9	0.8716	2.28	33.15	130	34.7
44	3.0	05/02/2012	-40.29	115.0	4775	AABW	370	442	4866	217.9	0.8716	2.28	33.15	130	34.7
45	0.1	05/02/2012	-40.29	115.0	1100	AAIW	601	779	1112	199.4	4.321	2.12	31.29	33.9	34.4
45	0.8	05/02/2012	-40.29	115.0	1100	AAIW	150	151	1112	199.4	4.321	2.12	31.29	33.9	34.4
45	3.0	05/02/2012	-40.29	115.0	1100	AAIW	118	124	1112	199.4	4.321	2.12	31.29	33.9	34.4
46	0.1	07/02/2012	-37.05	115.0	1100	AAIW	166	176	1112	201.7	5.233	2.20	32.12	39.5	34.4
46	0.8	07/02/2012	-37.05	115.0	1100	AAIW	227	312	1112	201.7	5.233	2.20	32.12	39.5	34.4
46	3.0	07/02/2012	-37.05	115.0	1100	AAIW	251	360	1112	201.7	5.233	2.20	32.12	39.5	34.4
47	0.1	07/02/2012	-37.05	115.0	5827	AABW	138	248	5952	217.2	1.030	2.29	33.00	129	34.7
47	0.8	07/02/2012	-37.05	115.0	5827	AABW	379	509	5952	217.2	1.030	2.29	33.00	129	34.7
47	3.0	07/02/2012	-37.05	115.0	5827	AABW	106	123	5952	217.2	1.030	2.29	33.00	129	34.7

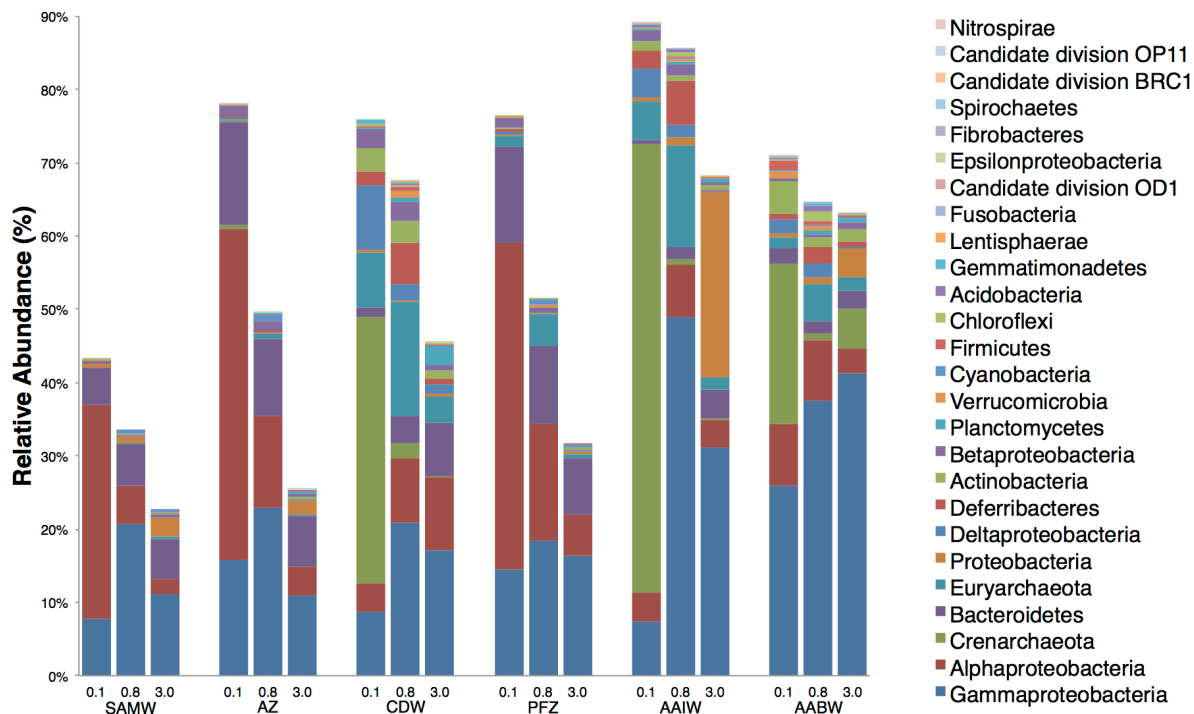


Figure 5.2: Taxonomic assignments for each sampled water mass. Water masses (x-axis): Subantarctic Mode Water (SAMW); Antarctic Zone (AZ); Circumpolar Deep Water (CDW); Polar Frontal Zone (PFZ); Antarctic Intermediate Water (AAIW); Antarctic Bottom Water (AABW). Size fractions are given in μm . All OTUs aggregated to phylum, except for members of the Proteobacteria which were aggregated to class when known. Relative abundance is percentage of all reads assigned to a given taxonomic group and has been scaled to account for unassigned reads.

nMDS ordination showed that the sampled water masses could be distinguished on the basis of taxonomic distance (Fig. 5.3). This was supported by ANOSIM analysis ($R = 0.77$, $p = 0.001$). While each water mass had a distinct taxonomic profile, some broad differences between surface and deep masses were observed (Fig. 5.2). Surface waters (AZ, PFZ, SAMW) were dominated by representatives of the Alphaproteobacteria, Bacteroidetes and Gammaproteobacteria. The high abundance of Bacteroidetes at the surface reflects their association with phytoplankton, as many species in this lineage specialise in the degradation of high molecular weight products of primary production (Williams *et al.*, 2012b). Alphaproteobacteria were represented primarily by the SAR11 clade, abundant in ocean surface communities (Morris *et al.*, 2002) including the SO (Brown *et al.*, 2012), and Roseobacter clades, which have also been associated with degradation of phytoplankton products (Williams *et al.*, 2012b; Giebel *et al.*, 2009). The dominant Gammaproteobacterial orders were the Alteromonadales and Oceanospirillales, typical of SO surface waters (Wilkins *et al.*, 2012b). Few archaeal OTUs were detected, consistent with their well-described decline in abundance during summer (Murray *et al.*, 1998; Grzymski *et al.*, 2012). The deep water masses (CDW, AAIW, AABW) were dominated by Crenarchaeota, Euryarchaeota and Gammaproteobacteria, again consistent with previous findings (López-García *et al.*, 2001).

Environment and distance effects

nMDS ordination showed that the sampled water masses clustered well on the basis of environmental distance (Fig. 5.4). This was supported by ANOSIM ($R = 0.84$, $p = 0.001$). A partial Mantel test, comparing the taxonomic to environmental matrices with the spatial matrix held constant, found a correlation of $r = 0.48$ ($p = 0.001$), indicating a strong environment effect.

distLM analysis of the individual physicochemical variables found that considered separately, each of phosphate, silicate, nitrate, oxygen, salinity and pressure explained 17–35% of the taxonomic variance between samples ($p = 0.001$). Temperature had no significant effect on taxonomic composition when considered separately ($p > 0.05$). When all combinations of variables were considered (BEST

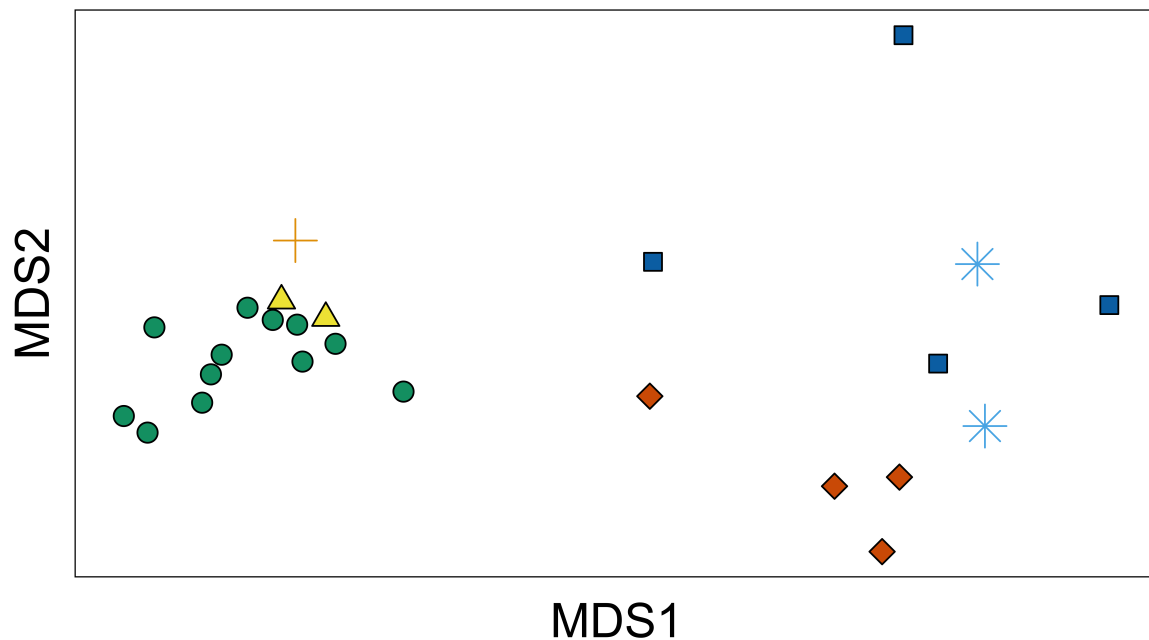


Figure 5.3: nMDS ordination of the taxonomic distance matrix (2D stress = 0.08). Antarctic Intermediate Waters (AAIW), light blue stars; Subantarctic Mode Water (SAMW), orange crosses; Antarctic Bottom Water (AABW), dark blue squares; Antarctic Zone (AZ), green circles; Polar Frontal Zone (PFZ), yellow triangles; Circumpolar Deep Water (CDW), red diamonds.

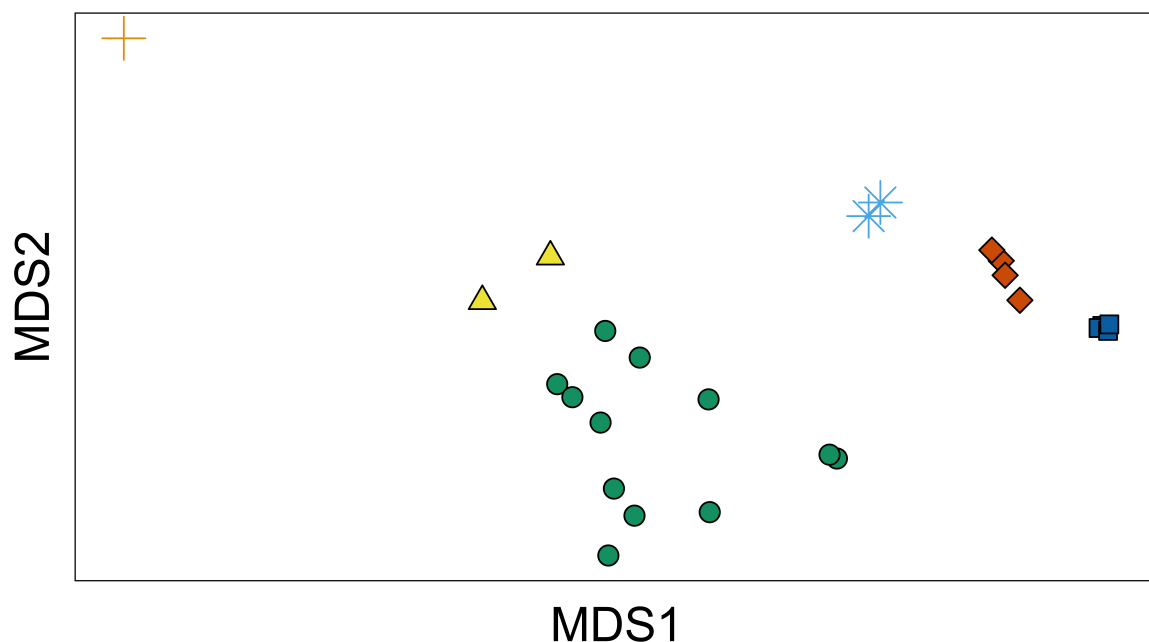


Figure 5.4: nMDS ordination of the environmental distance matrix (2D stress = 0.02). Antarctic Intermediate Waters (AAIW), light blue stars; Subantarctic Mode Water (SAMW), orange crosses; Antarctic Bottom Water (AABW), dark blue squares; Antarctic Zone (AZ), green circles; Polar Frontal Zone (PFZ), yellow triangles; Circumpolar Deep Water (CDW), red diamonds.

modelling), the best model consisted of all variables with the exception of phosphate (adjusted $R^2 = 0.44$), with the full set of variables only marginally worse (adjusted $R^2 = 0.43$). The rejection of phosphate may reflect a redundancy in the measurement of both phosphate and nitrate; these are often held to be constant throughout the ocean at the Redfield ratio of N:P $\sim 16:1$ (Anderson and Sarmiento, 1994). However, deviation from this ratio has been observed in the SO and related to iron concentration (which was not measured in this study) and to phytoplankton abundance (Weber and Deutsch, 2010). For these reasons, and because of the marginal effect of discarding phosphate from the variable selection, it was retained when generating the environmental distance matrix.

The dbRDA plot showed the six variables retained by the distLM model (i.e. all except phosphate) structured the samples first along an axis separating surface and deep samples (dbRDA1), strongly related to dissolved oxygen ($r = 0.79$) (Fig. 5.5). The second axis was best correlated with temperature ($r = -0.75$). All six retained variables had a moderate correlation with at least one of the first two axes (Table 5.2). As with the nMDS ordinations (Figs. 5.3, 5.4 and 5.6), the water masses were generally well separated by the first two dbRDA axes. Samples from the AABW and AAIW, which were not separated by the first two axes, were clearly separated along the third (Table 5.2), which was best correlated with pressure ($r = -0.79$). This suggests that these two masses had similar physicochemical properties, and were mainly distinguished by depth, consistent with their common origin in sinking Antarctic Surface Waters (Foldvik and Gammelsrød, 1988).

Table 5.2: Correlations between dbRDA coordinate axes and physicochemical variables (multiple partial correlations).

Variable	dbRDA1	dbRDA2	dbRDA3	dbRDA4	dbRDA5	dbRDA6
Pressure	- 0.316	- 0.485	- 0.787	- 0.148	- 0.144	- 0.048
Oxygen	0.792	- 0.171	- 0.125	0.069	- 0.567	0.050
Temperature	- 0.025	- 0.750	0.366	0.236	0.180	0.463
Nitrate	- 0.311	0.007	0.325	- 0.636	- 0.561	0.281
Silicate	- 0.303	0.341	- 0.166	0.615	- 0.371	0.498
Salinity	- 0.290	- 0.239	0.311	0.368	- 0.417	- 0.673

A distance effect was detected by comparing the taxonomic and spatial matrices with the environmental matrix held constant (partial Mantel; $r = 0.38$, $p = 0.003$). This indicated that a process other than contemporary environmental selection was appreciably affecting variation in microbial community composition.

Testing the advection effect

244,000 encounters were recorded between particles and sample sites during the 100 year advection simulation. Encounter times spanned the full range of the simulation (5 days–100 years), with a median of 30 days and mean of 3018 days. 47 pairs of samples did not yield mutual encounters (i.e. at least one particle from one sample encountering the other). Of these, every pair included at least one AABW sample.

nMDS ordination showed that the sampled water masses could be broadly distinguished on the basis of their mutual advection distances (Fig. 5.6). This was supported by ANOSIM ($R = 0.41$, $p = 0.002$).

A partial Mantel test, comparing the taxonomic and advection matrices with the spatial and environmental matrices held constant, showed that advection has a moderate ($r = 0.28$) and significant ($p = 0.010$) correlation with taxonomic composition independent of spatial and environmental factors. To ensure this result was not unduly influenced by the samples on which the 100 year ceiling was imposed (AABW) and those for which particle releases were not simulated (samples 11, 13, 17 and 22), the test was repeated with these samples removed. The correlation was stronger and remained significant despite the smaller sample size ($r = 0.36$, $p = 0.025$). To ensure the result was robust to the choice of advection distance metric, correlations were recalculated for both the full set of samples and the subset (excluding AABW and samples 11, 13, 17 and 22) with pairwise advection distance

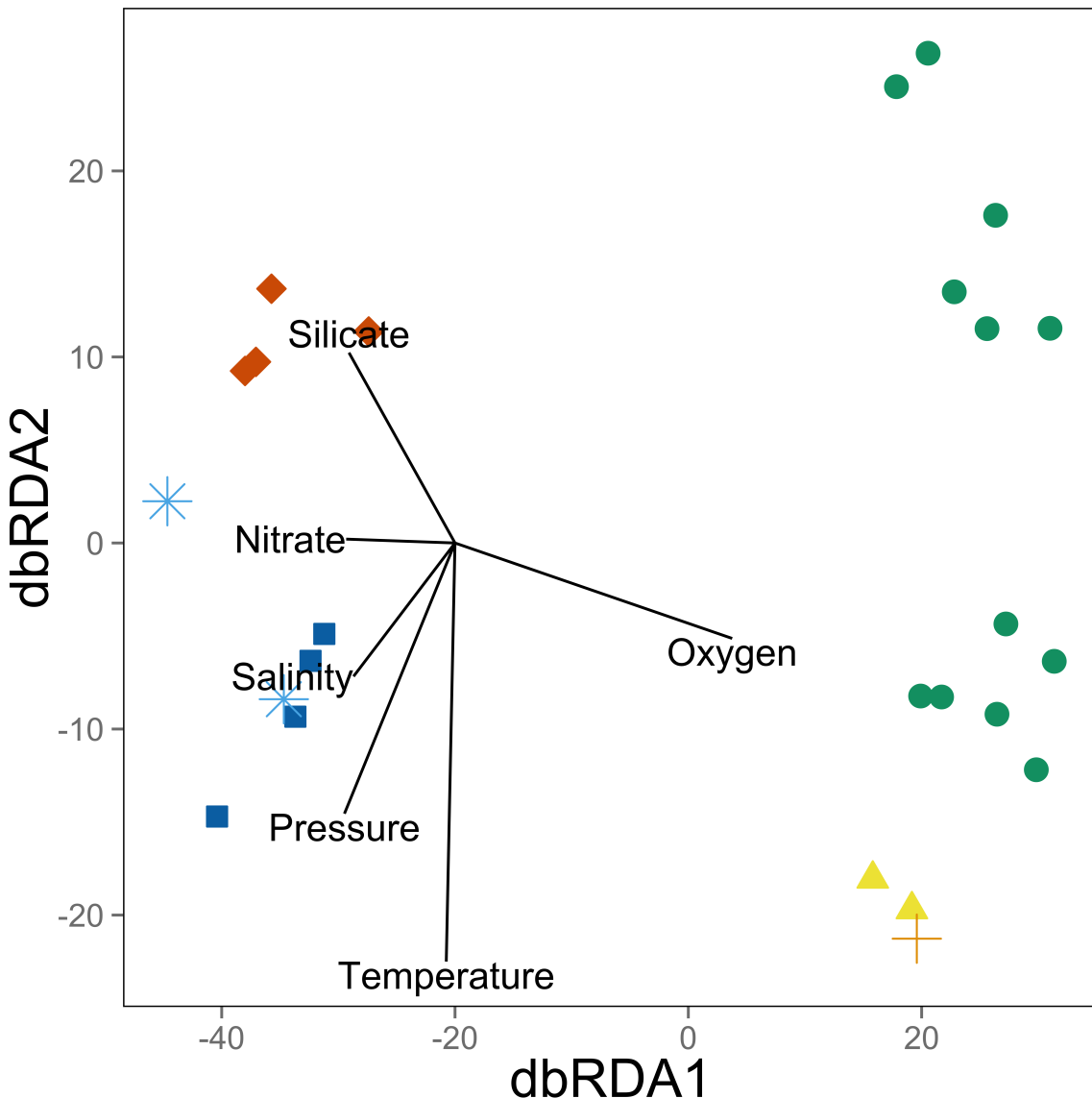


Figure 5.5: dbRDA ordination of the distLM model describing the relationship between the BEST-selected set of predictor physicochemical variables (pressure, oxygen, temperature, salinity, silicate, and nitrate) and the taxonomic dissimilarity between samples. Vectors represent the effect of each predictor variable on the two visualised axes. Vector length corresponds to the relative size of the effect, while direction represents the correlations to the two displayed axes. The first axis (dbRDA1) captures 64% of fitted and 37% of total variation between the samples' taxonomic profiles; the second (dbRDA2) captures 14% of fitted and 8% of total variation. Antarctic Intermediate Waters (AAIW), light blue stars; Subantarctic Mode Water (SAMW), orange crosses; Antarctic Bottom Water (AABW), dark blue squares; Antarctic Zone (AZ), green circles; Polar Frontal Zone (PFZ), yellow triangles; Circumpolar Deep Water (CDW), red diamonds.

defined as the mean time for all particle encounters between samples. The observed correlation was higher using this metric for both the full set ($r = 0.40, p = 0.0090$) and subset ($r = 0.52, p = 0.0070$). SOURCETRACKER analysis confirmed that the effect was moderately directional, with the proportion of OTUs contributed from a given “source” sample to a “sink” sample correlated with the proportion of particle encounters it generates (Spearman’s $\rho = 0.15, p = 0.0015$).

To explore the role of taxonomic resolution in the detection of an advection effect, partial Mantel tests were repeated as above with OTUs aggregated to each of the seven standard taxonomic ranks.

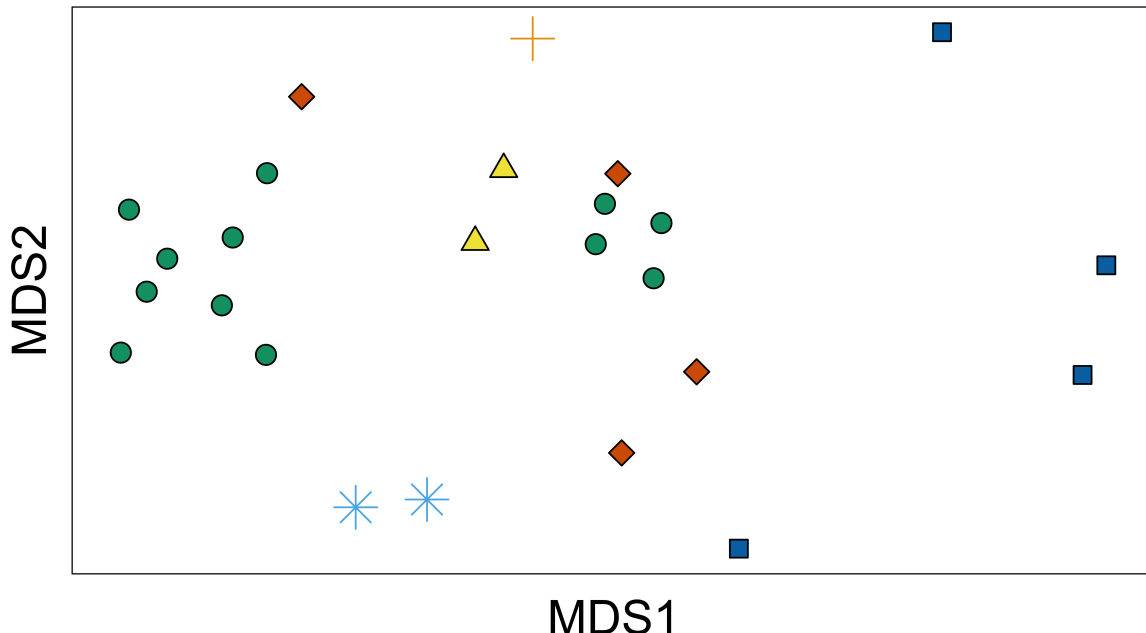


Figure 5.6: nMDS ordination of the advection distance matrix (2D stress = 0.19). Antarctic Intermediate Waters (AAIW), light blue stars; Subantarctic Mode Water (SAMW), orange crosses; Antarctic Bottom Water (AABW), dark blue squares; Antarctic Zone (AZ), green circles; Polar Frontal Zone (PFZ), yellow triangles; Circumpolar Deep Water (CDW), red diamonds.

Aggregation to genus resulted in a higher correlation ($r = 0.29$, $p = 0.02$) than to species, but with this exception a pattern of decreasing correlation with coarser rank was observed (Fig. 5.7).

Testing advection effect mechanisms

Two explanations can be proposed for the relationship between advection and community composition. The first is that advection increases microbial dispersal by increasing the probability that OTUs from one site will encounter and colonise another (the “dispersal mechanism”). This assumes microbial dispersal is less than perfect; i.e. that “everything is not everywhere”. The second is that advection transports a large numbers of cells at a rate measurably outpacing environmental selection, regardless of whether or not those cells are able to successfully colonise (i.e. grow and reproduce in) downstream sites: that “the environment selects, but not fast enough” (the “bulk transport mechanism”). Considering the long advection times between sites in this study, the relatively rapid growth of marine microorganisms, and the ability of small numbers of cells to rapidly reduce β -diversity between isolated marine sites (Declerck *et al.*, 2013), the dispersal mechanism seems the more plausible.

Two tests were performed to distinguish between these hypotheses. Firstly, the advection distance matrix was reconstructed using the absolute pairwise number of particle encounters as the distance metric between samples (distance metric for given sample pair = maximum number of encounters across all sample pairs – encounters for given pair + 1). There was no significant correlation between this matrix and the taxonomic distance matrix when the environmental and spatial matrices were held constant ($p > 0.05$). This suggests that advection time, not the absolute number of transported cells, is the relevant factor, supporting the dispersal mechanism.

Secondly, it was reasoned that under the dispersal mechanism, advection would have a large effect on the presence and diversity of taxa and a smaller effect on their abundances; while if the bulk transport hypothesis held, the effect would largely be on the relative abundances. To test this, the taxonomic profiles were transformed to a presence/absence measure (OTU present = 1, absent = 0), and a matrix of Sørensen dissimilarities generated. The advection effect was stronger ($r = 0.33$, $p = 0.004$) than when abundances were considered, again supporting the dispersal hypothesis.

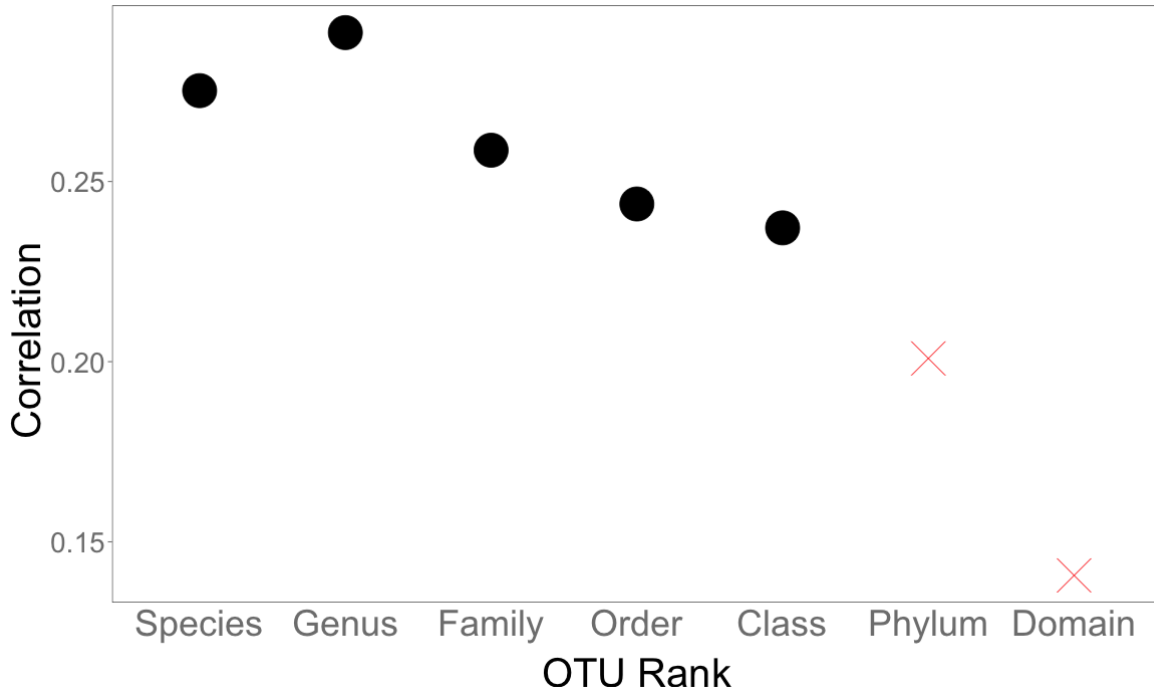


Figure 5.7: Effect of taxonomic resolution on partial Mantel correlation between advection and taxonomic distances, with environmental and spatial distances held constant. Significant correlations (right-tailed p-value after 999 random permutations > 0.05), black circles; not significant correlations (≤ 0.05), red crosses.

Discussion

This study found good support for the hypothesis that advection shapes microbial assemblages independent of an environment or distance effect. Communities that are more closely connected by advection are more similar, and this effect exists even when environment and distance effects are controlled for. The results also indicate that advection primarily shapes microbial community structure by increasing opportunities for colonisation, rather than transporting large numbers of cells to downstream sites.

The major alternative hypothesis for the observed correlation is that there exists an unmeasured environmental variable (e.g. iron concentration, pH) which correlates well with both advection and community composition. As in all studies of historical influences on microbial biogeography, it is impossible to eliminate all potential confounding variables. However, a rigorous confirmation of the advection effect will require future work to measure physicochemical parameters as comprehensively as possible.

The amount of variance in taxonomic composition explained by the advection effect can be estimated as the square of the correlation coefficient (r^2). This value, 7%, is likely to be a conservative estimate, as this study only captured advective pathways from one sample to another; it is possible that some samples with a large mutual advective distance shared a common advective source outside the study area. A recent review of studies partitioning variance in microbial community composition found that the mean reported variance explained by a distance effect was 10%, and by an environment effect 27% (Hanson *et al.*, 2012). The estimated proportions of variance in this study, 14% ($p = 0.001$) for distance and 23% ($p = 0.001$) for environment, were close to these values. While there are no comparative data for the advection effect in other systems, the value of at least 7% for the SO indicates that advection is important relative to both distance and environment effects.

Taxonomic resolution (i.e. the level of genetic difference at which OTUs are discriminated) often determines whether or not a pattern is detected in studies of microbial distance effects, with finer resolutions generally leading to an increased likelihood of detecting a significant effect (Hanson *et al.*, 2012). Surprisingly, aggregation to genus resulted in a higher correlation than to species (Fig. 5.7). This

may be because of the selection of the V6–V8 hypervariable regions as the sequencing target. Amplification of the V6 region alone has been shown to underestimate species richness, while targeting the V7–V8 region overestimates it (Youssef *et al.*, 2009). It is possible that due to this choice of target, the “species”-level aggregation represents a much finer taxonomic resolution at which intra-species variability begins to overwhelm the advection effect. With this exception, the pattern of a decreasing effect with coarser taxonomic resolution was confirmed, with no statistically significant effect for aggregation to phylum or domain.

Future work

To obtain a better understanding of the advection effect, it would be useful to determine whether particular taxonomic or physiological groups are more amenable to dispersal by advection; e.g. through the formation of dormant spores (Sul *et al.*, 2013; Bissett *et al.*, 2010). As it is possible that an unmeasured environmental variable (e.g. iron concentration, see Discussion) also correlates with both advection and community composition, future studies should address this. Finally, further mesocosm experiments like those reported by Declerck *et al.* (2013) will be useful to confirm the effect of small-scale exchange of cells between sites on colonisation and community structure.

References

- Abell G. C. J. and Bowman J. P. (2005). Colonization and community dynamics of class *Flavobacteria* on diatom detritus in experimental mesocosms based on Southern Ocean seawater. *FEMS Microbiology Ecology*, 53(3):379–391.
- Abell G. G. J. and Bowman J. P. (2005). Ecological and biogeographic relationships of class Flavobacteria in the Southern Ocean. *FEMS Microbiology Ecology*, 51:265–277.
- Agogué H., Lamy D., Neal P. R., Sogin M. L., and Herndl G. J. (2011). Water mass-specificity of bacterial communities in the North Atlantic revealed by massively parallel sequencing. *Molecular Ecology*, 20(2):258–274.
- Alonso C. and Pernthaler J. (2006). Roseobacter and SAR11 dominate microbial glucose uptake in coastal North Sea waters. *Environmental Microbiology*, 8(11):2022–2030.
- Anderson L. A. and Sarmiento J. L. (1994). Redfield ratios of remineralization determined by nutrient data analysis. *Global Biogeochemical Cycles*, 8(1):65–80.
- André J. M., Navarette C., Blanchot J., and Radenac M. H. (1999). Picophytoplankton dynamics in the equatorial Pacific: Growth and grazing rates from cytometric counts. *Journal of Geophysical Research*, 104(C2):3369–3380.
- Angly F. E., Felts B., Breitbart M., Salamon P., Edwards R. A., Carlson C., Chan A. M., Haynes M., Kelley S., Liu H., Mahaffy J. M., Mueller J. E., Nulton J., Olson R., Parsons R., Rayhawk S., Suttle C. A., and Rohwer F. (2006). The marine viromes of four oceanic regions. *PLoS Biology*, 4(11):e368.
- Angly F. E., Willner D., Prieto-Davó A., Edwards R. A., Schmieder R., Vega-Thurber R., Antonopoulos D. A., Barott K., Cottrell M. T., Desnues C., Dinsdale E. A., Furlan M., Haynes M., Henn M. R., Hu Y., Kirchman D. L., McDole T., McPherson J. D., Meyer F., Miller R. M., Mundt E., Naviaux R. K., Rodriguez-Mueller B., Stevens R., Wegley L., Zhang L., Zhu B., and Rohwer F. (2009). The GAAS Metagenomic Tool and Its Estimations of Viral and Microbial Average Genome Size in Four Major Biomes. *PLoS Computational Biology*, 5(12):e1000593.
- Aoki S., Yoritaka M., and Masuyama A. (2003). Multidecadal warming of subsurface temperature in the Indian sector of the Southern Ocean. *Journal of Geophysical Research*, 108(C4):8081–8088.
- Baas Becking L. G. M. *Geobiologie Of Inleiding Tot De Milieukunde*. W.P. Van Stockum & Zoon, The Hague, 1934.
- Beja O., Aravind L., Koonin E. V., Suzuki M. T., Hadd A., Nguyen L. P., Jovanovich S. B., Gates C. M., Feldman R. A., Spudich J. L., Spudich E. N., and DeLong E. F. (2000). Bacterial rhodopsin: evidence for a new type of phototrophy in the sea. *Science*, 289(5486):1902–1906.
- Béjà O., Suzuki M. T., Heidelberg J. F., Nelson W. C., Preston C. M., Hamada T., Eisen J. A., Fraser C. M., and DeLong E. F. (2002). Unsuspected diversity among marine aerobic anoxygenic phototrophs. *Nature*, 415(6872):630–633.
- Berg I. A., Kockelkorn D., Buckel W., and Fuchs G. (2007). A 3-Hydroxypropionate/4-Hydroxybutyrate Autotrophic Carbon Dioxide Assimilation Pathway in Archaea. *Science*, 318(5857):1782–1786.

- Bidle K. D. and Azam F. (2001). Bacterial control of silicon regeneration from diatom detritus: significance of bacterial ectohydrolases and species identity. *Limnology and Oceanography*, 46(7):1606–1623.
- Biebl H., Allgaier M., Tindall B. J., Kobližek M., Lünsdorf H., Pukall R., and Wagner-Döbler I. (2005). *Dinoroseobacter shibae* gen. nov., sp. nov., a new aerobic phototrophic bacterium isolated from dinoflagellates. *International Journal of Systematic and Evolutionary Microbiology*, 55(Pt 3):1089–1096.
- Bissett A., Richardson A. E., Baker G., Wakelin S., and Thrall P. H. (2010). Life history determines biogeographical patterns of soil bacterial communities over multiple spatial scales. *Molecular Ecology*, 19(19):4315–4327.
- Böning C. W., Dispert A., Visbeck M., Rintoul S. R., and Schwarzkopf F. U. (2008). The response of the Antarctic Circumpolar Current to recent climate change. *Nature Geoscience*, 1(12):864–869.
- Bowman J. P. and McCuaig R. D. (2003). Biodiversity, community structural shifts, and biogeography of prokaryotes within Antarctic continental shelf sediment. *Applied and Environmental Microbiology*, 69(5):2463–2483.
- Bowman J. P., Rea S. M., McCammon S. A., and McMeekin T. A. (2000). Diversity and community structure within anoxic sediment from marine salinity meromictic lakes and a coastal meromictic marine basin, Vestfold Hills, Eastern Antarctica. *Environmental Microbiology*, 2(2):227–237.
- Boyd P. W., Jickells T., Law C. S., Blain S., Boyle E. A., Buesseler K. O., Coale K. H., Cullen J. J., Baar H. J. W.de, Follows M., Harvey M., Lancelot C., Levasseur M., Owens N. P. J., Pollard R., Rivkin R. B., Sarmiento J., Schoemann V., Smetacek V., Takeda S., Tsuda A., Turner S., and Watson A. J. (2007). Mesoscale Iron Enrichment Experiments 1993–2005: Synthesis and Future Directions. *Science*, 315(5812):612–617.
- Brinkhoff T., Giebel H.-A., and Simon M. (2008). Diversity, ecology, and genomics of the Roseobacter clade: a short overview. *Archives of Microbiology*, 189(6):531–539.
- Brinkmeyer R., Knittel K., Jürgens J., Weyland H., Amann R., and Helmke E. (2003). Diversity and Structure of Bacterial Communities in Arctic versus Antarctic Pack Ice. *Applied and Environmental Microbiology*, 69(11):6610–6619.
- Brown M. V. and Bowman J. P. (2001). A molecular phylogenetic survey of sea-ice microbial communities (SIMCO). *FEMS Microbiology Ecology*, 35(3):267–275.
- Brown M. V., Lauro F. M., DeMaere M. Z., Muir L., Wilkins D., Thomas T., Riddle M. J., Fuhrman J. A., Andrews-Pfannkoch C., Hoffman J. M., McQuaid J. B., Allen A., Rintoul S. R., and Cavicchioli R. (2012). Global biogeography of SAR11 marine bacteria. *Molecular systems biology*, 8.
- Buchan A., González J. M., and Moran M. A. (2005). Overview of the marine Roseobacter lineage. *Applied and Environmental Microbiology*, 71(10):5665–5677.
- Callahan J. E. (1972). The structure and circulation of deep water in the Antarctic. *Deep Sea Research and Oceanographic Abstracts*, 19(8):563–575.
- Campanaro S., Williams T. J., Burg D. W., De Francisci D., Treu L., Lauro F. M., and Cavicchioli R. (2011). Temperature-dependent global gene expression in the Antarctic archaeon *Methanococcoides burtonii*. *Environmental Microbiology*, 13(8):2018–2038.
- Canfield D. E., Stewart F. J., Thamdrup B., De Brabandere L., Dalsgaard T., DeLong E. F., Revsbech N. P., and Ulloa O. (2010). A Cryptic Sulfur Cycle in Oxygen-Minimum-Zone Waters off the Chilean Coast. *Science*, 330(6009):1375–1378.
- Caporaso J. G., Kuczynski J., Stombaugh J., Bittinger K., Bushman F. D., Costello E. K., Fierer N., Pena A. G., Goodrich J. K., and Gordon J. I. (2010). QIIME allows analysis of high-throughput community sequencing data. *Nature methods*, 7(5):335–336.
- Carlson C. A., Morris R., Parsons R., Treusch A. H., Giovannoni S. J., and Vergin K. (2009). Seasonal dynamics of SAR11 populations in the euphotic and mesopelagic zones of the northwestern Sargasso Sea. *The ISME Journal*, 3(3):283–295.

- Cavicchioli R. (2006). Cold-adapted archaea. *Nature Reviews Microbiology*, 4(5):331–343.
- Cerovečki I., Talley L. D., and Mazloff M. R. (2011). A comparison of Southern Ocean air-sea buoyancy flux from an ocean state estimate with five other products. *Journal of Climate*, 24:6283–6306.
- Chiba S., Ishimaru T., Hosie G. W., and Fukuchi M. (2001). Spatio-temporal variability of zooplankton community structure off east Antarctica (90 to 160°E). *Marine Ecology Progress Series*, 216:95–108.
- Cho J. C. and Giovannoni S. J. (2004). Cultivation and Growth Characteristics of a Diverse Group of Oligotrophic Marine Gammaproteobacteria. *Applied and Environmental Microbiology*, 70(1):432–440.
- Cho J.-C. and Tiedje J. M. (2000). Biogeography and degree of endemism of fluorescent Pseudomonas strains in soil. *Applied and Environmental Microbiology*, 66(12):5448–5456.
- Christaki U., Obernosterer I., Van Wambeke F., Veldhuis M., Garcia N., and Catala P. (2008). Microbial food web structure in a naturally iron-fertilized area in the Southern Ocean (Kerguelen Plateau). *Deep Sea Research Part II: Topical Studies in Oceanography*, 55(5-7):706–719.
- Church M. J., DeLong E. F., Ducklow H. W., Karner M. B., Preston C. M., and Karl D. M. (2003). Abundance and distribution of planktonic Archaea and Bacteria in the waters west of the Antarctic Peninsula. *Limnology and Oceanography*, 48(5):1893–1902.
- Clarke K. R. and Gorley R. N. *PRIMER v6: User Manual / Tutorial*, 1st edition edition, 2006.
- Clarke K. R. and Warwick R. M. (1998). Quantifying structural redundancy in ecological communities. *Oecologia*, 113(2):278–289.
- Clarke K. R. and Warwick R. M. *Change in marine communities: an approach to statistical analysis and interpretation*. PRIMER-E, Plymouth, 2nd edition, 2001.
- Coleman M. L. M. and Chisholm S. W. S. (2010). Ecosystem-specific selection pressures revealed through comparative population genomics. *Proceedings Of The National Academy Of Sciences Of The United States Of America*, 107(43):18634–18639.
- Cottrell M. T. and Kirchman D. L. (2000). Community Composition of Marine Bacterioplankton Determined by 16S rRNA Gene Clone Libraries and Fluorescence In Situ Hybridization. *Applied and Environmental Microbiology*, 66(12):5116–5122.
- Cottrell M. T., Waidner L. A., Yu L., and Kirchman D. L. (2005). Bacterial diversity of metagenomic and PCR libraries from the Delaware River. *Environmental Microbiology*, 7(12):1883–1895.
- Cox P. M., Betts R. A., Jones C. D., Spall S. A., and Totterdell I. J. (2000). Acceleration of global warming due to carbon-cycle feedbacks in a coupled climate model. *Nature*, 408(6809):184–187.
- Crump B. C., Armbrust E. V., and Baross J. A. (1999). Phylogenetic analysis of particle-attached and free-living bacterial communities in the Columbia River, its estuary, and the adjacent coastal ocean. *Applied and Environmental Microbiology*, 65(7):3192–3204.
- Curson A. R. J., Todd J. D., Sullivan M. J., and Johnston A. W. B. (2011). Catabolism of dimethylsulphoniopropionate: microorganisms, enzymes and genes. *Nature Reviews Microbiology*, 9(12):849–859.
- Wit R.de and Bouvier T. (2006). 'Everything is everywhere, but, the environment selects'; what did Baas Becking and Beijerinck really say? *Environmental Microbiology*, 8(4):755–758.
- Deacon G. E. R. (1982). Physical and biological zonation in the Southern Ocean. *Deep Sea Research Part A: Oceanographic Research Papers*, 29(1):1–15.
- Declerck S. A. J., Winter C., Shurin J. B., Suttle C. A., and Matthews B. (2013). Effects of patch connectivity and heterogeneity on metacommunity structure of planktonic bacteria and viruses. *The ISME Journal*, 7(3):533–542.
- DeLong E. F., Franks D. G., and Alldredge A. L. (1993). Phylogenetic Diversity of Aggregate-Attached vs. Free-Living Marine Bacterial Assemblages. *Limnology and Oceanography*, 38(5):924–934.

- DeLong E. F., Wu K. Y., Prézelin B. B., and Jovine R. V. (1994). High abundance of Archaea in Antarctic marine picoplankton. *Nature*, 371(6499):695–697.
- Dinsdale E. A., Edwards R. A., Hall D., Angly F., Breitbart M., Brulc J. M., Furlan M., Desnues C., Haynes M., Li L., McDaniel L., Moran M. A., Nelson K. E., Nilsson C., Olson R., Paul J., Brito B. R., Ruan Y., Swan B. K., Stevens R., Valentine D. L., Thurber R. V., Wegley L., White B. A., and Rohwer F. (2008). Functional metagenomic profiling of nine biomes. *Nature*, 452(7187):629–632.
- Dixon J. L., Beale R., and Nightingale P. D. (2011). Rapid biological oxidation of methanol in the tropical Atlantic: significance as a microbial carbon source. *Biogeosciences Discussions*, 8(2):3899–3921.
- Ducklow H. W., Myers K., Erickson M., Ghiglione J. F., and Murray A. E. (2011). Response of a summertime Antarctic marine -bacterial community to glucose and ammonium enrichment. *Aquatic Microbial Ecology*, 64(3):205–220.
- Dupont C. L., Rusch D. B., Yooseph S., Lombardo M.-J., Richter R. A., Valas R., Novotny M., Yee-Greenbaum J., Selengut J. D., Haft D. H., Halpern A. L., Lasken R. S., Nealson K., Friedman R., and Venter J. C. (2011). Genomic insights to SAR86, an abundant and uncultivated marine bacterial lineage. pages 1–14.
- Eilers H., Pernthaler J., Glöckner F. O., and Amann R. (2000). Culturability and In Situ Abundance of Pelagic Bacteria from the North Sea. *Applied and Environmental Microbiology*, 66(7):3044–3051.
- El-Sayed S. Z. (2005). History and evolution of primary productivity studies of the Southern Ocean. *Polar Biology*, 28(6):423–438.
- Esper O. and Zonneveld K. A. F. (2002). Distribution of organic-walled dinoflagellate cysts in surface sediments of the Southern Ocean (eastern Atlantic sector) between the Subtropical Front and the Weddell Gyre. *Marine Micropaleontology*, 46(1):177–208.
- Evans C., Pearce I., and Brussaard C. P. D. (2009). Viral-mediated lysis of microbes and carbon release in the sub-Antarctic and Polar Frontal zones of the Australian Southern Ocean. *Environmental Microbiology*, 11(11):2924–2934.
- Evans C., Thomson P. G., Davidson A. T., Bowie A. R., Enden R. van den, Witte H., and Brussaard C. P. D. (2011). Potential climate change impacts on microbial distribution and carbon cycling in the Australian Southern Ocean. *Deep Sea Research Part II: Topical Studies in Oceanography*, 58(21-22):2150–2161.
- Fandino L. B., Riemann L., Steward G. F., Long R. A., and Azam F. (2001). Variations in bacterial community structure during a dinoflagellate bloom analyzed by DGGE and 16S rDNA sequencing. *Aquatic Microbial Ecology*, 23:119.
- Feller G. and Gerday C. (2003). Psychrophilic enzymes: hot topics in cold adaptation. *Nature Reviews Microbiology*, 1(3):200–208.
- Firing Y. L., Chereskin T. K., and Mazloff M. R. (2011). Vertical structure and transport of the Antarctic Circumpolar Current in Drake Passage from direct velocity observations. *Journal of Geophysical Research*, 116(C8):C08015.
- Foldvik A. and Gammelsrød T. (1988). Notes on Southern Ocean hydrography, sea-ice and bottom water formation. *Palaeogeography, Palaeoclimatology, Palaeoecology*, 67(1-2):3–17.
- Freitas S., Hatosy S., Fuhrman J. A., Huse S. M., Welch D. B. M., Sogin M. L., and Martiny A. C. (2012). Global distribution and diversity of marine *Verrucomicrobia*. *The ISME Journal*, 6(8):1499–1505.
- Fuhrman J. A., Schwalbach M. S., and Stingl U. (2008). Proteorhodopsins: an array of physiological roles? *Nature Reviews Microbiology*, 6:488–494.
- Fyfe J. C. and Saenko O. A. (2005). Human-induced change in the Antarctic Circumpolar Current. *Journal of Climate*, 18(15):3068–3073.

- Galand P. E., Potvin M., Casamayor E. O., and Lovejoy C. (2009). Hydrography shapes bacterial biogeography of the deep Arctic Ocean. *Nature*, 4(4):564–576.
- García-Martínez J. and Rodríguez-Valera F. (2000). Microdiversity of uncultured marine prokaryotes: the SAR11 cluster and the marine Archaea of Group I. *Molecular Ecology*, 9(7):935–948.
- Gentile G., Giuliano L., D'Auria G., Smedile F., Azzaro M., De Domenico M., and Yakimov M. M. (2006). Study of bacterial communities in Antarctic coastal waters by a combination of 16S rRNA and 16S rDNA sequencing. *Environmental Microbiology*, 8(12):2150–2161.
- Ghiglione J. F. and Murray A. E. (2011). Pronounced summer to winter differences and higher wintertime richness in coastal Antarctic marine bacterioplankton. *Environmental Microbiology*, 14(3): 617–629.
- Ghiglione J.-F., Galand P. E., Pommier T., Pedrós-Alió C., Maas E. W., Bakker K., Bertilson S., Kirchmanj D. L., Lovejoy C., Yager P. L., and Murray A. E. (2012). Pole-to-pole biogeography of surface and deep marine bacterial communities. *Proceedings Of The National Academy Of Sciences Of The United States Of America*, 109(43):17633–17638.
- Giebel H.-A., Brinkhoff T., Zwisler W., Selje N., and Simon M. (2009). Distribution of *Roseobacter* RCA and SAR11 lineages and distinct bacterial communities from the subtropics to the Southern Ocean. *Environmental Microbiology*, 11(8):2164–2178.
- Giebel H.-A., Kalhoefer D., Lemke A., Thole S., Gahl-Janssen R., Simon M., and Brinkhoff T. (2010). Distribution of *Roseobacter* RCA and SAR11 lineages in the North Sea and characteristics of an abundant RCA isolate. *The ISME Journal*, 5:8–19.
- Gille S. T. (2002). Warming of the Southern Ocean Since the 1950s. *Science*, 295(5558):1275–1277.
- Giovannoni S. J., Tripp H. J., Givan S., Podar M., Vergin K. L., Baptista D., Bibbs L., Eads J., Richardson T. H., Noordewier M., Rappé M. S., Short J. M., Carrington J. C., and Mathur E. J. (2005). Genome streamlining in a cosmopolitan oceanic bacterium. *Science*, 309(5738):1242–1245.
- Giovannoni S. J., Hayakawa D. H., Tripp H. J., Stingl U., Givan S. A., Cho J.-C., Oh H.-M., Kitner J. B., Vergin K. L., and Rappé M. S. (2008). The small genome of an abundant coastal ocean methylotroph. *Environmental Microbiology*, 10(7):1771–1782.
- Glöckner F. O., Fuchs B. M., and Amann R. (1999). Bacterioplankton compositions of lakes and oceans: a first comparison based on fluorescence in situ hybridization. *Applied and Environmental Microbiology*, 65(8):3721–3726.
- González J. M., Fernández-Gómez B., Fernández-Guerra A., Gómez-Consarnau L., Sánchez O., Coll-Lladó M., Del Campo J., Escudero L., Rodríguez-Martínez R., Alonso-Sáez L., Latasa M., Paulsen I., Nedashkovskaya O., Lekunberri I., Pinhassi J., and Pedrós-Alió C. (2008). Genome analysis of the proteorhodopsin-containing marine bacterium *Polaribacter* sp. MED152 (Flavobacteria). *Proceedings Of The National Academy Of Sciences Of The United States Of America*, 105(25):8724–8729.
- Grossart H. P., Schlingloff A., Bernhard M., Simon M., and Brinkhoff T. (2004). Antagonistic activity of bacteria isolated from organic aggregates of the German Wadden Sea. *FEMS Microbiology Ecology*, 47(3):387–396.
- Grote J., Bayindirli C., Bergauer K., Moraes P.Carpintero de, Chen H., D'Ambrosio L., Edwards B., Fernández-Gómez B., Hamisi M., Logares R., Nguyen D., Rii Y. M., Saeck E., Schutte C., Widner B., Church M. J., Steward G. F., Karl D. M., DeLong E. F., Eppley J. M., Schuster S. C., Kyprides N. C., and Rappé M. S. (2011). Draft genome sequence of strain HIMB100, a cultured representative of the SAR116 clade of marine *Alphaproteobacteria*. *Standards in Genomic Sciences*, 5(3):269–278.
- Grzymski J. J., Carter B. J., DeLong E. F., Feldman R. A., Ghadiri A., and Murray A. E. (2006). Comparative Genomics of DNA Fragments from Six Antarctic Marine Planktonic Bacteria. *Applied and Environmental Microbiology*, 72(2):1532–1541.

- Grzymski J. J., Riesenfeld C. S., Williams T. J., Dussaq A. M., Ducklow H., Erickson M., Cavicchioli R., and Murray A. E. (2012). A metagenomic assessment of winter and summer bacterioplankton from Antarctica Peninsula coastal surface waters. *The ISME Journal*, 6(10):1901–1915.
- Guixa-Boixereu N., Vaqué D., Gasol J. M., Sánchez-Cámarra J., and Pedrós-Alio C. (2002). Viral distribution and activity in Antarctic waters. *Deep Sea Research Part II: Topical Studies in Oceanography*, 49 (4):827–845.
- Hamdan L. J., Coffin R. B., Sikaroodi M., Greinert J., Treude T., and Gillevet P. M. (2013). Ocean currents shape the microbiome of Arctic marine sediments. *The ISME Journal*, 7(4):685–696.
- Hamilton A. K., Lovejoy C., Galand P. E., and Ingram R. G. (2008). Water masses and biogeography of picoeukaryote assemblages in a cold hydrographically complex system. *Limnology and Oceanography*, pages 922–935.
- Hanson C. A., Fuhrman J. A., Horner-Devine M. C., and Martiny J. B. H. (2012). Beyond biogeographic patterns: processes shaping the microbial landscape. *Nature Reviews Microbiology*, 10(7):497–506.
- Head I. M., Hiorns W. D., Embley T. M., McCarthy A. J., and Saunders J. R. (1993). The phylogeny of autotrophic ammonia-oxidizing bacteria as determined by analysis of 16S ribosomal RNA gene sequences. *Journal of General Microbiology*, 139(6):1147–1153.
- Heikes B. G., Chang W., Pilson M. E. Q., Swift E., Singh H. B., Guenther A., Jacob D. J., Field B. D., Fall R., Riemer D., and Brand L. (2002). Atmospheric methanol budget and ocean implication. *Global Biogeochemical Cycles*, 16(4):1133.
- Hessen D. O., Ågren G. I., Anderson T. R., Elser J. J., and de Ruiter, P.C. (2004). Carbon sequestration in ecosystems: the role of stoichiometry. *Ecology*, 85(5):1179–1192.
- Hollibaugh J. T., Bano N., and Ducklow H. W. (2002). Widespread Distribution in Polar Oceans of a 16S rRNA Gene Sequence with Affinity to *Nitrosospira*-Like Ammonia-Oxidizing Bacteria. *Applied and Environmental Microbiology*, 68(3):1478–1484.
- Howard E. C., Sun S., Biers E. J., and Moran M. A. (2008). Abundant and diverse bacteria involved in DMSP degradation in marine surface waters. *Environmental Microbiology*, 10(9):2397–2410.
- Hunt B. P. V., Pakhomov E. A., and McQuaid C. D. (2001). Short-term variation and long-term changes in the oceanographic environment and zooplankton community in the vicinity of a sub-Antarctic archipelago. *Marine Biolog*, 138:369–381.
- Huntley M. E., Lopez M. D., and Karl D. M. (1991). Top predators in the Southern ocean: a major leak in the biological carbon pump. *Science*, 253(5015):64–66.
- Huson D. H., Auch A. F., Qi J., and Schuster S. C. (2007). MEGAN analysis of metagenomic data. *Genome Research*, 17(3):377–386.
- Huston A. L., Krieger-Brockett B. B., and Deming J. W. (2000). Remarkably low temperature optima for extracellular enzyme activity from Arctic bacteria and sea ice. *Environmental Microbiology*, 2(4): 383–388.
- Ingalls A. E., Shah S. R., Hansman R. L., Aluwihare L. I., Santos G. M., Druffel E. R. M., and Pearson A. (2006). Quantifying archaeal community autotrophy in the mesopelagic ocean using natural radiocarbon. *Proceedings Of The National Academy Of Sciences Of The United States Of America*, 103 (17):6442–6447.
- Iverson V., Morris R. M., Frazer C. D., Berthiaume C. T., Morales R. L., and Armbrust E. V. (2012). Untangling Genomes from Metagenomes: Revealing an Uncultured Class of Marine Euryarchaeota. *Science*, 335(6068):587–590.
- Jacobs S. S. (2004). Bottom water production and its links with the thermohaline circulation. *Antarctic Science*, 16(04):427–437.

- Jamieson R. E., Rogers A. D., Billett D., Smale D. A., and Pearce D. A. (2012). Patterns of marine bacterioplankton biodiversity in the surface waters of the Scotia Arc, Southern Ocean. *FEMS Microbiology Ecology*, 80:452–468.
- Jung S.-Y., Oh T.-K., and Yoon J.-H. (2006). *Colwellia aestuarii* sp. nov., isolated from a tidal flat sediment in Korea. *International Journal of Systematic and Evolutionary Microbiology*, 56(1):33–37.
- Junge K., Eicken H., and Deming J. W. (2003). Motility of *Colwellia psychrerythraea* Strain 34H at Subzero Temperatures. *Applied and Environmental Microbiology*, 69(7):4282–4284.
- Kalanetra K. M., Bano N., and Hollibaugh J. T. (2009). Ammonia-oxidizing Archaea in the Arctic Ocean and Antarctic coastal waters. *Environmental Microbiology*, 11(9):2434–2445.
- Kawahata H. and Ishizuka T. (2000). Amino acids in interstitial waters from ODP Sites 689 and 690 on the Maud Rise, Antarctic Ocean. *Geochemical Journal*, 34(4):247–261.
- King G. M. (2003). Molecular and Culture-Based Analyses of Aerobic Carbon Monoxide Oxidizer Diversity. *Applied and Environmental Microbiology*, 69(12):7257–7265.
- Kirchman D. L. (2002). The ecology of *Cytophaga–Flavobacteria* in aquatic environments. *FEMS Microbiology Ecology*, 39(2):91–100.
- Kirchman D. L. *Microbial ecology of the oceans*. John Wiley & Sons, Inc., Hoboken, New Jersey, second edition, 2008.
- Kjelleberg S., Hermansson M., and Mårdén P. (1987). The transient phase between growth and non-growth of heterotrophic bacteria, with emphasis on the marine environment. *Annual Review of Microbiology*, 41:25–49.
- Knights D., Kuczynski J., Charlson E. S., Zaneveld J., Mozer M. C., Collman R. G., Bushman F. D., Knight R., and Kelley S. T. (2011). Bayesian community-wide culture-independent microbial source tracking. *Nature methods*, 8(9):761–763.
- Koh E. Y., Phua W., and Ryan K. G. (2011). Aerobic anoxygenic phototrophic bacteria in Antarctic sea ice and seawater. *Environmental Microbiology Reports*, 3(6):710–716.
- Kuwahara H., Yoshida T., Takaki Y., Shimamura S., Nishi S., Harada M., Matsuyama K., Takishita K., Kawato M., Uematsu K., Fujiwara Y., Sato T., Kato C., Kitagawa M., Kato I., and Maruyama T. (2007). Reduced Genome of the Thioautotrophic Intracellular Symbiont in a Deep-Sea Clam, *Calyptogena okutanii*. *Current Biology*, 17(10):881–886.
- Laubscher R. K., Perissinotto R., and McQuaid C. D. (1993). Phytoplankton production and biomass at frontal zones in the Atlantic sector of the Southern Ocean. *Polar Biology*, 13(7).
- Lauro F. M., Chastain R. A., Blankenship L. E., Yayanos A. A., and Bartlett D. H. (2007). The unique 16S rRNA genes of piezophiles reflect both phylogeny and adaptation. *Applied and Environmental Microbiology*, 73(3):838–845.
- Lauro F. M., McDougald D., Thomas T., Williams T. J., Egan S., Rice S., DeMaere M. Z., Ting L., Ertan H., Johnson J., Ferriera S., Lapidus A., Anderson I., Kyrpides N., Munk A. C., Detter C., Han C. S., Brown M. V., Robb F. T., Kjelleberg S., and Cavicchioli R. (2009). The genomic basis of trophic strategy in marine bacteria. *Proceedings Of The National Academy Of Sciences Of The United States Of America*, 106(37):15527–15533.
- Lauro F. M., DeMaere M. Z., Yau S., Brown M. V., Ng C., Wilkins D., Raftery M. J., Gibson J. A., Andrews-Pfannkoch C., Lewis M., Hoffman J. M., Thomas T., and Cavicchioli R. (2011). An integrative study of a meromictic lake ecosystem in Antarctica. *The ISME Journal*, 5(5):879–895.
- Legendre P. and Anderson M. J. (1999). Distance-based redundancy analysis: testing multispecies responses in multifactorial ecological experiments. *Ecological Monographs*, 69(1):1–24.

- Liu H., Nolla H. A., and Campbell L. (1997). *Prochlorococcus* growth rate and contribution to primary production in the equatorial and subtropical North Pacific Ocean. *Aquatic Microbial Ecology*, 12(1): 39–47.
- Liu H., Campbell L., Landry M. R., Nolla H. A., Brown S. L., and Constantinou J. (1998). *Prochlorococcus* and *Synechococcus* growth rates and contributions to production in the Arabian Sea during the 1995 Southwest and Northeast Monsoons. *Deep Sea Research Part II: Topical Studies in Oceanography*, 45 (10-11):2327–2352.
- Lo Giudice A., Caruso C., Mangano S., Bruni V., Domenico M., and Michaud L. (2011). Marine Bacterioplankton Diversity and Community Composition in an Antarctic Coastal Environment. *Microbial Ecology*, 63(1):210–223.
- Lomas M. W. and Moran S. B. (2011). Evidence for aggregation and export of cyanobacteria and nano-eukaryotes from the Sargasso Sea euphotic zone. *Biogeosciences*, 8(1):203–216.
- López-García P., López-López A., Moreira D., and Rodríguez-Valera F. (2001). Diversity of free-living prokaryotes from a deep-sea site at the Antarctic Polar Front. *FEMS Microbiology Ecology*, 36(2-3): 193–202.
- Ludwig W., Strunk O., Westram R., Richter L., Meier H., Yadhukumar , Buchner A., Lai T., Steppi S., Jobb G., Förster W., Brettske I., Gerber S., Ginhart A. W., Gross O., Grumann S., Hermann S., Jost R., König A., Liss T., Lüssmann R., May M., Nonhoff B., Reichel B., Strehlow R., Stamatakis A., Stuckmann N., Vilbig A., Lenke M., Ludwig T., Bode A., and Schleifer K.-H. (2004). ARB: a software environment for sequence data. *Nucleic Acids Research*, 32(4):1363–1371.
- Malmstrom R. R., Cottrell M. T., Elifantz H., and Kirchman D. L. (2005). Biomass production and assimilation of dissolved organic matter by SAR11 bacteria in the Northwest Atlantic Ocean. *Applied and Environmental Microbiology*, 71(6):2979–2986.
- Marchant H. J., Davidson A. T., and Wright S. W. (1987). The distribution and abundance of chroococoid cyanobacteria in the Southern Ocean. *Proc. NIPR Symp. Polar Biol*, 1:1–9.
- Martiny J. B. H., Bohannan B. J. M., Brown J. H., Colwell R. K., Fuhrman J. A., Green J. L., Horner-Devine M. C., Kane M., Krumins J. A., Kuske C. R., Morin P. J., Naeem S., Ovreas L., Reysenbach A.-L., Smith V. H., and Staley J. T. (2006). Microbial biogeography: putting microorganisms on the map. *Nature Reviews Microbiology*, 4(2):102–112.
- Mary I., Heywood J. L., Fuchs B. M., Amann R., Tarran G. A., Burkhill P. H., and Zubkov M. V. (2006). SAR11 dominance among metabolically active low nucleic acid bacterioplankton in surface waters along an Atlantic meridional transect. *Aquatic Microbial Ecology*, 45(2):107–113.
- Massana R., Taylor L. T., Murray A. E., Wu K. Y., Jeffrey W. H., and DeLong E. F. (1998). Vertical Distribution and Temporal Variation of Marine Planktonic Archaea in the Gerlache Strait, Antarctica, During Early Spring. *Limnology and ...*, 43(4):607–617.
- Massana R., DeLong E. F., and Pedrós-Alio C. (2000). A Few Cosmopolitan Phylotypes Dominate Planktonic Archaeal Assemblages in Widely Different Oceanic Provinces. *Applied and Environmental Microbiology*, 66(5):1777–1787.
- Mayali X., Franks P. J. S., and Azam F. (2008). Cultivation and Ecosystem Role of a Marine *Roseobacter* Clade-Affiliated Cluster Bacterium. *Applied and Environmental Microbiology*, 74(9):2595–2603.
- Mazloff M. R., Heimbach P., and Wunsch C. (2010). An eddy-permitting Southern Ocean state estimate. *Journal of physical oceanography*, 40:880–899.
- Merbt S. N., Stahl D. A., Casamayor E. O., Martí E., Nicol G. W., and Prosser J. I. (2012). Differential photoinhibition of bacterial and archaeal ammonia oxidation. *FEMS Microbiology Letters*, 327(1): 41–46.

- Methé B. A., Nelson K. E., Deming J. W., Momen B., Melamud E., Zhang X., Moult J., Madupu R., Nelson W. C., Dodson R. J., Methé B. A., Nelson K. E., Deming J. W., Momen B., Melamud E., Zhang X., Moult J., Madupu R., Nelson W. C., Dodson R. J., Brinkac L. M., Daugherty S. C., Durkin A. S., DeBoy R. T., Kolonay J. F., Sullivan S. A., Zhou L., Davidsen T. M., Wu M., Huston A. L., Lewis M., Weaver B., Weidman J. F., Khouri H., Utterback T. R., Feldblyum T. V., and Fraser C. M. (2005). The psychrophilic lifestyle as revealed by the genome sequence of *Colwellia psychrerythraea* 34H through genomic and proteomic analyses. *Proceedings Of The National Academy Of Sciences Of The United States Of America*, 102(31):10913–10918.
- Meyer B. and Kuever J. (2007). Molecular Analysis of the Diversity of Sulfate-Reducing and Sulfur-Oxidizing Prokaryotes in the Environment, Using *aprA* as Functional Marker Gene. *Applied and Environmental Microbiology*, 73(23):7664–7679.
- Mikaloff Fletcher S. E., Gruber N., Jacobson A. R., Doney S. C., Dutkiewicz S., Gerber M., Follows M., Joos F., Lindsay K., Menemenlis D., Mouchet A., Müller S. A., and Sarmiento J. L. (2006). Inverse estimates of anthropogenic CO₂ uptake, transport, and storage by the ocean. *Global Biogeochemical Cycles*, 20(2):GB2002.
- Miller T. R. and Belas R. (2004). Dimethylsulfoniopropionate Metabolism by *Pfiesteria*-Associated *Roseobacter* spp. *Applied and Environmental Microbiology*, 70(6):3383–3391.
- Mira A., Ochman H., and Moran N. A. (2001). Deletional bias and the evolution of bacterial genomes. *Trends in genetics : TIG*, 17(10):589–596.
- Moore J. K., Abbott M. R., and Richman J. G. (1999). Location and dynamics of the Antarctic Polar Front from satellite sea surface temperature data. *Journal of Geophysical Research*, 104:3052–3073.
- Moran M. A., Belas R., Schell M. A., González J. M., Sun F., Sun S., Binder B. J., Edmonds J., Ye W., Orcutt B., Howard E. C., Meile C., Palefsky W., Goesmann A., Ren Q., Paulsen I., Ulrich L. E., Thompson L. S., Saunders E., and Buchan A. (2007). Ecological Genomics of Marine Roseobacters. *Applied and Environmental Microbiology*, 73(14):4559–4569.
- Moran M. A., González J. M., and Kiene R. P. (2003). Linking a Bacterial Taxon to Sulfur Cycling in the Sea: Studies of the Marine Roseobacter Group. *Geomicrobiology Journal*, 20(4):375–388.
- Moran M. A., Buchan A., González J. M., Heidelberg J. F., Whitman W. B., Kiene R. P., Henriksen J. R., King G. M., Belas R., Fuqua C., Brinkac L., Lewis M., Johri S., Weaver B., Pai G., Eisen J. A., Rahe E., Sheldon W. M., Ye W., Miller T. R., Carlton J., Rasko D. A., Paulsen I. T., Ren Q., Daugherty S. C., Deboy R. T., Dodson R. J., Durkin A. S., Madupu R., Nelson W. C., Sullivan S. A., Rosovitz M. J., Haft D. H., Selengut J., and Ward N. (2004). Genome sequence of *Silicibacter pomeroyi* reveals adaptations to the marine environment. *Nature*, 432(7019):910–913.
- Morris R. M., Rappé M. S., Connon S. A., Vergin K. L., Siebold W. A., Carlson C. A., and Giovannoni S. J. (2002). SAR11 clade dominates ocean surface bacterioplankton communities. *Nature*, 420(6917):806–810.
- Morris R. M., Longnecker K., and Giovannoni S. J. (2006). *Pirellula* and OM43 are among the dominant lineages identified in an Oregon coast diatom bloom. *Environmental Microbiology*, 8(8):1361–1370.
- Murray A. E. and Grzymski J. J. (2007). Diversity and genomics of Antarctic marine micro-organisms. *Philosophical Transactions of the Royal Society B: Biological Sciences*, 362(1488):2259–2271.
- Murray A. E., Wu K. Y., Moyer C. L., Karl D. M., and DeLong E. F. (1999). Evidence for circumpolar distribution of planktonic Archaea in the Southern Ocean. *Aquatic Microbial Ecology*, 18(3):263–273.
- Murray A. E. A., Preston C. M. C., Massana R. R., Taylor L. T. L., Blakis A. A., Wu K. K., and DeLong E. F. (1998). Seasonal and spatial variability of bacterial and archaeal assemblages in the coastal waters near Anvers Island, Antarctica. *Applied and Environmental Microbiology*, 64(7):2585–2595.
- Murray A. E., Peng V., Tyler C., and Wagh P. (2011). Marine bacterioplankton biomass, activity and community structure in the vicinity of Antarctic icebergs. *Deep Sea Research Part II: Topical Studies in Oceanography*, 58(11-12):1407–1421.

- Newton I. L. G., Woyke T., Auchtung T. A., Dilly G. F., Dutton R. J., Fisher M. C., Fontanez K. M., Lau E., Stewart F. J., Richardson P. M., Barry K. W., Saunders E., Detter J. C., Wu D., Eisen J. A., and Cavanaugh C. M. (2007). The *Calyptogena magnifica* Chemoautotrophic Symbiont Genome. *Science*, 315(5814):998–1000.
- Ng C., DeMaere M. Z., Williams T. J., Lauro F. M., Raftery M., Gibson J. A., Andrews-Pfannkoch C., Lewis M., Hoffman J. M., Thomas T., and Cavicchioli R. (2010). Metaproteogenomic analysis of a dominant green sulfur bacterium from Ace Lake, Antarctica. *The ISME Journal*, 4(8):1002–1019.
- Nikrad M. P., Cottrell M. T., and Kirchman D. L. (2012). Abundance and Single-Cell Activity of Heterotrophic Bacterial Groups in the Western Arctic Ocean in Summer and Winter. *Applied and Environmental Microbiology*, 78(7):2402–2409.
- Obernosterer I., Catala P., Lebaron P., and West N. J. (2011). Distinct bacterial groups contribute to carbon cycling during a naturally iron fertilized phytoplankton bloom in the Southern Ocean. *Limnology and Oceanography*, 56(6):2391–2401.
- Oh H. M., Kwon K. K., Kang I., Kang S. G., Lee J. H., Kim S. J., and Cho J. C. (2010). Complete Genome Sequence of "Candidatus Puniceispirillum marinum" IMCC1322, a Representative of the SAR116 Clade in the Alphaproteobacteria. *Journal of Bacteriology*, 192(12):3240–3241.
- Oliver J. L., Barber R. T., Smith Jr W. O., and Ducklow H. W. (2004). The heterotrophic bacterial response during the Southern Ocean iron experiment (SOFeX). *Limnology and Oceanography*, 49(6): 2129–2140.
- Orsi A. H., Whitworth T., and Nowlin W. D. (1995). On the meridional extent and fronts of the Antarctic Circumpolar Current. *Deep Sea Research Part I: Oceanographic Research Papers*, 42(5):641–673.
- Orsi A. H., Johnson G. C., and Bullister J. L. (1999). Circulation, mixing, and production of Antarctic Bottom Water. *Progress in Oceanography*, 43(1):55–109.
- O'Sullivan L. A., Fuller K. E., Thomas E. M., Turley C. M., Fry J. C., and Weightman A. J. (2004). Distribution and culturability of the uncultivated 'AGG58 cluster' of the *Bacteroidetes* phylum in aquatic environments. *FEMS Microbiology Ecology*, 47(3):359–370.
- Paris C. B., Helgers J., Sebille E.van, and Srinivasan A. (2013). Connectivity Modeling System: A probabilistic modeling tool for the multi-scale tracking of biotic and abiotic variability in the ocean. *Environmental Modelling and Software*, 42(C):47–54.
- Partensky F., Hess W. R., and Vaulot D. (1999). *Prochlorococcus*, a marine photosynthetic prokaryote of global significance. *Microbiology and Molecular Biology Reviews*, 63(1):106–127.
- Paul J. H., DeFlaun M. F., and Jeffrey W. H. (1988). Mechanisms of DNA utilization by estuarine microbial populations. *Applied and Environmental Microbiology*, 54(7):1682–1688.
- Pham V. D., Konstantinidis K. T., Palden T., and DeLong E. F. (2008). Phylogenetic analyses of ribosomal DNA-containing bacterioplankton genome fragments from a 4000 m vertical profile in the North Pacific Subtropical Gyre. *Environmental Microbiology*, 10(9):2313–2330.
- Pinhassi J., Sala M. M., Havskum H., Peters F., Guadayol Ò., Malits A., and Marrasé C. (2004). Changes in bacterioplankton composition under different phytoplankton regimens. *Applied and Environmental Microbiology*, 70(11):6753–6766.
- Piquet A. M. T., Bolhuis H., Meredith M. P., and Buma A. G. J. (2011). Shifts in coastal Antarctic marine microbial communities during and after melt water-related surface stratification. *FEMS Microbiology Ecology*, 76(3):413–427.
- Pollard R. T., Lucas M. I., and Read J. F. (2002). Physical controls on biogeochemical zonation in the Southern Ocean. *Deep Sea Research Part II: Topical Studies in Oceanography*, 49(16):3289–3305.
- Pommier T., Canbäck B., Riemann L., Boström K. H., Simu K., Lundberg P., Tunlid A., and Hagström Å. (2007). Global patterns of diversity and community structure in marine bacterioplankton. *Molecular Ecology*, 16(4):867–880.

- Poorvin L., Rinta-Kanto J. M., Hutchins D. A., and Wilhelm S. W. (2004). Viral release of iron and its bioavailability to marine plankton. *Limnology and Oceanography*, 49(5):1734–1741.
- Powell L. M., Bowman J. P., Skerratt J. H., Franzmann P. D., and Burton H. R. (2005). Ecology of a novel *Synechococcus* clade occurring in dense populations in saline Antarctic lakes. *Marine Ecology Progress Series*, 291(28 April):65–80.
- Preston C. M., Wu K. Y., Molinski T. F., and DeLong E. F. (1996). A psychrophilic crenarchaeon inhabits a marine sponge: *Cenarchaeum symbiosum* gen. nov., sp. nov. *Proceedings Of The National Academy Of Sciences Of The United States Of America*, 93(13):6241–6246.
- Qin J., Li R., Raes J., Arumugam M., Burgdorf K. S., Manichanh C., Nielsen T., Pons N., Levenez F., Yamada T., Mende D. R., Li J., Xu J., Li S., Li D., Cao J., Wang B., Liang H., Zheng H., Xie Y., Tap J., Lepage P., Bertalan M., Batto J.-M., Hansen T., Le Paslier D., Linneberg A., Nielsen H. B., Pelletier E., Renault P., Sicheritz-Ponten T., Turner K., Zhu H., Yu C., Li S., Jian M., Zhou Y., Li Y., Zhang X., Li S., Qin N., Yang H., Wang J., Brunak S., Doré J., Guarner F., Kristiansen K., Pedersen O., Parkhill J., Weissenbach J., MetaHIT Consortium , Bork P., Ehrlich S. D., and Wang J. (2010). A human gut microbial gene catalogue established by metagenomic sequencing. *Nature*, 464(7285):59–65.
- Quast C., Pruesse E., Yilmaz P., Gerken J., Schweer T., Yarza P., Peplies J., and Glöckner F. O. (2013). The SILVA ribosomal RNA gene database project: improved data processing and web-based tools. *Nucleic Acids Research*, 41(Database issue):D590–6.
- Ramette A. and Tiedje J. M. (2007). Multiscale responses of microbial life to spatial distance and environmental heterogeneity in a patchy ecosystem. *Proceedings Of The National Academy Of Sciences Of The United States Of America*, 104(8):2761–2766.
- Rappé M. S., Connon S. A., Vergin K. L., and Giovannoni S. J. (2002). Cultivation of the ubiquitous SAR11 marine bacterioplankton clade. *Nature*, 418(6898):630–633.
- Rath J., Wu K. Y., Herndl G. J., and DeLong E. F. (1998). High phylogenetic diversity in a marine-snow-associated bacterial assemblage. *Aquatic Microbial Ecology*, 14(3):261–269.
- Reisch C. R., Stoudemayer M. J., Varaljay V. A., Amster I. J., Moran M. A., and Whitman W. B. (2011). Novel pathway for assimilation of dimethylsulphoniopropionate widespread in marine bacteria. *Nature*, 473(7346):208–211.
- Rosenberg M. and Rintoul S. R. Aurora Australis Marine Science Cruise AU1203 – Oceanographic Field Measurements and Analysis. Technical report, 2012.
- Rosenberg M. S. and Anderson C. D. (2011). PASSaGE: pattern analysis, spatial statistics and geographic exegesis. Version 2. *Methods in Ecology and Evolution*, 2(3):229–232.
- Rusch D. B., Halpern A. L., Sutton G., Heidelberg K. B., Williamson S., Yooseph S., Wu D., Eisen J. A., Hoffman J. M., Remington K., Beeson K., Tran B., Smith H., Baden-Tillson H., Stewart C., Thorpe J., Freeman J., Andrews-Pfannkoch C., Venter J. E., Li K., Kravitz S., Heidelberg J. F., Utterback T., Rogers Y.-H., Falcón L. I., Souza V., Bonilla-Rosso G., Eguiarte L. E., Karl D. M., Sathyendranath S., Platt T., Bermingham E., Gallardo V., Tamayo-Castillo G., Ferrari M. R., Strausberg R. L., Nealson K., Friedman R., Frazier M., and Venter J. C. (2007). The Sorcerer II Global Ocean Sampling expedition: northwest Atlantic through eastern tropical Pacific. *PLoS Biology*, 5(3):e77–e77.
- Sabine C. L., Feely R. A., Gruber N., Key R. M., Lee K., Bullister J. L., Wanninkhof R., Wong C. S., Wallace D. W. R., Tilbrook B., Millero F. J., Peng T.-H., Kozyr A., Ono T., and Rios A. F. (2004). The Oceanic Sink for Anthropogenic CO₂. *Science*, 305(5682):367–371.
- Scanlan D. J., Ostrowski M., Mazard S., Dufresne A., Garczarek L., Hess W. R., Post A. F., Hagemann M., Paulsen I., and Partensky F. (2009). Ecological Genomics of Marine Picocyanobacteria. *Microbiology and Molecular Biology Reviews*, 73(2):249–299.
- Selje N. N., Simon M. M., and Brinkhoff T. T. (2004). A newly discovered *Roseobacter* cluster in temperate and polar oceans. *Nature*, 427(6973):445–448.

- Short C. M. and Suttle C. A. (2005). Nearly Identical Bacteriophage Structural Gene Sequences Are Widely Distributed in both Marine and Freshwater Environments. *Applied and Environmental Microbiology*, 71(1):480–486.
- Short S. M. and Suttle C. A. (2002). Sequence Analysis of Marine Virus Communities Reveals that Groups of Related Algal Viruses Are Widely Distributed in Nature. *Applied and Environmental Microbiology*, 68(3):1290–1296.
- Simon M., Glöckner F. O., and Amann R. (1999). Different community structure and temperature optima of heterotrophic picoplankton in various regions of the Southern Ocean. *Aquatic Microbial Ecology*, 18(3):275–284.
- Sinha V., Williams J., Meyerhöfer M., Riebesell U., Paulino A. I., and Larsen A. (2007). Air-sea fluxes of methanol, acetone, acetaldehyde, isoprene and DMS from a Norwegian fjord following a phytoplankton bloom in a mesocosm experiment. *Atmospheric Chemistry and Physics*, 7(3):739–755.
- Sokolov S. and Rintoul S. R. (2002). Structure of Southern Ocean fronts at 140°E. *Journal of Marine Systems*, 37(1):151–184.
- Sokolov S. and Rintoul S. R. (2009). Circumpolar structure and distribution of the Antarctic Circumpolar Current fronts: 1. Mean circumpolar paths. *Journal of Geophysical Research*, 114(C11):C11018.
- Sowell S. M., Wilhelm L. J., Norbeck A. D., Lipton M. S., Nicora C. D., Barofsky D. F., Carlson C. A., Smith R. D., and Giovannoni S. J. (2009). Transport functions dominate the SAR11 metaproteome at low-nutrient extremes in the Sargasso Sea. *The ISME Journal*, 3(1):93–105.
- Speer K., Rintoul S. R., and Sloyan B. (2000). The Diabatic Deacon Cell. *Journal of physical oceanography*, 30(12):3212–3222.
- Steindler L., Schwalbach M. S., Smith D. P., Chan F., and Giovannoni S. J. (2011). Energy Starved *Candidatus Pelagibacter* Ubique Substitutes Light-Mediated ATP Production for Endogenous Carbon Respiration. *PLoS ONE*, 6(5):e19725.
- Stingl U., Tripp H. J., and Giovannoni S. J. (2007). Improvements of high-throughput culturing yielded novel SAR11 strains and other abundant marine bacteria from the Oregon coast and the Bermuda Atlantic Time Series study site. *The ISME Journal*, 1:361–371.
-). The concept of taxon invariance in ecology: do diversity patterns vary with changes in taxonomic resolution? *Folia Geobotanica*, 43:329–344.
- Straza T. R. A., Ducklow H. W., Murray A. E., and Kirchman D. L. (2010). Abundance and single-cell activity of bacterial groups in Antarctic coastal waters. *Limnology and Oceanography*, 55(6):2526–2536.
- Strous M., Fuerst J. A., Kramer E. H. M., Logemann S., Muyzer G., Van De Pas-Schoonen K. T., Webb R., Kuenen J. G., and Jetten M. S. M. (1999). Missing lithotroph identified as new planctomycete. *Nature*, 400(6743):446–449.
- Strutton P. G., Griffiths F. B., Waters R. L., Wright S. W., and Bindoff N. L. (2000). Primary productivity off the coast of East Antarctica (80–150°E): January to March 1996. *Deep Sea Research Part II: Topical Studies in Oceanography*, 47:2327–2362.
- Sul W. J., Oliver T. A., Ducklow H. W., Amaral-Zettler L. A., and Sogin M. L. (2013). Marine bacteria exhibit a bipolar distribution. *Proceedings Of The National Academy Of Sciences Of The United States Of America*, 110(6):2342–2347.
- Swan B. K., Martinez-Garcia M., Preston C. M., Sczyrba A., Woyke T., Lamy D., Reinthal T., Poulton N. J., Masland E. D. P., Gomez M. L., Sieracki M. E., DeLong E. F., Herndl G. J., and Stepanauskas R. (2011). Potential for Chemolithoautotrophy Among Ubiquitous Bacteria Lineages in the Dark Ocean. *Science*, 333(6047):1296–1300.

- Swingley W. D., Sadekar S., Mastrian S. D., Matthies H. J., Hao J., Ramos H., Acharya C. R., Conrad A. L., Taylor H. L., Dejesa L. C., Shah M. K., O'Huallachain M. E., Lince M. T., Blankenship R. E., Beatty J. T., and Touchman J. W. (2007). The Complete Genome Sequence of *Roseobacter denitrificans* Reveals a Mixotrophic Rather than Photosynthetic Metabolism. *Journal of Bacteriology*, 189(3):683–690.
- Teske A., Alm E., Regan J. M., Toze S., Rittmann B. E., and Stahl D. A. (1994). Evolutionary relations among ammonia- and nitrite-oxidizing bacteria. *Journal of Bacteriology*, 176(21):6623–6630.
- Thomalla S. J., Waldron H. N., Lucas M. I., Read J. F., Ansorge I. J., and Pakhomov E. (2011). Phytoplankton distribution and nitrogen dynamics in the southwest Indian subtropical gyre and Southern Ocean waters. *Ocean Science*, 7(1):113–127.
- Thompson D. W. J. and Solomon S. (2002). Interpretation of Recent Southern Hemisphere Climate Change. *Science*, 296(5569):895–899.
- Topping J. N., Heywood J. L., Ward P., and Zubkov M. V. (2006). Bacterioplankton composition in the Scotia Sea, Antarctica, during the austral summer of 2003. *Aquatic Microbial Ecology*, 45(3):229–235.
- Tréguer P., Nelson D. M., Van Bennekom A. J., DeMaster D. J., Leynaert A., and Quéquier B. (1995). The silica balance in the world ocean: a reestimate. *Science*, 268(5209):375–379.
- Tripp H. J., Kitner J. B., Schwalbach M. S., Dacey J. W. H., Wilhelm L. J., and Giovannoni S. J. (2008). SAR11 marine bacteria require exogenous reduced sulphur for growth. *Nature*, 452(7188):741–744.
- Trull T., Rintoul S. R., Hadfield M., and Abraham E. R. (2001). Circulation and seasonal evolution of polar waters south of Australia: implications for iron fertilization of the Southern Ocean. *Deep Sea Research Part II: Topical Studies in Oceanography*, 48(11):2439–2466.
- Sebille E. van, Johns W. E., and Beal L. M. (2012). Does the vorticity flux from Agulhas rings control the zonal pathway of NADW across the South Atlantic? *Journal of Geophysical Research*, 117(C5):C05037.
- Venter J. C., Remington K., Heidelberg J. F., Halpern A. L., Rusch D., Eisen J. A., Wu D., Paulsen I., Nelson K. E., Nelson W., Fouts D. E., Levy S., Knap A. H., Lomas M. W., Nealson K., White O., Peterson J., Hoffman J., Parsons R., Baden-Tillson H., Pfannkoch C., Rogers Y.-H., and Smith H. O. (2004). Environmental Genome Shotgun Sequencing of the Sargasso Sea. *Science*, 304(5667):66–74.
- Vila-Costa M., Simó R., Harada H., Gasol J. M., Slezak D., and Kiene R. P. (2006). Dimethylsulfonio-propionate Uptake by Marine Phytoplankton. *Science*, 314(5799):652–654.
- Wagner-Döbler I. and Biebl H. (2006). Environmental Biology of the Marine *Roseobacter* Lineage. *Annual Review of Microbiology*, 60(1):255–280.
- Walker C. B., Torre J. R. de la, Klotz M. G., Urakawa H., Pinel N., Arp D. J., Brochier-Armanet C., Chain P., Chan P. P., Gollabgir A., Hemp J., Hüglar M., Karr E. A., Könekke M., Shin M., Lawton T. J., Lowe T., Martens-Habbena W., Sayavedra-Soto L. A., Langf D., Sievert S. M., Rosenzweig A. C., Manning G., and Stahl D. A. (2010). *Nitrosopumilus maritimus* genome reveals unique mechanisms for nitrification and autotrophy in globally distributed marine crenarchaea. *Proceedings Of The National Academy Of Sciences Of The United States Of America*, 107(19):8818–8823.
- Walsh D. A., Zaikova E., Howes C. G., Song Y. C., Wright J. J., Tringe S. G., Tortell P. D., and Hallam S. J. (2009). Metagenome of a Versatile Chemolithoautotroph from Expanding Oceanic Dead Zones. *Science*, 326(5952):578–582.
- Ward P., Whitehouse M., Brandon M., Shreeve R., and Wood-Walker R. (2003). Mesozooplankton community structure across the Antarctic Circumpolar Current to the north of South Georgia: Southern Ocean. *Marine Biology*, 143(1):121–130.
- Weber T. S. and Deutsch C. (2010). Ocean nutrient ratios governed by plankton biogeography. *Nature*, 467(7315):550–554.

- Weinbauer M. G., Arrieta J. M., Griebler C., and Herndl G. J. (2009). Enhanced viral production and infection of bacterioplankton during an iron-induced phytoplankton bloom in the Southern Ocean. *Limnol. Oceanogr.*, 54(3):774–784.
- West N. J., Obernosterer I., Zemb O., and Lebaron P. (2008). Major differences of bacterial diversity and activity inside and outside of a natural iron-fertilized phytoplankton bloom in the Southern Ocean. *Environmental Microbiology*, 10(3):738–756.
- Whitworth T. (1980). Zonation and geostrophic flow of the Antarctic Circumpolar Current at Drake Passage. *Deep Sea Research Part I: Oceanographic Research Papers*, 27(7):497–507.
- Whitworth III T. and Nowlin Jr. W. D. (1987). Water masses and currents of the Southern Ocean at the Greenwich Meridian. *Journal of Geophysical Research*, 92(C6):6462–6476.
- Wilhelm S. W. and Suttle C. A. (1999). Viruses and nutrient cycles in the sea. *BioScience*, 49(10):781–788.
- Wilkins D., Lauro F. M., Williams T. J., DeMaere M. Z., Brown M. V., Hoffman J. M., Andrews-Pfannkoch C., McQuaid J. B., Riddle M. J., Rintoul S. R., and Cavicchioli R. (2012). Biogeographic partitioning of Southern Ocean microorganisms revealed by metagenomics. *Environmental Microbiology*.
- Wilkins D., Yau S., Williams T. J., Allen M. A., Brown M. V., DeMaere M. Z., Lauro F. M., and Cavicchioli R. (2012). Key microbial drivers in Antarctic aquatic environments. *FEMS Microbiology Reviews*.
- Williams G. D., Nicol S., Aoki S., Meijers A. J. S., Bindoff N. L., Iijima Y., Marsland S. J., and Klocker A. (2010). Surface oceanography of BROKE-West, along the Antarctic margin of the south-west Indian Ocean (30–80°E). *Deep Sea Research Part II: Topical Studies in Oceanography*, 57(9-10):738–757.
- Williams T. J., Lauro F. M., Ertan H., Burg D. W., Poljak A., Raftery M. J., and Cavicchioli R. (2011). Defining the response of a microorganism to temperatures that span its complete growth temperature range (-2 °C to 28 °C) using multiplex quantitative proteomics. *Environmental Microbiology*, 13 (8):2186–2203.
- Williams T. J., Long E., Evans F., DeMaere M. Z., Lauro F. M., Raftery M. J., Ducklow H., Grzymski J. J., Murray A. E., and Cavicchioli R. (2012). A metaproteomic assessment of winter and summer bacterioplankton from Antarctic Peninsula coastal surface waters. *The ISME Journal*, 6(10):1883–1900.
- Williams T. J., Wilkins D., Long E., Evans F., DeMaere M. Z., Raftery M. J., and Cavicchioli R. (2012). The role of planktonic Flavobacteria in processing algal organic matter in coastal East Antarctica revealed using metagenomics and metaproteomics. *Environmental Microbiology*.
- Wright T. D., Vergin K. L., Boyd P. W., and Giovannoni S. J. (1997). A novel α -subdivision proteobacterial lineage from the lower ocean surface layer. *Applied and Environmental Microbiology*, 63 (4):1441–1448.
- Wunsch C. and Heimbach P. (2007). Practical global oceanic state estimation. *Physica D: Nonlinear Phenomena*, 230(1):197–208.
- Ye Y. and Doak T. G. (2009). A parsimony approach to biological pathway reconstruction/inference for genomes and metagenomes. *PLoS Computational Biology*, 5(8):e1000465.
- Yoon J., Yasumoto-Hirose M., Katsuta A., Sekiguchi H., Matsuda S., Kasai H., and Yokota A. (2007). *Coraliomargarita akajimensis* gen. nov., sp. nov., a novel member of the phylum 'Verrucomicrobia' isolated from seawater in Japan. *International Journal of Systematic and Evolutionary Microbiology*, 57(5): 959–963.
- Youssef N., Sheik C. S., Krumholz L. R., Najar F. Z., Roe B. A., and Elshahed M. S. (2009). Comparison of species richness estimates obtained using nearly complete fragments and simulated pyrosequencing-generated fragments in 16S rRNA gene-based environmental surveys. *Applied and Environmental Microbiology*.

Zaballos M., López-López A., Ovreas L., Bartual S. G., D'Auria G., Alba J. C., Legault B., Pushker R., Daae F. L., and Rodriguez-Valera F. (2006). Comparison of prokaryotic diversity at offshore oceanic locations reveals a different microbiota in the Mediterranean Sea. *FEMS Microbiology Ecology*, 56(3): 389–405.

Zhang R., Liu B., Lau S. C. K., Ki J.-S., and Qian P.-Y. (2007). Particle-attached and free-living bacterial communities in a contrasting marine environment: Victoria Harbor, Hong Kong. *FEMS Microbiology Ecology*, 61(3):496–508.

Zubkov M. V., Sleigh M. A., Tarran G. A., Burkill P. H., and Leakey R. J. G. (1998). Picoplanktonic community structure on an Atlantic transect from 50°N to 50°S. *Deep Sea Research Part I: Oceanographic Research Papers*, 45(8):1339–1355.